Design of a continuous autohydrolysis pretreatment process of annual lignocellulose for industrial application

Vom Promotionsausschuss der
Technischen Universität Hamburg

Zur Erlangung des akademischen Grades

Doktor-Ingenieur (Dr.-Ing.)

genehmigte Dissertation

Von
Marc-Julian Conrad

Aus
Pinneberg

2023

1. Gutachterin:	Prof. Dr.-Ing. Irina Smirnova
2. Gutachterin:	Prof. Dr. rer. nat. Andrea Kruse
3. Gutachter:	Prof. Dr. Ola Wallberg
Prüfungsausschussvorsitzender:	Prof. Dr. rer. nat. Raimund Horn
Tag der mündlichen Prüfung:	20. Januar 2023

ORCID: https://orcid.org/0009-0009-0992-6014

DOI: https://doi.org/10.15480/882.5105

Acknowledgment

The present work was created solely and independently by myself. Anyhow, several people did support and inspire me, whom I cannot name all of. Some of them I want to thank explicitly here:

First and most importantly, I want to thank my **parents,** who continuously supported and motivated me to find my way. They created possibilities and chances that were crucial for my personal development. I dedicate this work to my parents.

I am genuinely thankful to **Simon Meyer** and **Katrin Korte,** who pursued the bachelor's degree with me. The constant strive for mindful and every better ways of studying and the impressive diligence were a fortune.

I thank **Dr. Jan Brummund** for supervising my first independent scientific work, the bachelor thesis. He taught the required basics of structured scientific work in a patient but demanding way. I thank **Dr. Wienke Reynolds** for the supervision of my project work. Finally, I was able to research the field of biorefining. I was trusted with complicated tasks and tremendous freedom to develop methods and concepts. I thank **Dr. Lisa Schmidt** for the supervision of my master's thesis. Working with modern techniques in reactive liquid-liquid extraction in a biorefinery context, I was responsible for selecting milestones and strategies to achieve them.

Big and special thanks are dedicated to **Prof. Dr.-Ing. Irina Smirnova** for the trust and supervision of my research as an employee at Institute for Thermal Separation Processes. She is an outstanding scientist and fantastic mentor and gave support in the most challenging uncertainties.

I thank **Dr. Hans Häring** of Sigmar Mothes Hochdrucktechnik GmbH for the kick-starting collaboration during the beginning of my studies. The perspective of plant manufacturing allowed me to develop process concepts with high realization feasibility.

I thank **Dr. Gerald Koch** of Thünen-Institut in Hamburg-Bergedorf for the chance to analyze pretreated straw samples with UV microspectrophotometry (UMSP) to gain insights relevant to my extraction process developments. I thank **Dr. Fabian Bonk** of Vereinigte Bioenergie GmbH (Verbio) for the perspective of an innovative company on process developments and investment cost calculations. I thank **Dr. Ireen Gebauer** of Fraunhofer CBP in Leuna for the support in the process Scale-Up and selection of

production-relevant equipment. I thank **Dr. Thibault Godard** of Mushlabs GmbH for the trust, the successful technology transfer project, and the provision of a technical hall-scale continuous screw press.

I am thankful for the unforgettable time with my **colleagues** at the institute, with numerous great experiences inside and outside the office and laboratories. Special thanks are dedicated to **Dr. Simon Müller**, **Alberto Bueno**, **Andrés Gonzales**, and **Philip Pein,** with whom I countlessly discussed mathematics, modeling, plant design, machining, thermodynamics, and scientific literature.

I am thankful to all the colleagues working with biorefinery topics, **Xihua Hu**, **Lennart Andersen**, **Dr. Anne Lamp**, **Stanislav Parsin,** and **Timo Steinbrecher,** for the inspiring discussions and mutual support in the laboratory.

I am thankful for **Dr. Carsten Zetzl**'s dedicated creation of technical concepts and grant proposals, for **Stefanie Meyer-Storckmann**'s cordial support of all non-engineering issues, for **Frank Sokolinski**'s fantastic developments in measurement and control systems, for **Dirk Manning**'s collaborative support in mechanical construction tasks.

I thank my wife **Gabriele** for her love, clearing space for my work, acknowledgments of my efforts, and motivational support. My work aims to contribute to climate change mitigation to allow good lives for future generations. The birth of my son **Emil** motivates me never to give up.

Summary

In the last decade, several factories were put into operation that used the pretreatment of lignocellulose as a central refining stage, mainly to convert cellulose, sometimes also a fraction of hemicellulose, to lignocellulosic ethanol. The focus is on cheap lignocellulosic ethanol; thus, other parts of the non-edible biomass are turned to low-value applications due to low quality. The potential of hemicellulose and lignin remains vastly untapped. To shift the feedstock of the chemical industry to renewable resources, it is required for all compounds of lignocellulose to be refined in high quality so that they can be used for the production of chemicals.

Such full-fractionation processes are under development but fail to deconstruct the recalcitrant biomass efficiently. A critical challenge is the hydrolysis of hemicellulose. Before the conversion of the polymer is sufficiently high, the formed products (water-soluble pentose) decay to unwanted, harmful, and reactive degradation products like furfural. Reactors with in-situ product removal allow a full-fractionation under the conditions of excessive water and energy consumption, which is economically not feasible.

In this work, a two-step pretreatment is proposed and investigated experimentally. The hemicellulose conversion is stopped before the degradations take place to extract the desired product at its peak concentration. In the second step, the hemicellulose conversion is continued to the required level. The kinetic of this concept was investigated in Liquid Hot Water reactors and transferred to steam pretreatment reactors. A rigorous mass balance approves the high separation yields and avoidance of degradation products. The resulting (intermediate) products, oligomer xylan, glucose, and solid lignin, were tested in relevant applications to conclude the high quality of the products. Finally, critical steps are validated in continuous steam pretreatment reactors to allow the scaling of the process to an industrial scale.

Using a steam environment allows a fast and homogenous pretreatment while a minimal amount of liquid water and energy are required for the process. The resulting high concentration in the pretreated biomass is beneficial for the necessary extraction process. The pretreated biomass was used to develop an extraction process for this purpose. A new counter-current extraction process is designed and filed for a patent based on fast extraction in a stirred suspension with mild compressive dewatering for

fast mass transport. Only a tiny amount of water can travel in the same direction as the solids to achieve a very low solvent (water) consumption, high extract concentrations, and a high extraction yield.

Contents

Latin Symbols

c_i	Concentration of component i [g/L], [g/1000g], [mol/L]
$c_{i,0}$	Initial concentration of component i [g/L], [g/1000g], [mol/L]
D	Reactor Diamter [m]
DM	Dry matter content [wt%], [g/g]
DM-i	Dry matter content of stream i [wt%], [g/g]
DS	Degree of Solubilisation [g/g], [wt%]
DS_j	Degree of Solubilisation after treatment step j [g/g], [wt%]
E_a	Energy of Activation [J/mol]
$E_{a,i}$	Energy of Activation of compound i [J/mol]
$k_{1,0}$	Preexponential factor
k_1^n	Rate constant for hemicellulose solubilization for reactorion order n
k_i	Reaction rate constant for substrate i [1/s], [L/mols], [g/gs]
L/D	Reactor length to diameter ratio [-]
L/S	Liquid to solid mass ratio [g/g]
M	Mass
m	Number of pretreatments [-]
M_{dryBM}	Mass of dry biomass
$M_{dryBM,in}$	Reactor output of dry solid biomass [kg/h]
$M_{dryBM,out}$	Reactor input of dry solid biomass [kg/h]
M_{HC}	Mass of hemicellulose in the solid [kg]
M_{LCB}	Lignocellulosic biomass mass flow [kg/h]
M^s_j	Mass of solids after treatment step j
$M^s_{j,0}$	Mass of solids in treatment step j at t=0
n	Reaction Order
n_{exp}	Number of experiments [-]
N_t	Number of tubes per reactor (SCR) [-]
R	Universal gas constant [J/K mol]
R_0	Severtiy
$R_{0,i}$	Severity of single step, if several are involed
R^2	Coefficient of determination [-]
Rec	Recovery [g/g], [wt%]
Rec_i	Recovery of compound i [g/g], [wt%]
$Rp_{0.2}$	0.2% offset yield strength [Mpa]
S_0	Severity Factor [-]
s_{min}	Minimum reactor wall thickness [mm]
T	Temperature [°C]
t	Reaction time / residence time [min]

T_g	Glass Transition Temperature [°C]
V_r	Reactor volume
w	Mass fraction [g/g], [wt%]
w_i	Mass fraction of compound i [g/g], [wt%]
X	Conversion
x	Reactor performance variable
x_a	Reactor performance variable worst value
y_a	Reactor performance variable normalized worst value
X_{HC}	Conversion of Hemicellulose [g/g]
x_w	Reactor performance variable best value
y_w	Reactor performance variable normalized best value
Y	Yield [g/g], [wt%]
y	Recycling factor [g/g], [-]
Y_i	Yield of compound i [g/g], [wt%]
y_i	Reactor performance variable normalized value

Greek Symbols

Symbol	**Word**
κ	Ratio of reaction rate constants [-]
ρ_{LCB}	Lignocellulosic biomass density [kg/m^3]

Abbreviations

AA	Acetic acid
BMBF	Bundesministerium für Bildung und Forschung
CSTE	Continuous Stirred Tank Extractor
CTR	Continuous Tubular Reactor
EH	Enzymatic Hydrolysis
ENEA	Italian National Agency for New Technologies, Energy and Sustainable Economic Development
FA	Formic acid
HC	Hemicellulose
HMF	5-Hydroxymethylfurfural
IUE	Institute of Environmental Technology and Energy Economics
LHW	Liquid hot water
min	Minutes
NREL	National Renewable Energy Laboratory
PFR	Plug flow reactor
PID	Proportional- integral- derivative controller
rel. Error	Relative error
RMSE	Root mean square error
RS	Reducing sugars
RTD	Residence time distribution
SCR	Screw conveyor reactor
SEC	Size exclusion chromatography
SEM	Scanning Electron Microscopy
SF	Severity Factor
SSF	Simultaneous saccharification and fermentation
st. Dev	Standard deviation
TUHH	Hamburg University of Technology (ger.: Technische Universität Hamburg)
TVT	Institute of Thermal Separation Processes
UMSP	UV Microspetrophotometry
WKI	Fraunhofer Institute for Wood Research Wilhelm-Klauditz-Institut
XOS	Xylo-Oligosaccharides

1. Introduction

Crude oil, natural gas, and coal-based chemical products contribute substantially to greenhouse gas emissions through production, transportation, refining, distribution, and disposal. A feedstock change to plant-based materials will mitigate global warming and environmental pollution if done right. Bioenergy, using plant-based fuels and heat sources, is a feasible method to lower the specific carbon dioxide emissions in heat, power, and transportation applications in a short-term manner. However, it is doubtful that it can be a major energy source due to the small amount of available plant matter and ethical concerns when edible or forest biomass is converted to biofuels. The insufficient supply argument does not apply to bio-based chemicals at all.

The chemical industry used 18.1 Mt fossil resources representing 87.0 % of the feedstock in Germany in 2017 [1]. Renewable resources take a minor role in the feedstock supply with only 2.7 Mt (13.0 wt%) [1], even though the potential is enormous: In 2017, 45.3 Mt of cereal grains were produced in Germany [2], resulting in a similar amount of cereal straw [3], which is a non-edible agricultural residue. This group of raw materials is called second-generation (2G) biomass, meaning derived from harvest residues in contrast to the use of energy crops directly (1G). Straw and other lignocellulosic materials like saw dust contain approximately 70 % carbohydrates, which can be converted to a large variety of chemicals via chemical or biological catalysis such as fermentation. The current use of cereal straw is animal bedding and soil improvement, thus lowering this material's availability for biorefining processes. Cereal straw is an abundantly available potential raw material for chemical production, and its production and use raise no ethical concerns. However, this potential raw material for biochemicals remains largely untapped. The main reason for higher specific production costs of 2G chemicals compared to petro-chemical routs is caused by externalization of environmental costs [4]. Another reason is the lack of efficient and scalable processes to fractionate the second-generation plant materials into steady and homogenous streams of valuable molecules for the chemical industry. Of the three lignocellulose biopolymers, lignin, hemicellulose, and cellulose, only the latter is used in the first commercial biorefineries producing lignocellulosic ethanol as car fuel by-mixtures. Other compounds are bioenergy for the plant, sold in low valorization pathways.

Further development is the catalytic conversion of lignocellulosic ethanol to chemicals. A strategy to turn 2G biomass into chemicals is using efficient fractionation processes that provide all three biopolymers in a high quality sufficient for chemical applications. Although under development, such processes do not exist yet but are critical to facilitate a feedstock change to renewables. Current limitations are the energy demand and product qualities. However, the rising demand on lignocellulosic material is expected to increase the substrate costs in the future. Thus, companies are motivated to turn a higher percentage of the substrate into high-value products. Full-fractionation processes that are efficient regarding space and expenses of energy and investment are critical for future developments.

This work focuses on developing economically relevant 2G full-fractionation processes. Therefore, the main criteria are energy, chemicals, and water consumption, scalability, and product quality. The methods are applied to wheat straw as a representative of the group of annual lignocellulose.

2. Fundamentals and state of the art

This chapter describes the fundamentals of biorefineries, relevant reference processes, and the theoretical basis for this work.

2.1. Second generation biorefineries

The primary refining of lignocellulose into its main constituent, cellulose, hemicellulose, both carbohydrates, and lignin, can be achieved with enzymatic hydrolysis of cellulose to glucose. Before, the enzymatic digestibility must be increased in a pretreatment step by removing the hemicellulose to increase the accessibility of cellulose to enzymes [5,6]. In industrial processes, dilute acid or severe acid-free direct steam heated methods are used.

2.1.1. Lignocellulosic materials

To produce starch-rich grains from wheat (*Triticum aestivum*) for human nutrition, similar straw mass is produced [7,8]. Wheat straw is an agricultural by-product consisting of dried stems and leaves. It is categorized as lignocellulosic material since it mainly contains structural components of the plant cell wall: cellulose, hemicellulose, and lignin. A typical composition of wheat straw is displayed in Fig. 2-1. Since straw is yearly re-growing from seeds, it belongs to the group of annual lignocellulose in contrast to woody-biomass. Annual lignocellulose, i.e., other cereal straw, rice straw, bagasse, and corn stover, is produced in large quantities on every continent. Yearly, 40 Mt of wheat grains and, thus, wheat straw is produced in Germany, and 240 Mt in Eastern Europe. Due to other uses, e.g., animal bedding and soil improvement, it is estimated that one-third or 13 Mt/a of wheat straw is available for chemical processing in Germany [7–9].

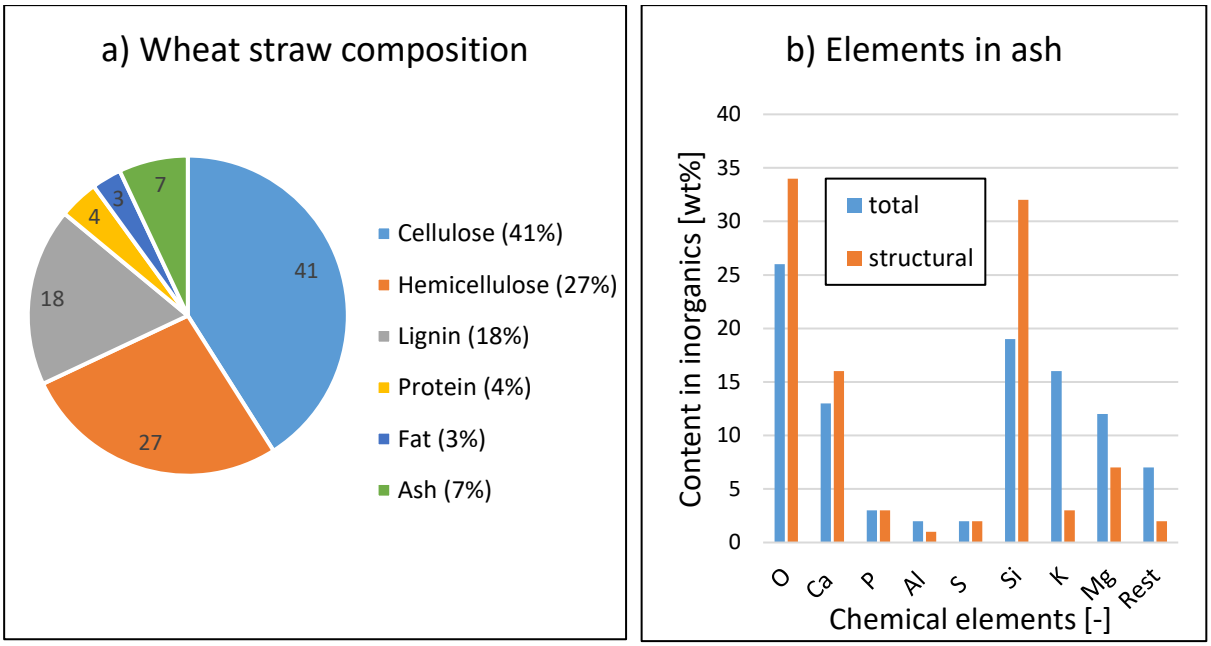

Fig. 2-1: Compositions of annual lignocellulose, **a)**Typical mass fractions in wheat straw *[10]*, **b)** chemical elements in inorganics (ash) in corn stover *[11]*.

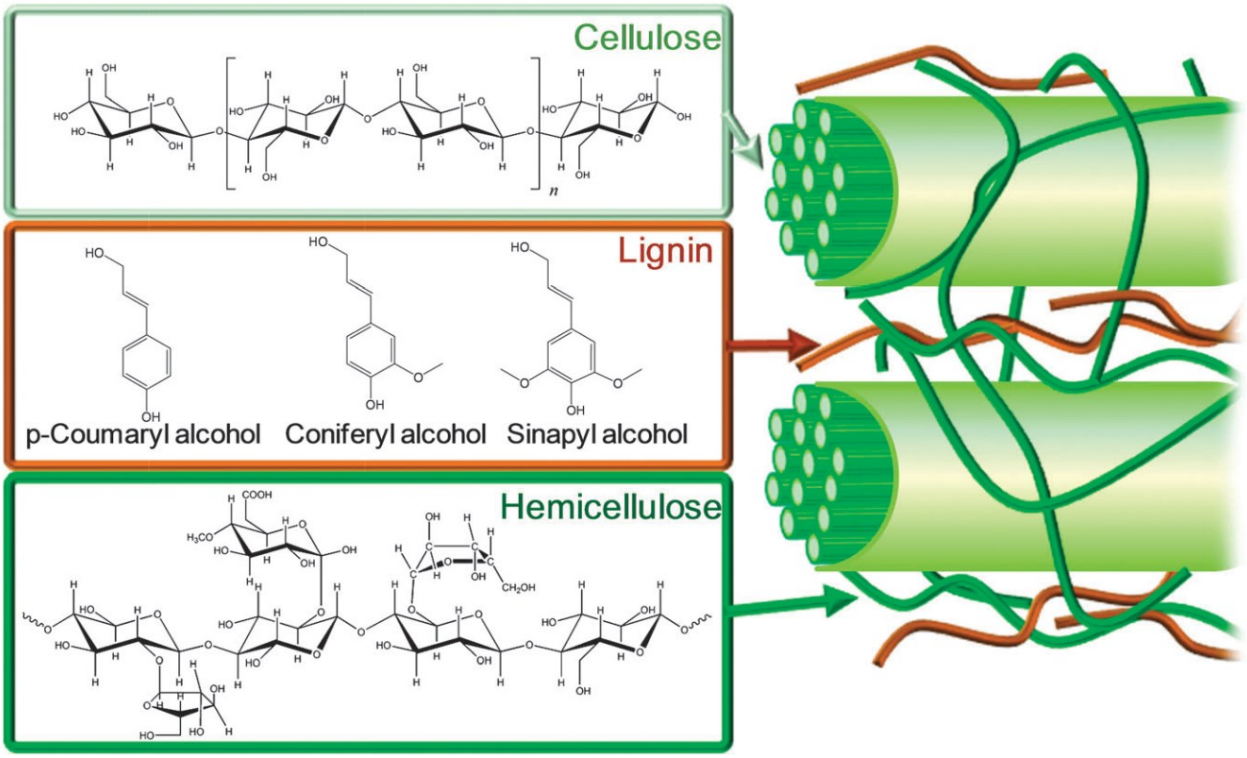

Fig. 2-2: Cell wall structure of lignocellulosic biomass with cellulose, hemicellulose, and lignin represented. *[12]*

The biomass cell wall consists of several layers with different compositions. The three biopolymers are finely interwoven on a nanometer scale, providing mechanical strength and an immense resistance to the biological decay, called biomass recalcitrance, to the plant, see Fig. 2-2. The following summary of the main contituents properties are discussed in [12–14].

Cellulose consists of β-D-glucopyranose subunits linked to each other via β-(1,4) glycosidic bonds. The fundamental repeating unit is cellobiose. The unbranched cellulose chain in the biomass is composed of 500-1400 D-glucose units. These units are arranged to form microfibrils, composing crystalline and amorphous sections. Hydrogen bonds between parallel polymer chains induce the high tensile strength of crystalline sections. In contrast, starch is a glucose-based biopolymer but linked with α-(1,4) glycosidic bonds and can form coils.

Hemicellulose is a branched and acetylated heterogeneous biopolymer. It contains randomly distributed pentoses (xylose and arabinose) and hexoses (glucose, mannose, galactose, and rhamnose). Xylan, xyloglucan, mannans, and glucomannans are various monomer subunits. Xylan is the most frequent subunit made from β-(1,4) glycosidic bonds of D-xylanpyranose. It has an amorphous structure and is known to contain little physical strength. The degree of polymerization of hemicelluloses ranges between 100-200 units. The plant cell wall hemicellulose forms hydrogen bonds to cellulose and covalent bonds to lignin, creating a rigid matrix. It is known for restricting the accessibility of enzymes.

Lignin is the second largest available organic compound in nature. It consists of phenyl propane units called monolignols, including p-coumaryl alcohol, sinapyl alcohol, and coniferyl alcohol, containing hydroxyl, methoxyl, and carbonyl functional groups. The units are connected with C-C and C-O-C bonds. The amorphous polymer’s structure is highly complex and hydrophobic. The aromatic compounds introduce resistance to pathogens.

The solid residue remaining after incineration is called ash. It consists of minerals, e.g., SiO_2 and metal salts [15], and will thus, be called inorganics in the following. The inorganics can be divided into structural and extractable components, see Fig. 2-1b. The first is incorporated in the cell wall structure; the latter adheres on the surface and is derived from soil [16]. Depending on the soil type weather conditions, the content of the extractable inorganic can vary [15]. Some inorganics can buffer the pH via cation

exchange [17,18], and feedstock washing with water is directly correlated with a drop in cation exchange capacity and the acid buffering capacity [15].

2.1.2. Enzymatic hydrolysis

Enzymes are biological catalysts. In enzymatic hydrolysis (EH) of pretreated lignocellulose, enzymes accelerate the cleavage of glycosidic bonds of cellulose and hemicellulose consuming water. The hemicellulases and cellulases, initially dissolved in water, adsorb on the biopolymers suspended in water [19]. The solid polysaccharides are converted to water-soluble monomers. The spatial accessibility of the cellulose, which is low in raw lignocellulose, is the main limitation for the conversion [20]. Pretreatment increases the surface area of the biomass, removes hemicellulose, and relocates lignin increasing the accessibility of cellulose. If accessible, remaining hemicellulose can be removed via EH to increase the accessibility of cellulose and vice versa. Thus, pretreatment is crucial to overcome the lignocellulose's inherent recalcitrance [20]. Several commercial enzyme mixtures are available, with optimal pH and temperature. Limitations for the hydrolysis rate are the enzyme inhibition by the product or by non-productive adsorption to the biopolymer lignin [21]. The development of enzymes mixtures results in a steady improvement in enzyme inhibitions, activity, and costs [22].

The EH can be conducted in a stirred tank with the initial water content controlling the transportation of enzymes to the polymer surfaces. A high water content dilutes the resulting monomers; a low water content prohibits sufficient contact of polymers and catalysts; thus, the initial water content is optimized for the regarded pretreated material. This trade-off can be avoided by starting with low solid content and adding more solids after particle dissolution starts. The technique allows to operate with suspended solids at any time and reach high final monomer concentration and is called fed-batch EH [23]. After EH, the suspension can be subjected to solid-liquid separation to gain a monomer-rich liquid and a stream containing lignin-rich solids. If the monomers are directly converted to fermentation products in the same vessel, the process is called simultaneous saccharification and fermentation (SSF). This technique is frequently used in the 2G- lignocellulosic ethanol production [24,25].

2.1.3. Autohydrolysis pretreatment

There are many pretreatment processes, such as alkali swelling, acid hydrolysis, and ionic liquid dissolution [26–28]. In the following, the mechanism of autohydrolysis pretreatment is described.

The hemicellulose chains are cleaved and their fragments are dissolved under acidic conditions. Without additional chemicals other than water, this process is called autohydrolysis and is conducted at higher temperatures. Thereby the autoprotolysis equilibrium constant of water is increased, raising the concentration of protons and hydroxide ions [29]. Under these conditions, the acetylated side groups of the hemicellulose are cleaved, releasing acetic acid lowering the pH. Thus, the acid-catalyzed hydrolysis of hemicellulose is accelerated. The biomass is (self-) auto hydrolyzed.

Hemicellulose is the most thermo-chemically sensitive compound in lignocellulose [26]. The hemicellulose content in the solids can be lowered from 27.4 wt% to 0,7 wt% by hydrolysis [30]. The chemical and structural features of the residual hemicelluloses after hydrothermal pretreatment are altered, i.e., the molecular weights exhibited a significant reduction of 60-75% [31].

Lignin strongly contributes to lignocellulose recalcitrance in the plant cell wall [20]. Depending on the difference of pretreatment and glass transition temperature (T-Tg), the lignin turns into a fluid-like state; subsequent cooling will cause the lignin to relocate within and on the cell wall material, and simultaneously, a small amount of lignin will dissolve in hot water [32–34]. The lignin relocation improves the accessibility of cellulose to enzymatic attack. The lignin removal depends on the biomass, process conditions, and reactor type [5]. Due to the cleavage of β-O-4 linkages in lignin, a decline of molecular weight is observed in mild pretreatment conditions before the recondensation reaction becomes more dominant [35,36].

The hemicellulose is hydrolyzed to shorter segments down to the monomers. Since some of the oligomers (2-100 units) are soluble in water, their presence can be detected in the hydrolysate (liquid fraction) early [29]. A fraction of the hemicellulose oligomers is the xylooligosaccharides (XOS) which are especially valuable for several processes. The oligomer concentration drops under more severe pretreatment to give

rise to organic acids, further lowering the pH, and monomers xylose, arabinose, and glucose. In the autohydrolysis conditions, the pentose and hexose cannot be further hydrolyzed but dehydrated forming furfural and 5-(hydroxymethyl)furfural (HMF), respectively [37]. Furfural does not accumulate in the liquid phase. Known furfural loss reactions are furfural-furfural-resinification and furfural-pentose condensation [38]. Both reactions form a polymer that can cover the remaining lignocellulose; thus, hindering the extraction and EH. In acidic conditions, pentose can condensate with lignin-derived aromatics to form another non-soluble polymer, called pseudo-lignin, that can be deposited as micro-spheres on the lignocellulose structure [39,40].

2.1.4. Kinetics modelling

The mathematical description of the hemicellulose hydrolysis rate in dependence of the remaining polymers content, the temperature, and the pH, called chemical kinetics, is an essential tool for designing lignocellulose pretreatment reactors. In the following, the rate-based models and the severity factor are described. A comprehensive overview of hemicellulose hydrolysis models is given by Ruiz [14].

Saeman first described the hydrolysis rate of non-water-soluble cellulose in 1945. Using the mathematical assumption that the reaction partners of the irreversible reaction, cellulose, and water, are in the same physical phase, the mass of the polymer is tuned into a concentration [41]. This allows the use of Arrhenius type rate models, here called pseudo-homogeneous first-order kinetics. This model was also applied to hemicellulose hydrolysis, considering xylan and oligomers as a individual components. The models are helpful but overestimate the reaction rate at high xylan conversions; thus, the xylan is divided into two groups with individual reaction rates. This model using a fast-reacting and slow-reacting fraction is called a bi-phasic model. A better fit to experimental data is allowed but more parameters are introduced.

For selected lignocellulose, the reaction time and temperature are the most critical process parameters in autohydrolysis pretreatment. Overend et al. [42] introduced an expression for the process severity based on the reaction time in minutes and the temperature in degrees Celsius, see equation (2-1). For isothermal reactors, the integral simplifies to an arithmetic expression that is most useful in its logarithmic form, here called severity factor (SF) S_0, see equation (2-2). The severity factor allows to plot conversion data from a wide range of temperature and residence times as a continuous function, see Fig. 2-3 [43].

$$R_0 = \int_0^t exp\left(\frac{T(t) - 100}{14{,}75}\right) dt \tag{2-1}$$

$$S_0 = \log_{10}(R_0) = \log_{10}\left(t[min] * exp\left(\frac{T[°C] - 100}{14{,}75}\right)\right) \tag{2-2}$$

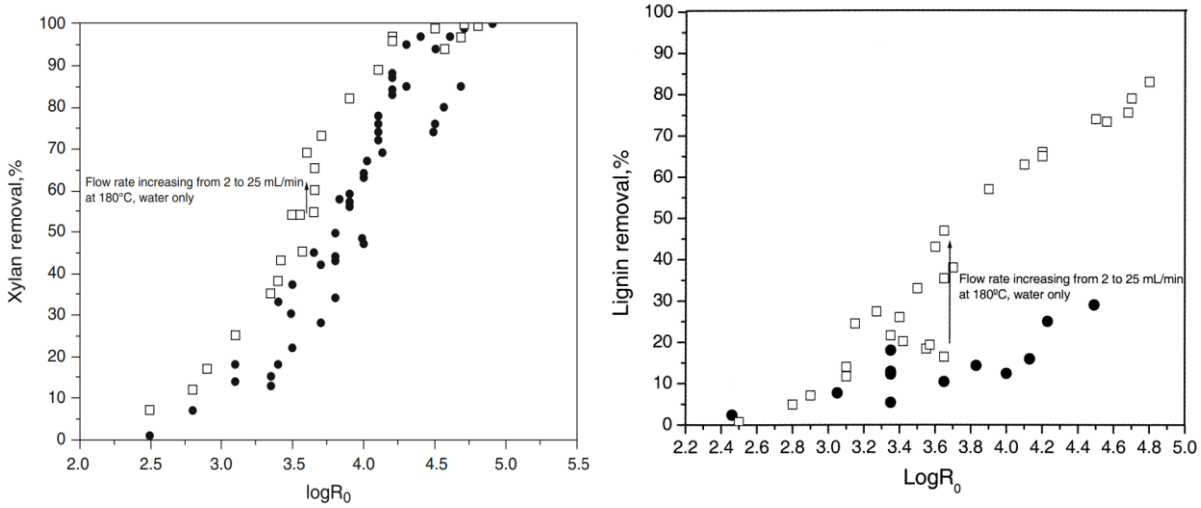

Fig. 2-3: Effect of severity factor on **(left)** xylan removal and **(right)** lignin removal for batch tube and flowthrough pretreatment of corn stover at 160-220 °C with water only, **filled circle)** batch tube at a 5% solid concentration, **open square)** flowthrough reactor at flow rates of 2-25 mL/min. [43]

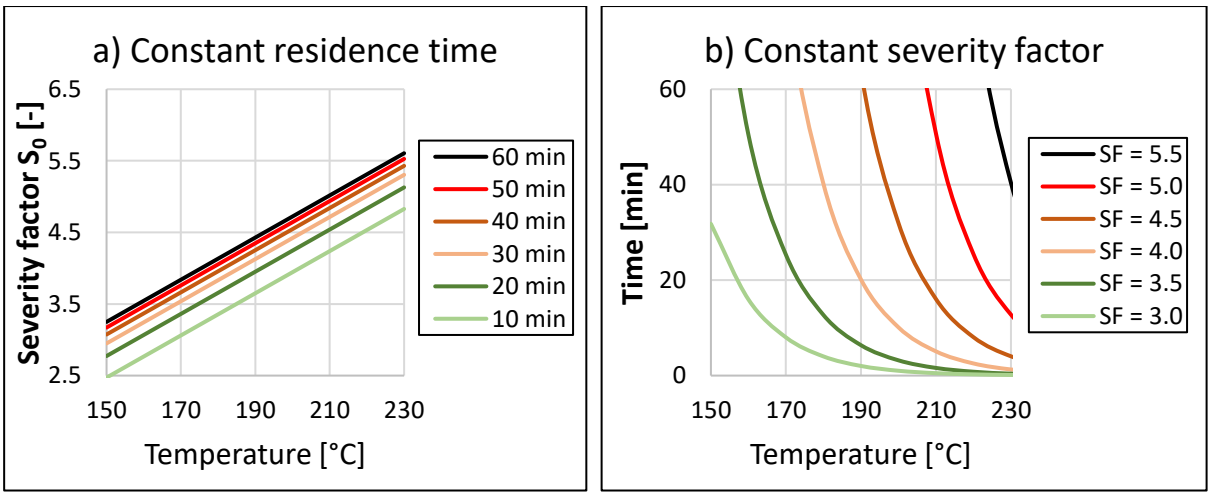

Fig. 2-4: Severity factor maps, **a)** Effect of temperature on the severity factor for different times, **b)** Effect of temperature on time for different severity factors. (SF= Severity factor).

The severity factor possesses a linear dependency on the temperature, see equation (2-3) and Fig. 2-4a. At a constant temperature, the residence time's effect on the SF drops rapidly with increasing residence time, see Fig. 2-4a. Depending on changing

temperature and/or time, the change in severity factor can be calculated using equation (2-4). If the severity factor plot results in a continuous function, each temperature has a matching residence time to result in the same severity factor, see equations (2-5) and (2-6). At a constant severity factor, a ten degrees increase in temperature leads to a halving of the residence time, see Fig. 2-4b.

$$S_0 = log_{10}(R_0) = log_{10}(t[min]) - 2{,}94 + 0.0294 * T[°C] \quad (2\text{-}3)$$

$$S_{0,2} - S_{0,1} = log\left(\frac{t_2}{t_1}\right) + \frac{(T_2 - T_1)}{33.96} \quad (2\text{-}4)$$

$$\frac{t_2}{t_1} = 10^{\frac{-(T_2 - T_1)}{33.96}}, \ for\ S_{0,2} = S_{0,1} \quad (2\text{-}5)$$

$$t = R_0 * exp\left(\frac{T[°C] - 100}{14{,}75}\right)^{-1} = 10^{S_0} * exp\left(\frac{T[°C] - 100}{14{,}75}\right)^{-1} \quad (2\text{-}6)$$

2.2. Pretreatment reactors

Several reactors for the autohydrolysis pretreatment are presented in literature, including designs aiming at a full-fractionation of annual lignocellulose. A comprehensive description can be found in Ruiz et al. [6].

2.2.1. Batch reactors (LHW and steam)

The batch reactor is the most common type and is operated in different scales from bench-scale (0.025 – 3 L) and pilot-scale (15 – 350 L). The reactor is loaded with liquid water and lignocellulose particles then heated. The process is called liquid hot water (LHW) when the biomass is suspended. Often gaseous nitrogen is used to introduce pressure and allow liquid water above 100 °C [44]. In LHW, the heat is introduced via an oil or electrical jacket or a heated fluidized sand bath. With low heat transfer rates, the process can be operated in non-isothermal conditions, increasing the temperature with sudden cooling, reaching the temperature set point. LHW heat transfer is faster if stirring at low solid concentrations is possible. Isothermal reactors remain at the temperature set point for the reaction time, then cooled. This setup is ideal for screening and kinetic studies and challenging for a scale-up. The co-processing of

water results in large space demand, diluted product, and high heat demands. Due to the immense heat capacity of liquid water (4.2 kJ/(kg K)), suspended systems face a tremendous heat demand per kg of initial biomass [45].

Direct saturated steam injection into a reactor filled with moist biomass results in faster heat transfer rates, lower energy demand and more concentrated products. Additionally, temperature control, often challenging, simplifies to controlling the pressure in the vapor phase. The pressure release can be done slowly, and the vapor can be condensed. The vapor and condensate will contain volatile compounds, like acetic acid and furfural. Furfural has a higher boiling temperature than water and becomes more volatile when mixed with water. Water and furfural form an azeotropic mixture with a higher furfural concentration in the vapor phase than water for the pretreatment relevant furfural concentration in the liquid phase [46]. A sudden pressure release into a blowdown vessel called steam explosion facilitates the phase change of intracellular water, disrupting cell walls. Thus a particle size reduction is added, improving the enzymatic digestibility.

All batch processes show the disadvantage that a simultaneous high conversion a high yield of the hemicellulose is impossible.

2.2.2. Semi-batch (Flow-through reactor)

A flow-through pretreatment without the addition of chemicals was first patented in 1968 by Ortwin Bobleter and Gerhard Pape [47]. The flow-through reactor (FTR) inherits an in-situ product removal to reduce or avoid its degradation. In the FTR, biomass is retained with gasket filters or sieves, while hot water is pumped through. Thus, a fluid residence time shorter than the solid pretreatment time is achieved. Moreover, the hot water simultaneously induces the autohydrolysis and extraction of the solubilized but thermally labile sugar products. The pressure is induced either by pressurizing with cold water or gaseous nitrogen. In the second half of that century, various materials were fractionated in laboratory-scale FTR reactors [48]. The hot water flow profile is commonly constant and upward in a vertical reactor. Several approaches were tested to reduce the water to liquid ratio and energy demand. Stepwise, fully or partially recirculated, flow profiles were presented [5,45].

A large variety of materials have been tested successfully using the FTR, including softwood and hardwood [49,50], straws [5,51,52,52,53], and other lignocellulose

biomasses from and food industry [54]. A one-liter scale reactor was first operated by Ingram et al. in 2009 [51]. The research group at the Hamburg University of Technology proposed using a cartridge for fast loading of a 3 L and 40 L FTR [52,55]. In 2014 Kilpeläinen et al. presented a scale-up to a 300 L reactor, which is the largest size published today [50]. The sawdust is first heated with direct saturated steam injection, then extracted with hot water.

The reactor's spatial productivity can be improved by densely filling the reactor, e.g., with pelleted, bracketed, or finely ground (particle size < 500 µm) biomass. A too dense biomass bed causes a massive press drop, further compacting the bed leading to an abortion of the process [56,57]. This behavior was reported for bagasse and wheat straw but not with more rigid ground softwood and hardwood.

The strengths of the FTR are the high yield of hemicellulose-derived sugars and the high enzymatic digestibility of the pretreated solids. The latter is due to almost complete hemicellulose solubilization, high lignin particle removal by fluid drag [43,57], and avoidance of condensation reactions [29]. Successful full-fractionation processes are in a small scale (< 1 L) and show substantial hot water consumption (L/S = 45 - 390) [48,49,53,58]. Larger scale reactors (3 – 300 L) with reduced water consumptions (L/S = 9 - 22) show hemicellulose yields (47 – 77 %) [50,52] with no or minor improvements compared to batch.

The thermal energy of the hot effluent can be partially recycled to preheat the inlet water. However, the dilute hydrolysates require energy in concentration steps, such as evaporation.

2.2.3. Continuous reactors (SCR and PFR)

Continuous, isothermal steam pretreatment with or without steam explosion can be conducted in a screw conveyor reactor (SCR). It is also called horizontal digester, Pandia digester, and continuous tubular reactor. The SCR is horizontal and tubular, designed for annular lignocellulose. A conveyor screw moves the biomass through a pressurized saturated steam atmosphere from one end to the other without exerting mechanical treatment. In Fig. 2-5a, reactor design for the first reported industrial operation and an illustration of the peripheral equipment are displayed. Today engineering and plant design solutions based on SCR autohydrolysis are supplied by companies like Andritz, Valmet, Metso, AdvanceBio Systems, and others on pilot and

industrial scales [25,59]. In the following, the feeding techniques, the conveying theory, the release systems, and the SCR limitations are summarized.

A comprehensive literature selection on high-pressure biomass feeders can be found at Dai et al. [60]. The feeding of the biomass into the reactor requires preliminary conditioning. A pre-steaming hopper is applied for wood chips preheating, moisturizing the biomass, and replacing entrapped air. Non-woody biomass requires a water mixing stage; air can be removed here. Preheating reduces steam consumption and reactor pressure fluctuations in the SCR. The devices used for SCR are realized as plug-forming machines based on a screw or a reciprocating screw. The material is metered and dosed into the screw feeder, where it is compressed to form a gas-tight plug. This apparatus can be equipped with a mechanical dewatering section, where air can escape too. The plug is pressed through a narrow channel called the throat. The outlet of the throat can be closed by a hydraulic piston called a choke or blowback preventer. The biomass is only released into the reactor when the axial force is high enough to move the plug along the throat, pushing the piston again air pressure. The blowback preventer aids in forming a dense plug. It limits the risk of a steam blowback, reduces the blowback flow, and promotes plug breaking. Blowback preventers can be designed with a conical tip for improved performance. The throat can be equipped with knives in flow directing to improve plug breaking.

Once entered into the reactor, the biomass bulk is moved toward the exit by a conveyor screw. The screw flights form segments that are not mixed; thus, a narrow residence time distribution can be achieved. The volumetric filling degree is the critical parameter affecting the throughput and the residence time distribution [61,62] and is optimal around 40 %. A too high volumetric filling degree of the reactor leads to a back-slipping of material: The flights do not separate the biomass into chambers; instead, fractions of a chamber fall over the shaft into the previous chamber; thus, the RTD is widened [61]. The slip of biomass through the gap of screw and wall is getting relatively larger for smaller filling degrees [62]. Thus, the optimal filling degree should be as high as possible and as low as required to prevent a falling to the previous chamber.

Several techniques can be applied to release the treated material from the pressurized reactor to atmospheric pressure. The hot blow pressure release is a semi-continuous steam explosion [59]. Here, the material drops into a vertical tube at the end of the reactor. Two valves form a lock that periodically releases the material into a blow line.

The rapid pressure drop causes the hot water to evaporate and accelerate along the blow line into a cyclone, where solids and vapor are separated. The hot blow can also be realized with a compression screw and a single valve [63]. For the cold blow technique, water is introduced into the vertical pipe to quench the mixture below 100°C. One ball valve releases the slurries exploiting the high reactor pressure.

The convertibility of results from lab-scale equipment to a continuous, scalable scale reactor is of great interest. It was successfully shown using the severity factor for corn stover in dilute acid pretreatment [64] and hardwood in autohydrolysis pretreatment [63]. The optimal parameters in LHW resulted in at least near-optimal parameters for the SCR.

The limitation of the screw conveyor reactor lay in the challenges to producing experimental data. The scale-down of the reactor to laboratory sizes is not possible. Depending on the producer, the smallest reactor types show nominal throughputs of 50 - 2000 kg/h [52,56,58–69]. The dense biomass plug in the feeding device acts as a dynamic pressure seal. Its rupture leads to blowback of the reactor content. Thus, the feeder operation requires careful optimization for each processed material. Also, installations are required to prevent damages in a blowback event. A blowback pipe attached to the feeder can lead the accelerated material to a cyclone to separate solids and safely release steam to the top. Optimal operational parameters, e.g., screw speed and pressures, must be adapted to each material. The formation of volatiles like furfural and acetic acid may require a gas purge. This is more likely for cold-blow since steam leakage is prevented. Abrasive feedstock, e.g., straws and bagasse, leads to increased wear in the plug feeder; thus, the requirement for the hardness of the construction steel and the maintenance is high.

To this day, there is no systematic techno-economical comparison of the reactor types. It remains unknown, which concepts show the most potential and what are the drawbacks for an industrial full fractionation process.

a) Furfural production in SCR in 1960s

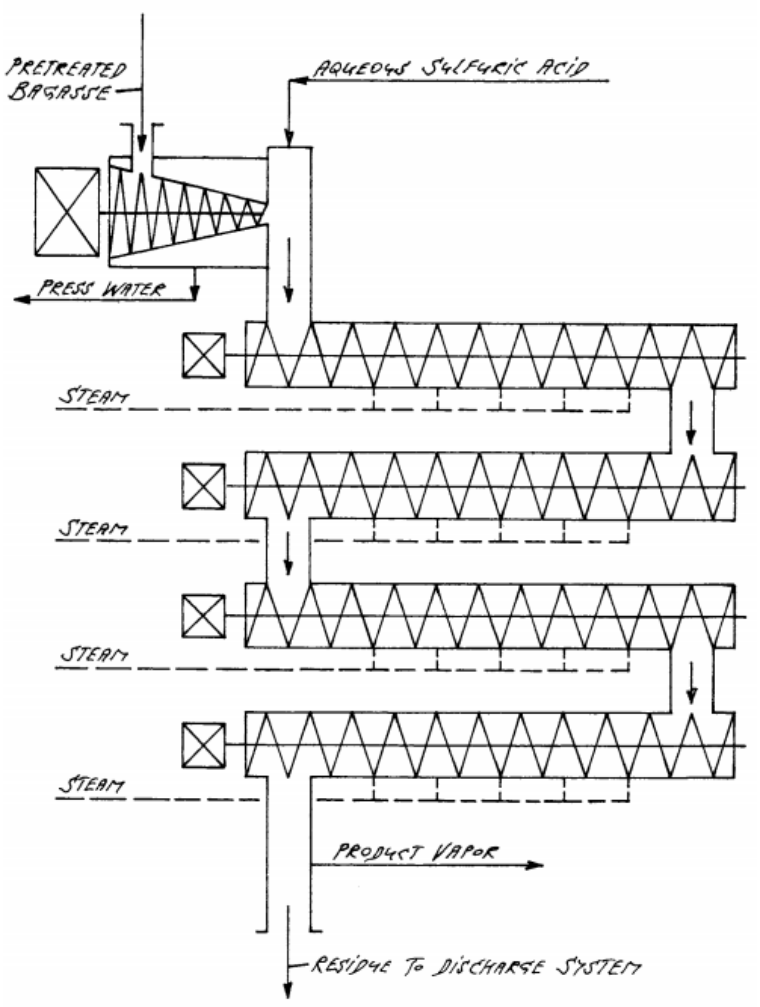

b) SCR and peripheral components

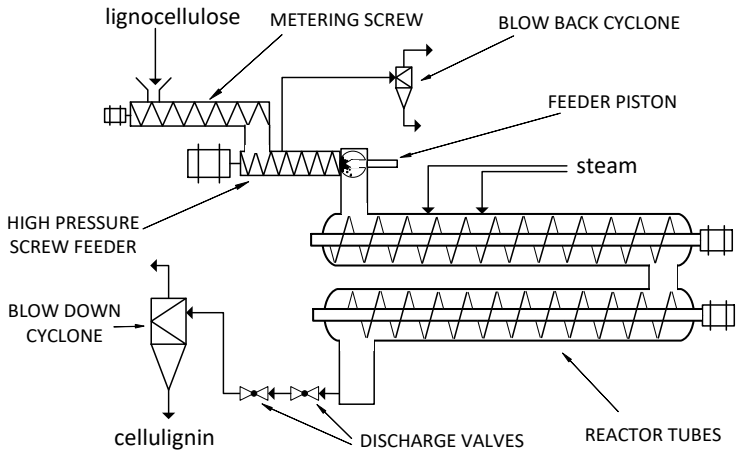

Fig. 2-5: Screw conveyor reactor (SCR), a) from bagasse to furfural processing at 11 bar and *[65]* b) reactor and peripheral equipment *[6]*.

2.2.4. Industrial applications

In the 1960s, the SCR was first used to produce furfural from bagasse by Quaker Oats, replacing a batch process [65]. For this purpose, four reactor tubes were stacked on

top of each other to allow a residence time of one hour, see Fig. 2-5. Several tubes are combined to increase the throughput or residence time. Each tube had a diameter of 1.8 m and a length of 16 m resulting in a total volume of 160 m^3. Each reactor had a throughput of 60 t/h; thus, the nominal capacity is 1.000.000 t/a. Three lines were installed, with two in operation and one available for maintenance. This process ran with sulfuric acid and superheated steam of 650°C at 10.8 bar. The Pandia digester is an SCR used for pulp production from wheat straw and bagasse, using chemical additives [66]. The Canadian company Stake Technology Ltd developed an SCR for the pretreatment of lignocellulose in the 1970s [67]. This technology was further developed to the Stake II pretreatment unit, which was used with and without adding acids in the 1980s 1990s [63,68]. In 2013 a 270,000 t/a annual lignocellulose to lignocellulosic ethanol production plant in Crescentino, Italy, was taken into operation based on the Proesa process. The pretreatment is based on a continuous steam autohydrolysis pretreatment reactor. Clariant developed the sunliquid process based on an SCR to produce lignocellulosic ethanol from wheat straw. The pilot plant was erected in Munich, Germany, and the demonstration plant in Straubing, Germany, with a capacity of 0.4 t/a and 200 t/a wheat straw processing capacity, respectively. The first sunliquid process production plant was finished in 2021 with a 250.000 t/a capacity in Podari, Romania. More plants in Poland and China are announced. The former Danish company Inbicon developed an SCR-based autohydrolysis pretreatment technology using saturated steam in 2008 [69]. This process was based on the IBUS process [70]. This process used two inclined SCRs with counter-current water flow to extract the product in-situ. This measure to increase the yield show low effectiveness or excessive hot water consumption. Only one pretreatment unit was used in the following scale, which was in a full-time operated demonstration plant with wheat straw throughput of 4 t/h (30,000 t/a) [24]. A treatment temperature of 180 - 200°C with a residence time of 5-15 minutes was used. The main product is lignocellulosic ethanol, the hemicellulose stream is converted to molasses and sold as a biogas booster. The company abandoned the operation and sold a license to new energy blue, which designed a plant 275,000 t/a of local crops. The Abengoa Bioenergy Biomass Kansas (ABBK) in Kansas, USA, and the UPM beech wood biorefinery currently under construction in Leuna, Germany, deserve mention.

All degradation products are unwanted for the fractionation performance, and the hemicellulose oligomers and monomers are the desired product in the complex

sequential reaction network. At the same time, a high hemicellulose conversion, thus, removal from the solids is the target to recover it and increase the cellulose's enzymatic digestibility. Undesirable for a full-fractionation, the removal of hemicellulose reaches only a limited conversion before the degradation of the formed pentose monomers begins [71].

In established industrial processes, the degradation of hemicellulose to a large extent is accepted, focusing on the preferred glucose. It shows generally higher biological conversion rates than xylose. The xylan thermal lability allows a xylose degradation to furfural in considerable amounts. Furfural is an inhibitor to several microorganisms [72,73]; thus, purification and detoxification of the hydrolysate are required for many applications. Furfural does not disturb the microbiological collective in a biogas fermenter[74]; thus, this low-value product is a used pathway for hemicellulose hydrolysates.

Another route for hemicellulose use on an industrial scale is the co-substrate fermentation of xylose and glucose to lignocellulosic ethanol. Here, hemicellulose is not separated, but whole-slurry EH and lignocellulosic ethanol fermentation are applied.

There is no process for the selective fractionation of the two carbohydrate sources and lignin on an industrial scale; straw-based xylooligosaccharides' potential is not used.

2.2.5. Sequential reactions

For sequential reactions and reversible reactions, the educt A is converted to the product P and the second reaction converts the product to an undesirable compound, here to the substance C.

$$A \rightarrow P \rightarrow C \qquad (2\text{-}7)$$

For petrochemical and organic reactions, the following chemical engineering solutions can be found in prominent textbooks [75,76], summarized in this section.

Assuming that both reactions are of the first reaction order, the concentration of the product P in a batch reactor can be expressed as:

$$\frac{dc_P}{dt} = k_A * c_A - k_P * c_P \qquad (2\text{-}8)$$

$$c_P(t) = \frac{k_A}{k_P - k_A} * c_{A,0} * [\exp(-k_A * t) - \exp(-k_P * t_P)] \quad (2\text{-}9)$$

For $k_A \sim k_P$ A and P will be present temporarily in similar amounts, and for a high conversion of A, P will also be mainly converted. The Yield of the product Y_P, see equation (2-10), cannot reach 100%.

$$Y_P = \frac{c_p}{c_{A,0}} = \frac{k_A}{k_P - k_A} * [\exp(-k_A * t) - \exp(-k_P * t_P)] \quad (2\text{-}10)$$

The maximum product yield $Y_{P,max}$ is reached if the condition $dY_P/dt = 0$ is true. Here an expression for the maximum yield and corresponding optimum residence time can be derived, which depends on the ratio of the two rate constants:

$$Y_{P,max} = \kappa^{\frac{\kappa}{1-\kappa}} \quad , for\ \kappa = \frac{k_P}{k_A} \neq 1 \quad (2\text{-}11)$$

$$Y_{P,max} = \frac{1}{e} = 0.368, for\ \kappa = 1 \quad (2\text{-}12)$$

$$t_{opt} = \frac{1}{k_P - k_A} * \ln\left(\frac{k_P}{k_A}\right), \quad for\ \kappa \neq 1 \quad (2\text{-}13)$$

$$t_{opt} = \frac{1}{k_P}, \quad for\ \kappa = 1 \quad (2\text{-}14)$$

In Fig. 2-6, the intermediate product yield P is plotted over time for different ratios of k_P to k_A called κ (kappa), based on equation (2-10). Also, the optimal residence time according to (2-13) is displayed. Fig. 2-6b shows the same data with the time converted to the severity factor using the arbitrary temperature T=230°C. It can be seen that the tailoring, maximum curve in the time domain is transformed to a curve similar to a bell shape.

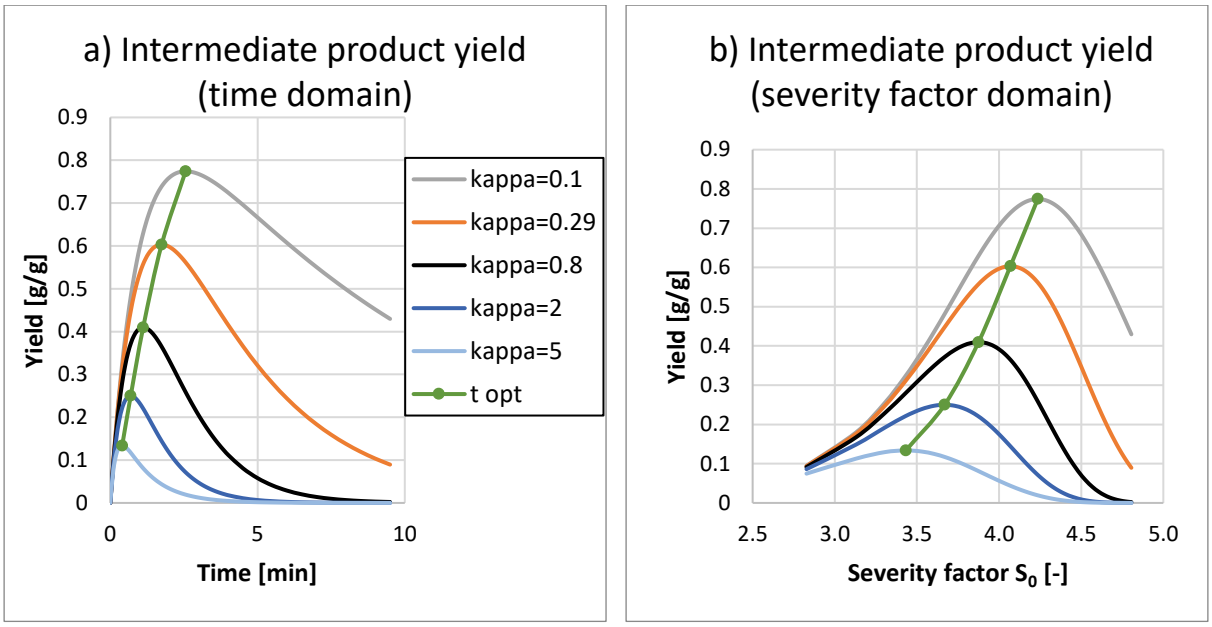

Fig. 2-6: Intermediate product yield and optimal time for k_A=1g/L*min. **a)** time domain (state of the art), **b)** converted to severity factor domain using T=230°C.

Since the reaction time determines the maximum yield for each temperature, a reactor with a sharp residence time distribution, such as a plug flow reactor (PFR) and a batch reactor, is advisable. Using a continuously stirred tank reactor will prohibit reaching the maximum product yield.

The energy of activation determines the dependency on the temperature; thus, the temperature of the reaction can be used to increase the maximum product yield if $E_{a,A} \neq E_{a,P}$ is true. For $E_{a,A} < E_{a,P}$ a low temperature increased the maximum product yield, and if $E_{a,A} > E_{a,P}$, a high temperature increases the maximum product yield. In the first case, the reaction temperature should be as high as possible to increase the conversion rate and the maximal product yield. In the second case, the temperature can be varied along the reactor, starting with a high temperature for an initially fast conversion rate and dropping to increase the maximum product yield.

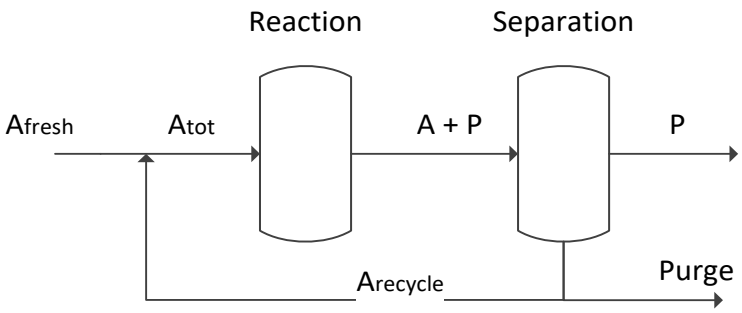

Fig. 2-7: Process layout for reactions with the incomplete conversion of the educt. After the reactor, the remaining educt and formed product are separated into product and educt; the latter is recycled to the reactor. **A:** educt, **P:** product.

Additionally, the plant layout can be adapted to reach a yield higher than the maximum product yield in a single step, see Fig. 2-7. After the reaction, the unconverted educt is separated from the product P and recycled to the reactor. A small purge stream is required to avoid an accumulation of impurities in the feed or other side products.

2.3. Solid-liquid extraction

Extraction is a thermal separation process where additions of a liquid phase separate a compound, compare Fig. 2-8. In solid-liquid extraction, the feed contains a solid and the solute. By contacting feed and solvent, the solute is removed by dissolution or transportation from the pores of the solid carrier. The extract is the liquid containing the solvent and solute. It is separated from the solid residue, called raffinate, by any means of liquid-solid separation. The solvent can be recovered from the extract and raffinate and recycled. The process is also called leaching if the solute is of high value and purified. Solid-liquid extraction is also called washing if the solvent is water and the solute is an unwanted substance. With hazardous solvents, a closed-loop solvent recycling is frequent; with water as a solvent, it can already be contained in the feed, and the recycling is integrated with other water-using processes and much more complex than displayed in Fig. 2-8.

Regarding biomass processing, solid-liquid extraction is used in sugar production from sugarbeet or sugarcane [77,78], production of vegetable oils [79,80], e.g., from soy beans or pressed rape seeds, the washing of cooking chemicals from wood pulp [81], and in biorefineries [82].

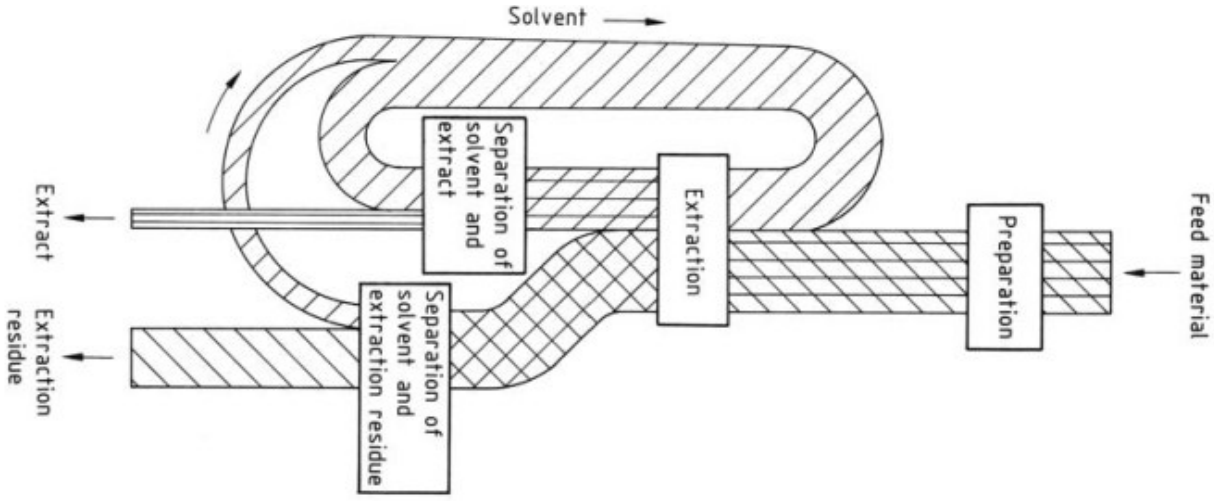

Fig. 2-8: Schematic diagram of liquid-solid extraction, with closed-loop solvent recycling *[83]*.

The feed material is porous and contains capillaries, and is not homogeneous. First, the solvent penetrates the capillary into the feed and dissolves the solute. This can be accompanied by particle swelling. Second, the solute is transported to the particle surface and the liquid bulk phase. The concentration gradient drives the solute mass transport. An equilibrium is reached when the internal and external concentrations are identical. The equilibration time is infinite and economic considerations determine when is process is stopped. High extraction rates are desired; thus, the solvent temperature should be as high as possible due to temperature-dependent viscosity and solubility [83]. Also, the solid should be prepared so that the parts with diffusion-dominant transport are as short as possible [83]. Fig. 2-9 displays the effect of flake thickness in soybean extraction on the extraction rate.

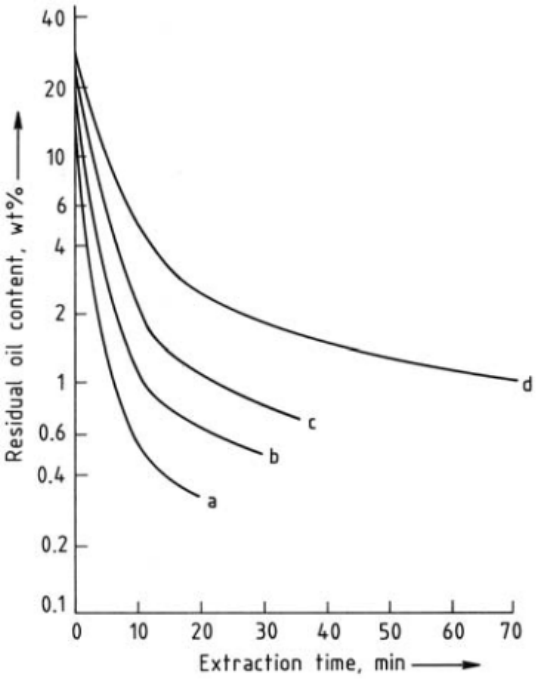

Fig. 2-9: Extraction of soybean flakes of different thicknesses during percolation with hexane. Flake thickness in mm: a) 0.22, b) 0.35, c) 0.43, d) 0.55 *[83]*

2.3.1. Extraction processes

Solid-liquid extractors come in many types, from batch to continuous countercurrent, tailored to the process requirements and applied extraction methods. Extractors can either be one complex apparatus or made from several units. In the following, two extractors from two reference processes are summarized relevant for extraction in biorefineries.

In the pulp washing, cooking chemicals are removed from the wood pulp consisting of liberated and cellulose-enriched fiber cells. The belt extractor in Fig. 2-10 is a counter-current continuous extractor. The suspended pulp feed is transported to a wire mesh that is permeable for liquids. While the forming pulp mat is transported from one end, the solvent/ extract is spayed on top, displacing the suspension liquid. The solute-enriched extract is collected below the belt and sprayed on the mat, a section closer to the pulp feed entry. This way, several stages of displacement washing are realized. The pulp washing operation is illustrated in Fig. 2-11. The displacement of the fluid is far from a plug flow profile due to axial dispersion and diffusion limitation of solute from trapped liquor inside fibers or fiber voids to free-flowing liquor. Thus several stages are required to achieve the desired extraction yield.

The stele process by ENEA, see Fig. 2-12, uses continuous steam explosion processes, followed by a belt extractor to separate the hemicellulose sugars [82]. The pretreatment is rather intensive, forming a biomass slurry. Here the extraction takes place in a suspension, and the belt extractor is used as an additional extractor, allowing high retention of the solid but further diluting the extract. A similarly high severity pretreatment in an SCR followed by belt filter/ extractor was systematically investigated by Sievers et al. in 2017 [84,85]. Experimental results are used to calculate the performance of a belt extractor, see Fig. 2-13. Severe pretreatments result in enormous wash water demands to extract 90% of the sugars (L/S = 15). The authors conclude that low severity conditions are recommended for good belt extractor performance [84].

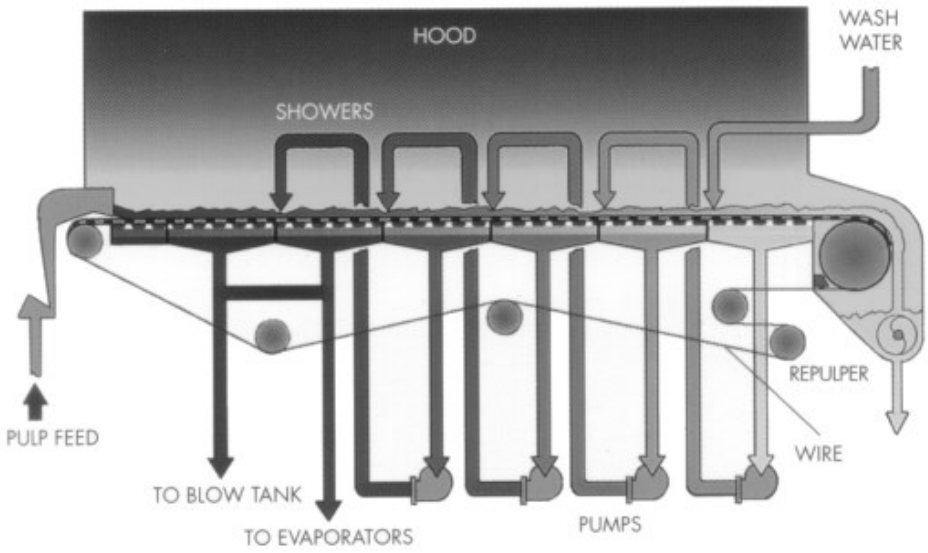

Fig. 2-10: Belt-extractor for pulp washing, countercurrent extraction with displacement washing with pulp mat formation *[81]*.

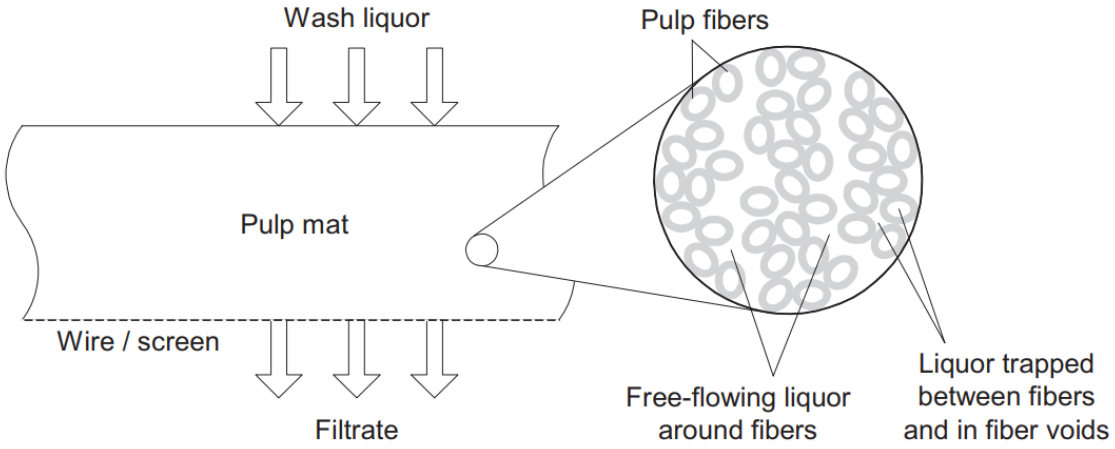

Fig. 2-11: Simplified illustration of the pulp washing operation. Wash liquor is added to the pulp mat, which is retained on the filter medium (wire or screen), and the filtrate is extracted through the filter medium. Right side: Simplified illustration of the pulp suspension, the free-flowing liquor around the fibers, and immobile liquor trapped between the fibers and in the fiber voids *[81]*.

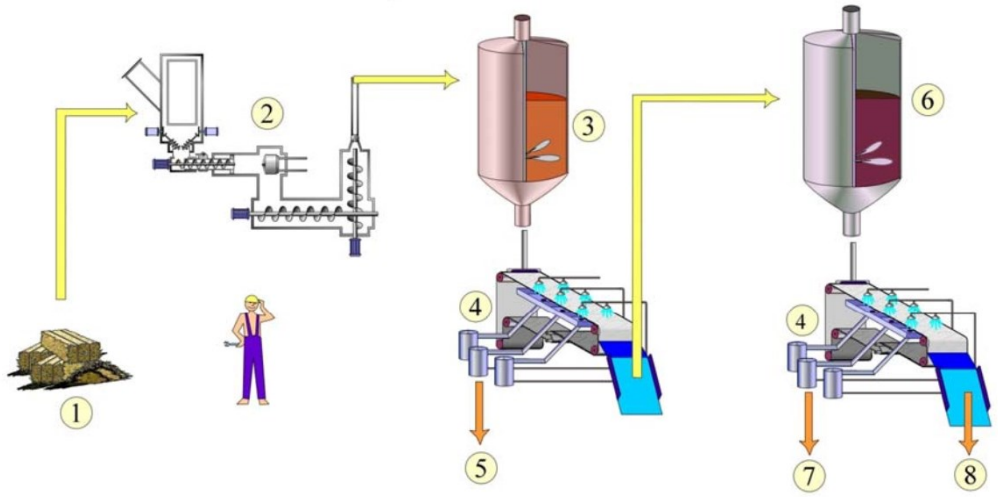

Fig. 2-12: Stele process at ENEA. The biomass (1) is continuously steamed and exploded in the digester (2), then slurried with warm water (3) and filtered with a belt machinery (4) to recover hemicellulose (5). The residue is slurried with alkaline solution (6), then filtered to separate the lignin (7) from cellulose (8) *[82]*.

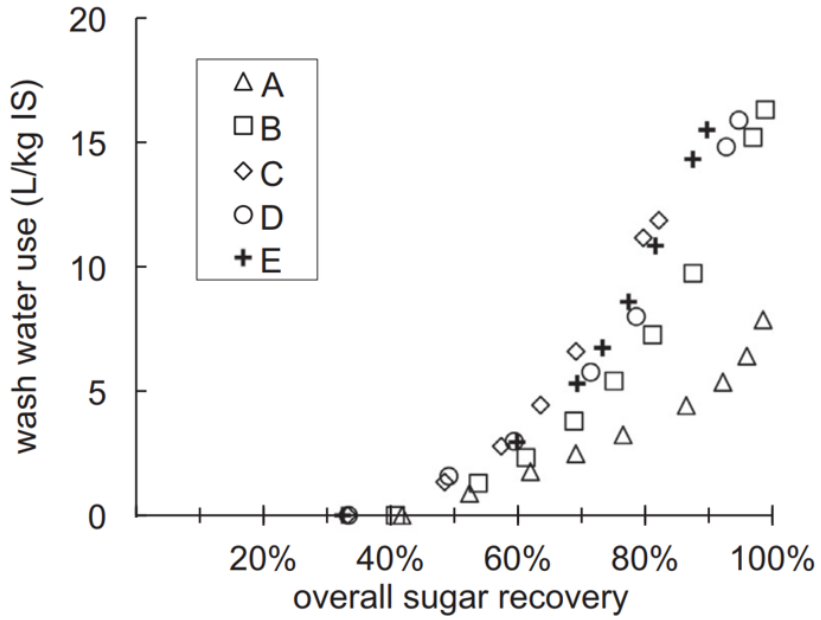

Fig. 2-13: Estimated performance of scaled vacuum belt filter based on VF [vacuum filtration] data. Incoming slurry solute recovery in the filtrate versus cake wash water usage. A-E pretreatment severity in dilute acid pretreatment in SCR. All particle sizes below 110 µm. All xylose feed concentrations below 50 g/L, more than 95 % as monomers, furfural feed concentrations 3 – 12 g/L *[84]*.

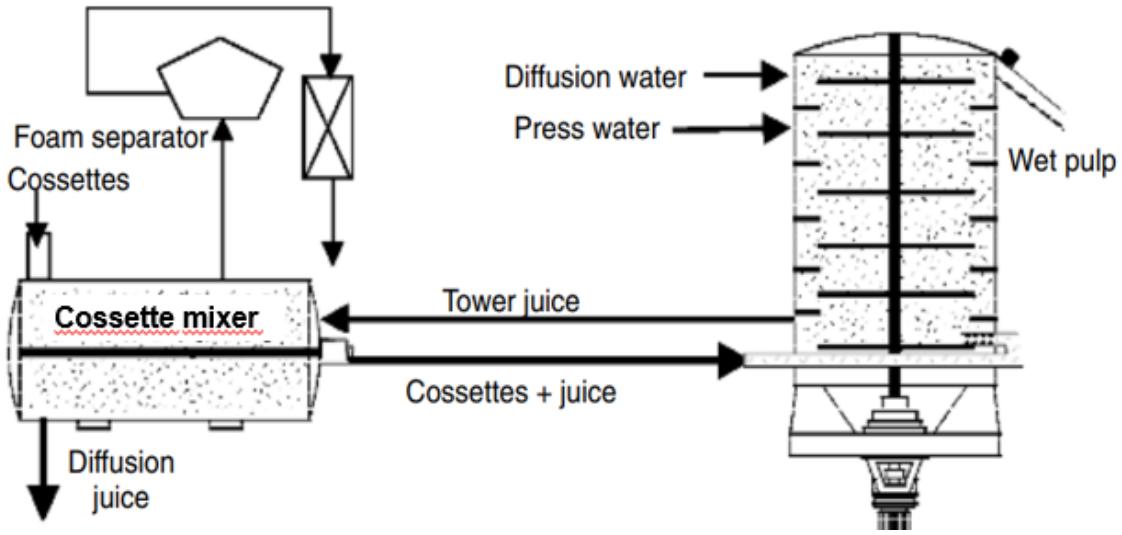

Fig. 2-14: BMA diffuser [extractor] for sugar beet extraction. Cossettes: sliced beets; diffusion juice: extract, wet pulp: raffinate, diffusion water: solvent; press water: from mechanical wet pulp dewatering *[78]*. BMA: Braunschweig Machinenbau Anstalt.

Fig. 2-14 shows a solid-liquid extraction process to gain sucrose from sugarbeet developed by Braunschweig Machinenbau Anstalt (BMA). The process uses countercurrent flow and comprises the cossette mixer, extraction tower, and beet pulp press (not shown). The press water is heated to operate the extraction at elevated temperatures. The heat is partly recovered in the cosset mixer preheating the feed. In

the same stage, the feed is suspended in the solvent, and the extract (diffusion juice) is withdrawn. After preheating, solvent penetration, and air removal in the cossette mixer, the soaked solids are pumped to the extraction tower. A vertical screw moves the material upwards, with solvent flowing downwards. The recycled and hot press water is added below the fresh solvent (diffusion water) to facilitate a beneficial concentration profile in the tower. The solvent can consist of fresh water, spent cooling water, or condensate from the juice evaporation units.

The raffinate pressing at the end reduces the water content in the raffinate and recovers some solute that was not extracted. A final intensive pressing can also be found in pulp washing after a series of drum washers [86]. First, the water extraction fills the solids void with solvent and reduces the solute concentration substantially. Second, most of the solvent and dissolved solute are recovered with compressive dewatering. Here, the filtrate initially contains mainly the free liquor around the fibers. Also, an increasing fraction of the liquor of fiber voids is removed with increasing compaction pressure [81]. Compressive dewatering is the more economical method to gain the solute than extraction, but relatively high residual solute content and undesirable heating are the consequence; thus, in the vegetable oil industry, an intensive but incomplete pressing is followed by solvent extraction [83]. The capital cost of pressing increases approximately in proportion to the throughput, whereas the relative capital cost of leaching decreases [83].

Solid-liquid extractions play an essential role in biorefining processes. They can be applied to remove the substrate’s contaminants or gain a product after (pre-) treatment. In both applications, solvent consumption, most often water, is significant. Low water consumption will not allow a high extraction yield. Enormous water will dilute the product and cause further problems. Improving solid-liquid extraction processes can reduce operating costs and valorize the biomass constituents in more profitable pathways. This work proposes a new counter-current, solid-liquid extraction process that aims to reach

As discussed above, numerous extraction processes exist and are tailored to different biomass extractions tasks. These biomasses are not similar enough to pretreated lignocellulose to allow a technology transfer, primarily if high extraction yields, high extract concentrations, low solvent consumption, and small space demand are targeted. There is no efficient extraction process for lignocellulosic biomass available.

Lignocellulosic biomass possesses challenging properties that must be considered to design improved extraction processes. These materials' high porosity [78,87] and low bulk density, compare to section 10.1, may lead to voluminous extractors. The cellular structure, compare to section 10.6, leads to a high water holding capacity for wheat straw of up to four times its weight and a long path for solute diffusion from the particle center to the surface. Thus, slow internal mass transport is the result. The fibrous nature of annual lignocellulose and reduced material flowability [87] increases diffusion limitations. Finally, the product concentration on pretreated lignocellulose is relatively low compared to leaching tasks in beet sugar processing [78].

2.3.2. Modeling and graphical representation

The methods and mathematical models depend on the extraction system, type, and extractor configuration [77,78,81,88]. In the following, an overview is given for the design of a multistage extractor, see Fig. 2-15. Here, the mass transport rates are not regarded since equilibrium in every stage is assumed. In solid-liquid extraction, the carrier solids are regarded inert, and the two liquids inside and around the particles are used in an overall and stage mass balance. The raffinate (underflow) concentration is represented with x, and the extract (overflow) concentration is represented with y. The equilibrium, both liquids show the same concentration, can be represented as angular bisector (x = y).

First, the process requirements, extraction yield, and extract concentration are used to determine the solvent consumption using an overall mass balance. Second, graphical and numerical methods can be used to estimate the ideal stage number. A stage efficiency can be used to account for mass transport limitations. Third, the solvent consumption and number of stages are the input to a rigorous calculation, determining the extraction yield and extract concentration. For that purpose, a mass balance for the first (or last) stage is carried out using the input and output and solvent throughputs from the overall mass balance and the equilibrium condition. In the same manner, the following stages are calculated. The concentrations in both liquids can be plotted before and after every stage in the operating diagram, see Fig. 2-16.

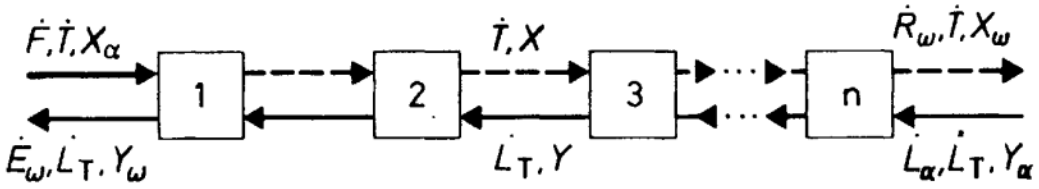

Fig. 2-15: Schematic drawing of counter-current extraction is separate stages *[88]*.

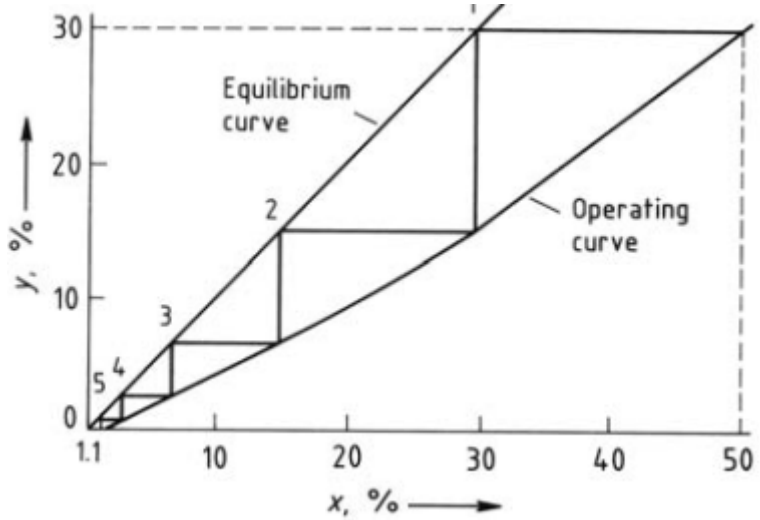

Fig. 2-16: Graphical determination of the number of theoretical extraction stages. The steps between $x_{a,total} = 50\%$ (corresponding to $y = 30\%$) and y=0 (corresponding to $x_{end} = 1.1\%$) product, five points, i.e., theoretical stages, on the equilibrium curve *[83]*.

3. Objectives

For a feedstock change in the chemical industry to renewables, full-fractionation processes for lignocellulosic materials are required but do not exist on an industrial scale. Proposed processes based on autohydrolysis and hemicellulose extraction, e.g., flow-through pretreatment, face substantial limitations. The objectives of this work are to improve the understanding of the sequential reactions during autohydrolysis pretreatment and to find a scalable method to overcome the resulting limitations regarding xylose and furfural yields. In-situ product removal methods are excluded in this work. The following six sections are defined to achieve the objective:

1. Understand how the maximum yield of intermediate product (water-soluble pentoses) can be affected by the reaction conditions in terms of temperature, residence time, and pH.
2. Find a mathematical description of the conditions leading to characteristic phenomena during autohydrolysis pretreatment, e.g., the start of product degradation.
3. Find a method to increase the recovery of pentoses, hexoses, and lignin in separated streams that is above the single-batch pretreatment performance and shows no limitations to be scaled to a production scale.
4. Develop a method for selecting pretreatment reactor concepts based on preliminary (low-quality) processing data for concept comparison and selection.
5. Based on previous results, develop and experimentally validate a processing concept in conditions relevant for commercial production. Demonstrate the product's quality.
6. Design and validate a continuous process for (i) the conditioning of annual lignocellulose before the pretreatment, avoiding excessive water consumption and (ii) the aqueous extraction of water-soluble pentose from porous lignocellulose with low product concentration achieving as high as possible extract concentration and extraction yield and low solvent (water) demand while allowing a low space demand.

4. Materials and methods

4.1. Materials

The straw of common wheat (*Triticum aestivum*) was used exclusively in this work. Three different forms of straw, see below, are used. The used straw form is indicated in the pretreatment method description or the results.

Pelleted wheat straw with 8 mm diameter was purchased from Speers Hoff in Stelle, Germany. This material was used for all LHW experiments. A granulated wheat straw litter with the product name “Bionesto Stroheinstreu” was purchased from Raiffeisen-Markt near Bremen, Germany. This material was used for 40 L steam pretreatment. Cut wheat straw with a length of around one cm with the product name “Q-Mehl” was purchased from Cordes-Grasberg in Grasberg, Germany. This material was used for 3 L and 400 L batch steam pretreatment and 230 L and 70 L continuous steam pretreatment.

4.2. Analytical methods

4.2.1. Solid analysis

The dry matter content was determined gravimetrically. Samples of at least two grams dry weight were weighed before and after oven drying at 105 °C for at least 4 hours, adapted from an NREL procedure [89].

The compositional analysis was conducted in a two-step analytical hydrolysis with sulfuric acid. The resulting solids residue was weighed and corrected for the remaining inorganic content using a muffle furnace. The residue is the “acid-insoluble” lignin. The “acid-soluble” lignin content was determined was photometrically using the acid hydrolysate. The carbohydrates in the hydrolysate are measured in an HPLC with an anion-exclusion column. Glucose and pentoses are corrected for the mass gain via hydrolysis to calculate the cellulose and hemicellulose content, respectively. The fresh sample was fully oxidized in a muffle furnace to determine the inorganic content gravimetrically. The procedure was done based on an NREL procedure and carried out at Thünen-Institute in Hamburg, Germany for the LHW experiments and at the TUHH-IUE in Hamburg, Germany, for the 40 L steam pretreatment experiments.

Thünen Institute in Hamburg, Germany, carried out the light microscope and Scanning UV microspectrophotometry (UMSP) according to a method developed by Prof. Koch [90]. “For UV-microspectrophotometry, 1 µm thick unstained sections of the same embedded specimens were prepared, transferred to quartz microscope slides, immersed in a drop of non-UV absorbing glycerin, and covered with a quartz cover slip. Cell wall analysis was performed using a UV-microspectrophotometer (UMSP 80, Zeiss) equipped with a scanning stage that enables determining image profiles at constant wavelengths (e.g., 280 nm maximum absorbance for conifer lignin). The specimens were scanned with a defined wavelength of 280 nm using the scan program APAMOS® (Zeiss). The new improved scan program digitizes rectangular fields of the tissue with a local geometrical resolution of 0.25 µm^2 and a photometrical resolution of 4096 grey scale levels which are converted in 14 basic colors to visualize the absorbance intensities.”[91]

The bulk density of the wheat straw pellets and uncompressed wheat straw were determined to calculate the reactor volume. The pellets were swollen with cold water for four hours and dried in a convective oven at 45 °C for at least 24 hours. To adjust the liquid to solid ratio, approximately (precisely measured) 150 g of dried wheat straw was mixed with the corresponding amount of cold tap water and stirred thoroughly. The mass of the probe that fits a beaker of known volume was determined in an adapted method according to DIN EN ISO 17828 [92]. The bulk density was modeled with a polynomial of the second degree and as a function of the liquid to solid mass ratio L/S (equation (4-1)). Here a, b and c are constants, which are fitted with the least-squares method.

$$\rho_{suspension}\left[\frac{g}{L}\right] = a * \left(\frac{L}{S}\right)^2 + b * \left(\frac{L}{S}\right) + c \qquad (4\text{-}1)$$

Biogas yields were determined according to the VDI guideline 4630 [93] by the TUHH-IUE in Hamburg, Germany. Under mesophilic conditions at 37 °C in batch tests. 500 mL glass bottles were filled with 400 g of digested sludge, obtained from a municipal sewage treatment plant south of Hamburg, Germany. This inoculum was gassing out for six days. Then 2.7 g of samples were placed in each of three identical reactors. Three reference measurements were carried out with microcrystalline cellulose from AlfaAesar. Three further reference measurement was carried out without the addition of the substrate. Each trial was conducted for 32 days from substrate addition, during which the samples were manually stirred once a day. The amount of biogas formed

was measured by the use of eudiometer tubes. Summary of the method was taken from [94]

The particle size distribution of AS-lignin samples was measured using a Beckman Coulter laser diffractometer (LS 13320) at TUHH Institute of Solids Process Engineering and Particle Technology. The AS-lignin samples were suspended in water and mixed thoroughly. The equipment's programs were used for automated degassing, background signal correction, sample dispersion, and a Fraunhofer model for near-spherical particles. The data were transformed to cumulative volume distributions; d10, d30 d50 d90, and d99 were automatically calculated prior to data export.

4.2.2. Liquid analysis

The liquid pH was measured after centrifugation and at room temperature using a Mettler Toledo Five Easy Plus pH/mV bench meter. The hydrolysates from pretreatment were analyzed for the composition regarding cellobiose, glucose, xylose, arabinose, acetic acid, formic acid, and degradation products HMF and furfural. The sample was neutralized and centrifuged and split into two specimens. The first was hydrolyzed with four percent sulfuric acid to convert the oligomer to detectable monomers. Both specimens are analyzed in an Agilent 1200 HPLC-RI system with a polymer-based HPLC phase column which combines steric exclusion, ligand exchange, and partition effects. Organic acids, HMF, furfural, and carbohydrate monomers were taken from the specimen without hydrolysis. The carbohydrates in the hydrolyzed specimen are regarded as derived from monomers and oligomers. This method was conducted by the TUHH central laboratory for chemical analysis and is based on an NREL procedure [95].

The reducing sugar (RS) analysis of EH hydrolysates was determined using a DNS (dinitrosalicylic acid) test according to a NREL procedure [96]. The test reagent was produced by mixing 5 g DNS powder 100 mL 2M sodium hydroxide solution and 150 g sodium potassium tartrate dissolved in water and filled with water to 500 mL. The mixture was intensively mixed and stored at four degrees Celsius in an opaque vessel. A glucose dilution series was produced and measured along with the samples. 0.167 mL sample, 0.333 mL 5 mM Citrate puffer at pH 5, and 1mL DNS reagent are mixed in a 2 mL micro tube. The tubes are closed, mixed, boiled in a water bath for 5.0 minutes, and cooled in a water bath. In a cuvette, 1.25 mL water and 0.10 mL reaction mixture are mixed, and the absorbance is analyzed at 540 nm. The glucose solution

series with known concentration was used to calculate the calibration curve to convert the sample absorbance to glucose equivalent, reducing sugar concentration.

4.3. Experimental methods

In the following, the experimental methods regarding the pretreatment, enzymatic hydrolysis, and extraction are presented.

4.3.1. Autohydrolysis experiments

In this work, six different pretreatment reactors are used for different purposes, see Fig. 4-1 and Tab. 4-1. The following sections describe the methods in detail.

4.3.1.1. Wheat straw preparation

The straw pellets for LHW experiments were not wetted outside the reactor. For the 3L-batch experiments, the straw was moistened with water and mixed thoroughly to reach 50 wt% moisture content. For the other operations in batch and continuous mode, the biomass was washed with 20 L demineralized water per kg of dry mass and pressed in a Wiltec hydro press. After pressing, the moisture content of around 68 wt% (L/S = 2.1) was reached. The wet biomass was prepared the same day of the hydrothermal pretreatment and stored in a closed container before usage. For the 70L-continuous experiments, the washed straw was pressed in a 35 L piston press to reach a moisture content of around 55 wt% (L/S = 1.2). After compressive dewatering, the pretreated material reached a moisture content of 60 wt% (L/S = 1.5).

4.3.1.2. 0.03 L LHW (Batch)

Experimental data from earlier published experiments [55] were used to determine the reaction kinetics. Wheat straw pellets with a moisture content of approximately 10 wt% were used as substrate. Autohydrolysis experiments were conducted in 30 mL batch reactors at 50 bar at temperatures of 170 °C, 185 °C, 200 °C, 215 °C and 230 °C for each 10, 20, 30, 45, 60 and 90 minutes. Each experiment was conducted in duplicate with 600 mg dry biomass and deionized water (added to result in 30 mL reaction volume). Nitrogen gas was used to pressurize the reactors. An electrical heating jacket was applied to control the temperature. When the reactor temperature reached 10 °C below its set point, the reaction time was started. The reaction was stopped by cooling each reactor with an ice bath. The composition of the solid phase and the hydrolysate was measured, and the remaining solid dry biomass. Testing the two-step

autohydrolysis pretreatment in LHW reactors, the following experimental conditions were used, see Tab. 4-2.

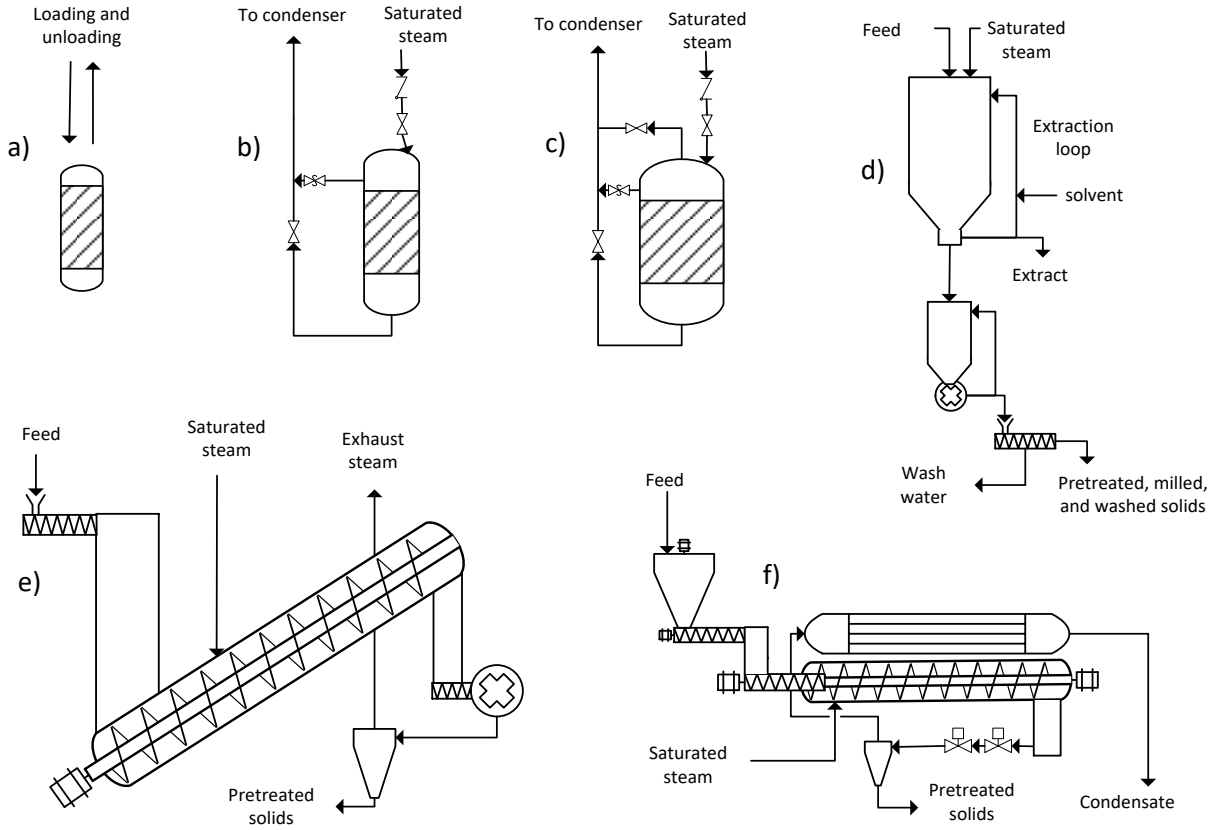

Fig. 4-1: Reactors investigated for the autohydrolysis pretreatment of wheat straw. a)-d) batch, **a)** Liquid Hot Water (0.03 L), **b)** steam (3 L), **c)** steam (40 L), **d)** steam and percolation (400 L), **e)** continuous steam pretreatment with refiner (230 L), **f)** continuous steam with hot blow (70 L).

Tab. 4-1: Pretreatment reactors in this work, with design and process characteristics.

i	Name	Vol.	M* [kg]	P	T	heating	mode	Use
[#]	[-]	[L]	[kg/h]	[bar]	[°C]	[-]	[-]	[-]
a	LHW	0.03	0.0006	300	250	jacket	batch	kinetic data
b	3L-batch	3	0.2	10	180	steam	batch	transfer to steam
c	40L-batch	40	5	10	180	steam	batch	Mass balance
d	400L-batch	400	17	15	180	steam	batch	scale up/ equipment
e	230L-contin.	230	30	10	175	steam	continuous	transfer to continuous
f	70L-contin.	70	3	17	204	steam	continuous	s. explosion/ screw feeding

*mass per batch or mass flow in continuous reactors based on dry solids input.

Tab. 4-2: LHW two-step autohydrolysis experiments. All combinations of temperature and residence time in the second step are used.

Step [#]	name [-]	T_1 [°C]	t_1 [min]	T_2 [°C]	t_2 [min]	repetitions [-]	$S_{0,1}$ [-]	$S_{0,2}$ [-]	S_0 [-]
1	A1	170	60			*30	3.84		3.84
1	B1	200	10			*30	3.94		3.94
1	Opt1	200	30			6	4.42		4.42
2	A2	170	60	170, 185 200, 215	10, 20 20, 60	2	3.84	3.06 - 5.16	3.91 - 5.18
2	B2	200	10	170, 185 200, 215	10, 20 20, 60	2	3.94	3.06 - 5.16	4.00 - 5.19

* Six repetitions are analyzed; the remaining ones are done to produce material for the second step.

The pH buffers were used in hydrothermal pretreatments in the 0.03 L LHW batch reactors to investigate the effect of the pH on the reaction rates. The reaction procedure is identical, but the correspondent buffer was used instead of deionized water. The reaction conditions can be found in Tab. 4-3.

Tab. 4-3: Experimental conditions for constant pH hydrothermal pretreatments. M: molar [mol/L].

pH [-]	T [°C]	t [min]	repetitions [-]	Buffers [-]
2	180, 200	5, 10, 20, 30	2	0.1 M, phosphate
3	180, 200	5, 10, 20, 30	2	0.1 M, phosphate
4	200	5, 10, 30, 50	1	0.05 M, acetate
5	200	5, 10, 20, 30, 50	1	0.05 M, acetate
no Buffer	200	5, 10, 20, 30, 50	2	non

4.3.1.3. 3 L steam (Batch)

The set-up consists of the reactor itself, a removable cartridge, a steam generator, pressure and temperature sensors at the bottom and top, and a condenser connected to the reactor bottom.

The cylindrical reactor with an oil heating jacket possesses a removable lit that allows sliding in and out a metal cartridge containing the biomass. The top is connected to the steam inlet; the bottom is connected to a vapor condenser operated with cold water. The cartridge has an inner diameter of 90 mm and a length of 495 mm. The top and bottom are a removable slot screen of 250 µm width. The 15 kW steam generator 200-15 manufactured from Stritzel Dampftechnische Geräte GmbH operates at nine bar gauge.

The cartridge filled with wet biomass is loaded into the preheated reactor closed afterward. The reaction mixture is preheated for 5 minutes with the oil jacket while keeping the outlet to the condenser open to allow hot air the escape. The steam inlet is opened slightly to flush the remaining air from the reactor and replace it with steam. After five minutes, the outlet to the condenser is closed, and the steam inlet is open. After seconds, the maximal pressure is reached, and the reaction time is started. The steam inlet is closed, and the outlet to the condenser is opened to stop the reaction. After approximately a minute, the depressurization is completed, and the cartridge is removed from the reactor. Condensate is weighted and cooled at 8°C prior to further analysis. The cartridge is cooled by running cold water over the surface. Experimental conditions can be found in Tab. 4-4.

Tab. 4-4: 3L batch reactor experimental conditions.

Step [#]	T [°C]	name [-]	t_1 [min]	t_2 [min]	repetitions [-]	$S_{0,1}$ [-]	$S_{0,2}$	S_0 [-]
1	180	A'1	20		*20	3.66		3.66
1	180		30		2	3.83		3.83
1	180	B'1	35		*20	3.90		3.90
1	180		39		2	3.95		3.95
1	180		45		2	4.01		4.01
1	180		60		2	4.13		4.13
2	180	A'2	20	20, 30, 35, 45, 60, 80	2	3.66	3.66 -4.26	3.96 -4.36
2	180	B'2	35	20, 30, 35, 45, 60, 80	2	3.90	3.66 -4.26	4.10 -4.42

* Two repetitions are analyzed; the remaining ones are done to produce material for the second step.

The hydrolysate is obtained by mechanical dewatering the pretreated straw using a self-made manual cylinder press. The cartridge is opened on top and placed in the cartridge holder. A piston connected to a threaded rod exerts an axial force on the biomass bed inside the cartridge to press out the liquid phase. The torque wrench was used to press the biomass up to 40 Nm. The hydrolysate collected below the cartridge was cooled at 8 °C until further use.

4.3.1.4. 40 L steam (Batch)

The set-up is identical to the 3 L reactor and consists of the reactor itself, a removable cartridge, a steam generator, pressure and temperature sensors at the bottom and top, and a condenser.

The cylindrical reactor with an oil heating jacket possesses a bayonet quick coupling lid. The top is connected to the steam inlet, the top and bottom are connected to a vapor condenser operated with cold water. The cartridge has an inner diameter of 320 mm and a length of 500 mm. The top and bottom are a removable slot screen of 250 µm width. The same steam generator is used for the 3L-batch experiments.

The cartridge filled with wet biomass is loaded into the preheated reactor and closed afterward. The reaction mixture is preheated for 12 minutes with the oil jacket and by flowing steam slowly in at the top to replace the air to the bottom outlet. The outlet to the condenser is closed when the outlet stream reaches 100 °C and the steam inlet is opened. After approximately eight minutes, the maximal pressure is reached, and the reaction time is started. The steam inlet is closed, and the top outlet to the condenser is opened to stop the reaction. After approximately three minutes, the depressurization is completed, and the cartridge is removed from the reactor using a hook and 1000 kg crane. The condensate is weighted and analyzed for furfural, HMF, and acetic acid.

The hydrolysate is obtained by water extraction and mechanical dewatering. The pretreated biomass is mixed with desalted water, wholly submerged the solids, and mixed for 20 minutes. A 40 L Wiltec hydro press (press filter) is used for dewatering the suspension. The hydrolysate is collected at the bottom and cooled at 8 °C until further use. The solids are weighted, and the moisture content is determined. Then the solids are washed with fresh desalted water (L/S>20), pressed, and weighted. The moisture content is determined. The used conditions for the autohydrolysis pretreatment can be seen in Tab. 4-5.

Tab. 4-5: Experimental conditions for the mass balance determination in the 40L-batch experiments

Name [-]	T [°C]	t_1 [min]	t_2 [min]	$S_{0,1}$ [-]	$S_{0,2}$ [-]	S_0 [-]	repetitions [-]	M_0 [kg]
A''	180	20	30	3.66	3.83	4.05	3	2.00
B''	180	35	35	3.90	3.90	4.20	3	2.00

4.3.1.5. 300 L steam (batch)

The autohydrolysis reaction was scaled up to the 400 L Organosolv reactor at Fraunhofer Center for Chemical-Biotechnological Processes CBP in Leuna, Germany. The wet biomass was loaded to the reactor and preheated with saturated steam, while the forming condensate was drained at the bottom. After 10 minutes, the bottom value was closed to pressurize the reactor. When a constant temperature of 140 °C was reached, saturated steam at 20 bar was injected into the reactor. Since the reactor temperature slowly increased after reaching 170 °C, live integration of the temperature profile was used to stop the reaction after a severity factor of $S_0 = 3.9$ was reached. 100 L of cold water was injected into the reactor to quench the reaction. Draining the biomass over a sieve, the water was circulated in a percolating manner for 20 minutes to extract the dissolved carbohydrates. The extract was removed and collected. The solid fraction was flushed with fresh water into a batch rotor-stator mill. After 10 minutes of milling, the solid and liquid phases are separated using a screw press.

The washed and pressed pretreated solids were treated again, applying the same procedure and reaction conditions. The extract was hydrolyzed enzymatically, filtered, and concentrated.

4.3.1.6. 230 L Steam (continuous)

A continuous screw conveyor reactor (CSR) manufactured by Andritz combined with a disk refiner was used at Fraunhofer Institute for Wood Research Wilhelm-Klauditz-Institut WKI in Braunschweig, Germany. The wet biomass was fed through a vertical lock chamber into the screw reactor. Saturated steam at 175 °C was injected at two positions on top of the reactor. The screw conveys the material with an approximate throughput of 36 kg h-1 based on dry matter and a residence time of up to 20 minutes into a disk refiner. After the release valve, the forming steam accelerates the reaction mixture into a cyclone to separate steam from the wet biomass. The discharged biomasses were suspended with boiling water and pressed in a Wiltec hydro press after 20 minutes of mixing. Washing was carried out to pretreat the pretreatment. Before enzymatic hydrolysis, the solids were stored in a closed container at below 10 °C.

4.3.1.7. 70 L steam (continuous)

A continuous screw conveyor reactor (CSR) manufactured by *AdvanceBio Systems LLC* equipped with a high-pressure feeder manufactured by *Tk energy ApS* was used at the Lund University of Technology in Lund, Sweden. The high-pressure screw feeder has a movable section in the plug zone connected to a hydraulic pump system. This setup allows a constant force on the plug with changing plug volume. The feeder was used to feed the biomass into the reactor. The screw speed of the feed hopper and the high-pressure feeder, and the feeder oil pressure are varied to find a combination that allows stable feeding for the washed and pretreated biomass. The reactor was operated at 200°C and ten minutes in both pretreatment steps. The pretreated biomass was extracted, washed, and pressed in a 35 L piston press.

4.3.2. Enzymatic hydrolysis

The enzymatic hydrolysis of pretreated solids from LHW and 3 L steam pretreatment are conducted with an excess of enzymes to determine the enzymatic hydrolysis of the pretreated solids. Economical use of the enzymes was not of interest. A more recent enzymes mixture and a scalable mixing tank were used for the mass balance in the 40 L steam pretreatment reactor to produce experimental data relevant for process scale-up. Here the amount of the used enzymes is of interest.

4.3.2.1. 0.05 L tank

The cellulignin from the LHW and 3L steam reactor is hydrolyzed enzymatically in 50 mL centrifugal tubes in a water bath for 72 hours. 800 mg of oven-dried (50 °C, 24 hours) cellulignin, 40 mL 5mM citric acid buffer of pH 5 and 196 µL Novozymes CTecII are mixed thoroughly and shaken at 50°C in a horizontal position. The reaction was quenched with a cold-water bath. The tubes are centrifuged to analyze the supernatant and its composition. The solid residue was washed with distilled water by mixing and separating in a centrifuge twice to remove any dissolved components from the solids. The solids are dried at 50 °C for 24 hours in a convective oven Afterward, the residual solid mass and composition are determined. Experiments are done in duplicate.

4.3.2.2. 10 L tank

A ten liter stirred tank with a flat bottom, and an anchor agitator was used to investigate the cellulignin after two-step steam pretreatment for the 40 L reactor under varying enzymes load. The solids were produced according to section 4.3.1.4. Seven liters of

50 mM Citric acid buffer at pH5 were heated to 50 °C at 100 RPM. Novozymes CTecIII was added to result in 2.5, 5.0, and 7.5 mL enzyme mixture per dry matter of added solids. To reach a high solid content, the wet biomass was added according to a fed-batch scheme, starting at time zero; every 20 minutes, so much cellulignin was added that homogeneous mixing was possible; the last amount was added after 60 minutes. In the first three hours, every 30 minutes, samples were taken.

4.3.3. Extraction of hydrothermally pretreated polids

4.3.3.1. Suspended stirred extraction

To determine the time required to reach equilibrium in stirred suspension extraction with pretreated biomass, a 10 L stirred tank was used. 3.000 kg deionized water is heated to 70 °C at 150 rpm. After the temperature was reached, pretreated wet wheat straw was added. The dry solids concentration is 2 wt% (L/S = 49). Samples are taken after 1, 2.5, 5, 10, 15, 20, 30 and 60 minutes. Samples are left for 30 seconds for solid settling; the supernatant is taken and filtered in a 0.02 µm syringe filter to remove residual particles. The sample is stored at 4 °C until analysis. The concentration of the total pentoses is converted to a dimensionless scale to account for different moisture contents and thus feed concentrations in the pretreated biomass. The average of the last three concentrations in each experiment defines the equilibrium concentration. Here the equilibrium is defined as the concentration in the bulk that is constant for at least three measurement points. It is assumed that the particle interior and the bulk phase concentrations are identical in this state, and no further mass transport occurs.

4.3.3.2. Analytical extraction

The pretreated solids from the 3 L steam pretreatment with varied initial moisture content were extracted with water in batch suspension extraction to determine the amount of extractable pentose. Four grams of dry matter of the wet sample was mixed with 160 mL distilled water in a 200 mL vessel. The vessel was closed, sealed, and treated in a water bath shaker at 70 °C for 60 minutes. Then the sample was centrifuged, and the supernatant was stored at 4 °C prior to carbohydrate analysis.

4.4. Modeling and calculations

4.4.1. Experimental parameters and calculation

The hemicellulose conversion X_{HC} was calculated based on the determined hemicellulose mass fraction in the solid w_{HC} and the degree of solubilization DS. The

latter needs to be considered since the solid mass was partly liquefied, including cellulose, lignin inorganics, and extractives affecting the hemicellulose mass fraction. Otherwise, the inorganics dissolution alone would result in a negative hemicellulose conversion since its mass fraction would be increase. The degree of solubilization DS, see equation (4-2), describes how much solid is liquefied during the autohydrolysis process. Note, the subscript index (0, 1, 2, th) refers to initial or after first/ second/ total thermal step(s). DS_{th} is the degree of solubilization after the hydrothermal treatment step (th = 1 for single-step pretreatment, th = 2 for two-step pretreatment) and is calculated according to equation (4-3).

In kinetic modeling, only the initial and final hemicellulose mass fractions are known. To be able to calculate the hemicellulose conversion, the change in total solid mass must be known. The latter can be derived from the initial and final hemicellulose mass fractions, thus the conversion formula for the lignocellulose hydrolysis is more complex compared to well-known conversion formula in liquids with no volume change. For the first and second-order reaction model described below, all components but hemicellulose are treated as inert. The total mass after pretreatment $M_1^{s,model}$ is the sum of intert mass and remaining hemicellulose mass. This allows the expression of $M_1^{s,model}$ in terms of $w_{HC,0}$ and $w_{HC,1}$, compare equation (4-4).

The combination of equations (4-2) and (4-4) results in an expression for DS^{model} that is only dependent on $w_{HC,0}$ and $w_{HC,1}$, compare equation (4-5).

The conversion of hemicellulose X_{HC} describes the solubilized mass fraction of hemicellulose, here the change of total solid mass must be considered, see equation (4-6). In the kinetic modeling, M_1^s is unknown, instead $M_1^{s,model}$ can be used, compare equations (4-4), (4-6) and (4-7). Here, X_{HC}^{model} depends only on the calculated hemicellulose content $w_{HC,0}$ and $w_{HC,1}$, see equation (4-7).

$$DS = \frac{M_0^s - M_1^s}{M_0^s} = 1 - \frac{M_1^s}{M_0^s} \qquad (4\text{-}2)$$

$$DS_{th} = \frac{M_0^s - M_2^s}{M_0^s} = 1 - (1 - DS_1)(1 - DS_2) \qquad (4\text{-}3)$$

$$M_1^{s,model} = M_0^s * \left(1 - w_{HC,0}\right) + M_1^{s,model} * w_{HC,1} = M_0^s * \frac{\left(1 - w_{HC,0}\right)}{\left(1 - w_{HC,1}\right)} \quad (4\text{-}4)$$

$$1 - DS^{model} = \frac{\left(1 - w_{HC,0}\right)}{\left(1 - w_{HC,1}\right)} \quad (4\text{-}5)$$

$$X_{HC} = \frac{M_{HC,0}^s - M_{HC,1}^s}{M_{HC,0}^s} = 1 - \frac{M_1^s * w_{HC,1}}{M_0^s * w_{HC,0}} \quad (4\text{-}6)$$

$$X_{HC}^{model} = 1 - \frac{(1 - DS^{model}) * w_{HC,1}}{w_{HC,0}} = 1 - \left(\frac{w_{HC}}{1 - w_{HC}}\right) * \left(\frac{1 - w_{HC,0}}{w_{HC,0}}\right) \quad (4\text{-}7)$$

The pH was calculated using the measured concentration of acetic acid c_{AA} and formic acid c_{FA} in mol/L, see equation (4-8). Here the mass action constants for the weak acids are expressed in dependence of their pKs values. The formic acid concentration is only quantifiable above 400 mg/L, which results in a sudden jump in concentration. To correct this artefact, the linear curve section of formic acid concentration versus severity factor was continued below the quantification limit.

$$pH = -\log_{10}\left(\sqrt{c_{FA}10^{-pK_{FA}} + c_{AA}10^{-pK_{AA}}}\right) \quad (4\text{-}8)$$

The recovery of the products i after step j $Rec_{i,j}$ is expressed as the component mass in the hydrolysate $M_{i,j}^l$ to the polymer mass in the untreated biomass from which the component is derived $M_{i,j-1}^s$. Here, the volume of the reaction mixture V_R and the concentration of component i after step j $c_{i,j}$ are used, compare equation (4-9). The recovery calculation in the second pretreatment step is based on the substrate mass in the untreated component. For this purpose, the untreated, dry biomass M_0^s was calculated using the initial dry biomass M_1^s and DS_1, compare equation (4-10)**.** The total recovery of component i after both hydrothermal pretreatment steps $R_{i,th}$ is the sum of both individual steps, compare equation (4-11) and equation (4-12).

$$Rec_{i,j} = \frac{M_{i,j}^{l}}{M_{i,0}^{s}} = \frac{c_{i,j}\, V_R}{w_{i,0}\; M_0^s}\; 10^{-6} \qquad (4\text{-}9)$$

$$M_0^s = \frac{M_1^s}{(1 - DS_1)} \qquad (4\text{-}10)$$

$$Rec_{i,th} = \frac{M_{i,1}^{l} + M_{i,2}^{l}}{M_{i,0}^{s}} = Rec_{i,1} + Rec_{i,2} \qquad (4\text{-}11)$$

$$Rec_{i,th} = Rec_{i,1} + Rec_{i,2} = \frac{c_{i,1}\, V_1^l}{w_{i,0}\; M_0^s}\; 10^{-6} + \frac{c_{i,2}\, V_2^l}{w_{i,0}\; \frac{M_1^s}{(1 - DS_1)}}\; 10^{-6} \qquad (4\text{-}12)$$

The yield of component i after step j $Y_{i,j}$ is calculated as mass component recovered in step j to the untreated, dry biomass. The AS-lignin yield can be calculated based on the three treatment's degrees of solubilization, see equation (4-13). The yield of the reducing sugars in the enzymatic hydrolysis experiment $Y_{RS,EH}$ is calculated with the reducing sugar concentration c_{RS} determined with the DNS test, see equation (4-14). The yield of the dissolved component i can be calculated based on its total recovery, see equation (4-15). Here, $Y_{Rest,TH}$ represents the organic acid and furfural in both hydrothermal pretreatments.

$$Y_{AS-Lignin} = \frac{M_{AS-lignin}}{M_0^s} = \prod_{k=1}^{j=EH} (1 - DS_k) \qquad (4\text{-}13)$$

$$Y_{RS} = \frac{M_{RS}^{l}}{M_0^s} = \frac{c_{RS}\, V_R\, (1 - DS_{th})}{M_{EH}^s} \qquad (4\text{-}14)$$

$$Y_i = \frac{M_i}{M_0^s} = Rec_{i,th}\; \cdot w_{i,0} \qquad (4\text{-}15)$$

4.4.2. Chemical kinetics modelling

4.4.2.1. Arrhenius rate models

For the scaling of an autohydrolysis reactor, a mathematical description of the changing hemicellulose content in the solid phase during the process is required.

For this propose the hemicellulose mass fraction in the remaining solids from a full-factorial design of temperatures of (170, 185, 200, 215, and 230)°C and residence times of (10, 20, 30, 45, 60, and 90) minutes in duplicate in a 0.03 L LHW experiment, compare 4.3.1.2, were used. It is assumed that the temperature was homogeneously distributed in the reaction mixture, and the hydrolysate composition did not show local gradients. The hemicellulose hydrolysis was modeled using first and second reaction orders using the hemicellulose mass fraction in the solid w_{HC} and an Arrhenius temperature approach, see equations (4-16) - (4-20). Here k_1 is the rate constant, n the reaction order, M_{HC} the mass of hemicellulose in the solid, M_{dryBM} the dry biomass, $k_{1,0}$ the preexponential factor, E_a the activation energy, R the universal gas constant and T the temperature. The Arrhenius constants (pre-exponential factor and E_a/R) were determined by the method of least squares using experimental values and those calculated with equations (4-19) and (4-20).

$$\frac{dw_{HC}}{dt} = k_1 * w_{HC}^n \qquad (4\text{-}16)$$

$$w_{HC} = \frac{M_{HC}}{M_{dryBM}} \qquad (4\text{-}17)$$

$$k_1 = k_{1,0} * \exp\left(-\frac{E_a}{R} * \frac{1}{T}\right) \qquad (4\text{-}18)$$

$$w_{HC} = w_{HC,0} * \exp(-k_1^{n=1} * t) \;\; ; \;\; for\; n = 1 \qquad (4\text{-}19)$$

$$w_{HC} = \frac{w_{HC,0}}{w_{HC,0} * k_1^{n=2} * t + 1} \;\; ; \;\; for\; n = 2 \qquad (4\text{-}20)$$

Evaluation of the model performance is determined using the root mean square error (RMSE).

$$RMSE = \sqrt{\frac{\sum_{k=1}^{n_{exp}} \left(Y_{H,i,k}^{exp} - Y_{H,i,k}^{mod}\right)^2}{n_{exp}}} \qquad (4\text{-}21)$$

Where $Y_{H,i,k}^{exp}$ are the experimental values, $Y_{\mathrm{H,i,k}}^{\mathrm{mod}}$ are the values predicted by the model and n_{exp} is the number of data points.

4.4.2.2. Severity Factor

For the comparison of different pretreatment severities, the severity R_0 and the severity factor $\mathrm{S}_0 = \log(R_0)$ is used, see equations (4-22) and (4-23). It combines the temperature T and the residence time t in a single variable. For consecutive pretreatments the overall severity factor is the summation of the individual severity with m being the number of pretreatments, see equation (4-24).

$$R_0 = t[min] * \exp\left(\frac{T[°C] - 100}{14.75}\right) \quad (4\text{-}22)$$

$$\mathrm{S}_0 = \log(R_0) = \log\left(t[min] * \exp\left(\frac{T[°C] - 100}{14.75}\right)\right) \quad (4\text{-}23)$$

$$R_0 = \sum_{i=1}^{m} R_{0i} \quad (4\text{-}24)$$

4.4.3. Heuristic evaluation of autohydrolysis reactors

Different reactor types in batch, semi-batch, and continuous mode are investigated for use in an industrial autohydrolysis pretreatment unit for a second-generation biorefinery. A fast evaluation of technical and economic characteristics is used to reduce bias in selection of a promising reactor type for further process development. Since not all plausible concepts can be developed in detail, a fast method based on available data is developed and applied. Missing data are estimated based on the reactor descriptions. The aim of this approach is the quick ranking of relevant parameters for the scale-up and operation the evaluation of potentials and risks in the further development.

Technical and economic design criteria are described below in detail. Each reactor concept i is evaluated according to the described functions with a score x_i. The scale from the best x_a to the worst x_w score is normalized to a new scale with values from

$y_a = 1$ (worst performance) to $y_w = 10$ (best performance), resulting in a normalized design criteria value y_i. Using a linear interpolation, the relative position of each concepts score to the best and worst performance is projected to the new limits, 1 and 10, see equations (4-25) and (4-26).

$$y_i = \frac{x_i - x_{i,a}}{x_{i,w} - x_{i,a}} * (y_w - y_a) + y_a \qquad (4\text{-}25)$$

$$y_i = \frac{x_i - x_{i,a}}{x_{i,w} - x_{i,a}} * (10 - 1) + 1 \qquad (4\text{-}26)$$

All design parameters are highly relevant for the success of further process development. To combine all design parameters, their product is formed, which ranks from 1 (worst reactor possible) to 10^n (best reactor possible), with n the number of design criteria. This method punished reactor concepts with at least one criteria with poor performance. Thus, it is essential to select crucial design parameters only.

4.4.3.1. Design Criteria

Based on experience, a techno-economical assessment of a fixed-bed autohydrolysis scale-up study [45] and further publications, reactor, and plant design criteria are developed and discussed below. Those will be used to evaluate different reactor types in an autohydrolysis pretreatment unit.

Water consumption

Water consumption is of great importance since water heating requires a considerable amount of energy considering its high heat capacity. It is expressed as the liquid to solid ratio L/S, which is often in the range of 1 to 10. Secondly, a large L/S leads to the dilution of the dissolved products. The required high concentration of the sugar stream will lead to a heat demand concentrating the product. As a default unit operation, the evaporation of the water is regarded, which in turn is regarded as energy-intensive. Thirdly, the throughput of large amounts of water can lead to the need to treat large amounts of waste water, which must be avoided. The water consumption should be low.

Heat duty and integration

The usually large energy consumption of autohydrolysis processes, which is coupled to the water consumption, is a major limitation towards its industrialization. In addition,

the heat transfer should be fast and efficient for reasonable process control and a reduction of the residence time. With a high water consumption, either the heat can be recovered at a high temperature resulting in a diluted product stream, or the heat is used to evaporate the product stream and can only be recovered at a low temperature level. The heat duty is evaluated as in equation

$$x_{i,Heat} = \frac{L}{S} + c_{heat} \quad (4\text{-}27)$$

Here, L/S accounts for the specific heat demand and c accounts for heating rates, see discussion above. The following values are defined, with fast heating for a good score: $c = 0$ for continuous operations with direct saturated steam heating, $c = 1$ for continuous operation with conductive heating, $c = 2$ for batch operation and direct saturated steam heating, and $c = 3$ for batch operation with conductive heating.

Handling

This criterion targets the loading and cleaning processes of the reactor types. Time-consuming loading processes can lead to long down times of the process. Long down times can lead to a numbering up in a semi-continuous production to maintain a steady material flow. Also, labor costs for the operation support this criterion. The handling of the reactor should be easy and fast.

$$x_{i,Handling} = \frac{t_{operation}}{t_{reaction}} \quad (4\text{-}28)$$

Here $t_{operation}$ stands for the operation time and $t_{reaction}$ for the time the reactor is carrying out a reaction. These times are estimated based on the reactor design and the literature. For continuous processes, the handling design criteria is 1.

Apparatus scalability

It is assumed to be beneficial to find an apparatus type that can be easily scaled to different sizes, especially industrial production scales. This criterion shall also be helpful to avoid the optimization of lab-scale apparatuses that will lead to a severe numbering-up or are not economically scalable to an industrial size. With increasing diameter and pressure, the reactor wall thickness increases. Large reactor diameters and thick reactor walls can lead to enormous investment costs. Industrial scales should be possible and already exist, and transport processes should not play a role in designing the criteria. Here, $x_{i,Scalability} = 10$ for a reactor that exists at a 10 t/h scale

and shows no transport limited phenomena, $x_{i,Scalability} = 5$ for reactors that do not exist at a 10 t/h scale and show no transport limited phenomena and $x_{i,Scalability} = 1$ for reactors that do not exist on a 10 t/h scale and show transport limited phenomena.

Apparatus complexity

As a rule of thumb, the cost for high-pressure closing systems increases with its diameter and complexity. The complexity should be low to reduce the investment cost and process development time. The complexity criterion is the number of critical parts and parts requiring individual testing for each biomass investigated. The definition of a complex part is that there is no accepted design rule for scaling. For example a solid agitator at unknown moisture levels for lignocellulose pressure reactor is regarded as one complex component. Both, the blade design for proper mixing, and the (multiaxial) sealing need experimental investigation in the process development.

Operation mode

Due to the high temperatures (170 °C – 230 °C) and the short residence times (5 – 30 minutes), the use of continuous apparatuses possesses outstanding advantages in terms of reactor size, down time, energy consumption, and temperature stress to the reactor compared to batch processes. In a batch process, the reaction mixture and the thick-walled pressure reactors must be heated and cooled to the desired temperatures, which takes time and consumes thermal energy, which is also challenging to recycle. Also, the reactor must be loaded and unloaded, which costs time and binds work force. Nevertheless, in a batch reactor, the process severity can be easily adapted to account for substrate composition changes and process other materials. If the process is realized in batch mode, the handling should be easy and fast, the heat consumption low, and possess heat recycling possibilities. If the process is realized in continuous mode, the residence times should be short, and the process parameters, e.g., L/S, T, t, substrate, particle size, adjustable. The operation mode criterion evaluates the reactor size and its effects on capital costs. Here the value is $x_{i,Mode} = 1$ for batch mode, $x_{i,Mode} = 5$ for semi-continuous and $x_{i,Mode} = 10$ for continuous operation mode.

4.4.4. Solid-liquid extractors

To investigate the extraction of the new counter-current solid-liquid extraction method, the process windows are calculated and compared with two other processes:

suspension extraction without recycling and suspension extraction with recycling. Two important design parameters for each process are varied, and the effect on the extract concentration C^E in g solute in 1000 g liquid and the extraction yield Y^E in g solute in extract per g solute in feed is evaluated. For each extraction vessel, thermodynamic equilibrium is assumed. A washing and a leaching scenario are investigated to account for these possible applications. Mass balance calculations and iterations are done in Microsoft excel 2016 using the solver function.

Each scenario is defined by its feed composition. Here solids, solute, and solvent (water) are considered. The solute is defined as entirely soluble in water. In the washing scenario, water and solute contents are small to represent freshly harvested lignocellulose. The solute represents ash, fine particles, and non-structural carbohydrates. The washing feed contains 86.4 wt% solids, 4.5 wt% solute, and 9.1 wt% solvent. The leaching scenario represents steam pretreated wheat straw. The solute represents soluble hemicellulose-derived components such as oligomer and monomer pentoses. The leaching feed contains 25.8 wt% solids, 7.5 wt% solute, and 66.7 wt% solvent.

4.4.4.1. Suspension extraction without recycling

In Fig. 4-2a, the block flow diagram of the suspension extraction with and without recycling is displayed. In the extraction process without recycling, the recycling stream is neglected. Feed and solvent (water) are mixed in a continuously stirred tank. The outflowing suspension is pressed in one or two consecutive presses, e.g., screw or roll presses. The first one may represent a press near the extraction plant. The second one represents a high-pressure plug screw feeder that dewaters the moist solids while pushing the material into a continuous screw conveyor reactor. The two presses are considered one press for the calculation since the effluents from both presses are mixed in one filtrate tank. Between the two presses – before the reactor - there might be presteaming unit that adds a small amount of condensate to the biomass and thus, to the filtrate. However, in this study the possible condensate additions is not considered.

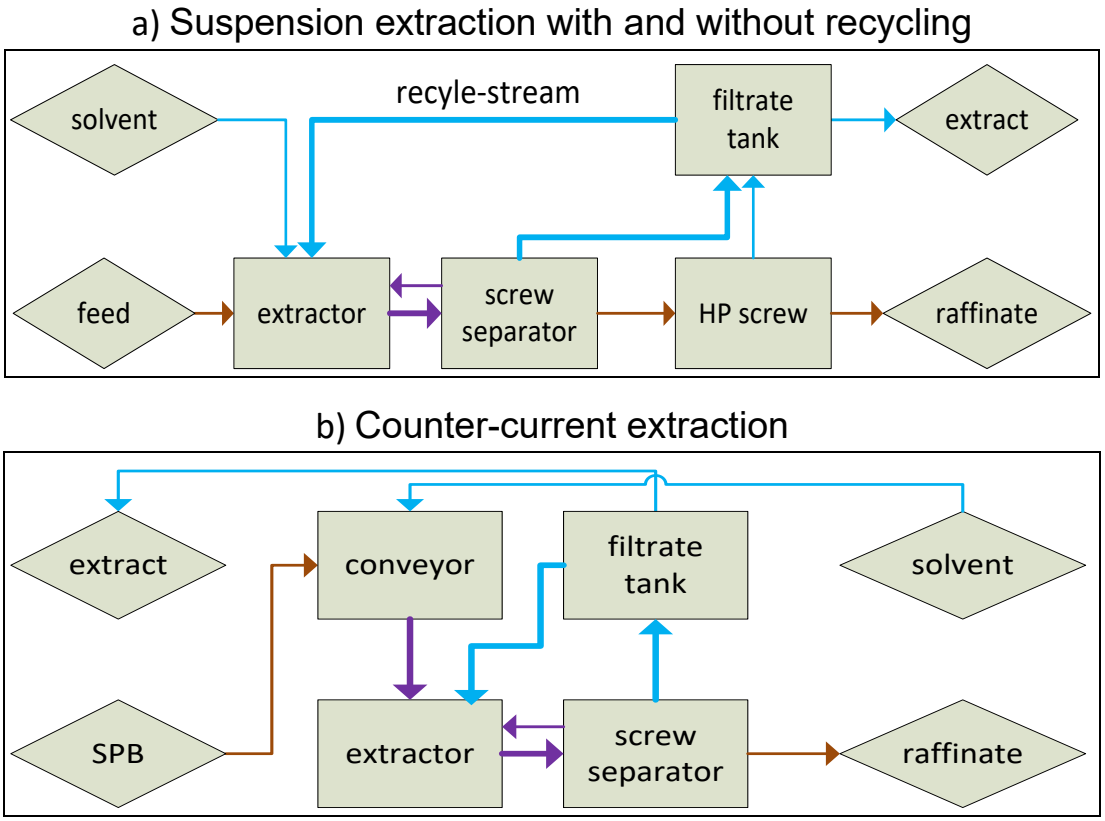

Fig. 4-2: Suspension extraction processes, Diamonds represent streams. Rectangles represent process units. Arrows represent mass flows, Brown: solids, purple: slurry, blue: liquid. **a)** Suspension extraction with and without recycling, **b)** proposed counter-current extraction process; steam pretreated biomass (SPB), conveyor (optional) with initial mixing of moist solids and solvent, extractor as a continuous stirred tank, screw separator as mechanical dewatering device, and filtrate tank. Recycle streams are overflow from the screw press feed tank (not shown) back to the extractor and fluid from the filtrate tank to the extractor.

The first design parameter is the dry matter content in the extraction tank DM-tank. It is used to determine the water intake. The second parameter is the dry matter content of the pressed material DM-out. It determines the amount of raffinate leaving the system. The solute mass and concentration are calculated assuming the identical solute concentrations in the extract and raffinate outflows, due to equilibration on every stage. The specific solvent consumption L/S in g of water input to g of dry solids is not displayed in the process window.

4.4.4.2. Suspension extraction with recycling

The block flow diagram is represented in Fig. 4-2a. The recycling stream is determined through the recycling split factor "y" It is the mass flow ratio of the recycle stream to the filtrate tank inflow. The recycling split factor can take values from 0 to 1. In the case of y = 0, this process is identical to the suspension extraction without recycling. The

largest possible value depends on the feed composition and the design parameters to be selected.

The recycling stream is used as tear stream to calculate the process by iteration. Firstly, random initial positive values for the tear stream amount and concentration are chosen to calculate the same parameters by mass balance. Secondly, the initial values are changed until they match the calculated ones. This is done by minimizing the error calculated as the sum of the squared differences.

The water flow to the extractor is calculated based on the dry matter content in the extractor DM-tank, which is set to 5 wt% and not varied in this study. The calculations are executed similarly to section 4.4.4.1. The recycling split factor is chosen to calculate the recycle flow and concentration. The extraction yield, the extract concentration, and solvent consumption are reported.

4.4.4.3. Counter-current suspension-dewatering extractor

Fig. 4-2b shows a block flow diagram of the proposed Counter-Current suspension-dewatering extraction process. A more detailed description and discussion of the process can be found in 5.3.5

The calculation of the counter-current extraction is based on an overall and a stepwise mass balance. The extraction yield is used to minimize the error of the extract concentration in the overall and the stepwise mass balance.

Only the liquid streams are considered in the mass balance calculation, and the solids are neglected. The underflow is the solvent and solute adhering to the solids particles; the screw press moisture content gives its mass on every stage, which was chosen to be 33 wt% in this study. The dry matter content in the final stage was chosen to be 50 wt%. The overflow is the solvent and solute in the extract phase. The initial solvent input is defined by the solvent usage L/S, which is varied in this study.

For the overall mass balance, a component and total mass balance are done to calculate the flow and composition of the raffinate and the extract, respectively. The overflow input (pure solvent) composition, amount, and feed composition are known. Choosing a random extraction yield allows calculating the solute mass flow in final underflow and overflow.

The stepwise mass balance starts at the last stage for the underflow. Here, the underflow output and overflow input are already known from the overall mass balance. The underflow input is known via the screw press moisture content. With the assumption of thermodynamic equilibrium in every stage, the outflowing concentrations of each stage are equal. Thus, the output overflow concentration equals the output underflow concentration, which is already known. The missing overflow input is calculated by the stepwise mass balance. This calculation scheme is repeated for the previous stages. The final overflow concentration must equal the overall mass balance's overflow output (extract). The extraction yield is varied in an iteration to minimize the error, expressed as the square of the stepwise and overall extract concentration difference. Thus, the extraction yield and extract concentration are calculated for a given number of stages and solvent usage.

4.4.5. SCR scaling

The scale of 3,000 t lignocellulose per year was chosen and assumed to be adequate for the supply of lignin for on-site usage. It represents a small industrial scale in a decentralized approach. The reaction parameters (temperature T and residence time t) were chosen according to the pretreatment strategy developed in this work. Taking the mass flow and the bulk density, the reaction volume V_r is calculated using a plug flow assumption, equation (4-29)). Here, V_r is the volume of the reaction mixture, $\dot{m}_{LCB}$ is the mass flow of the straw and water mixture and ρ_{LCB} its density.

$$V_r = \frac{\dot{M}_{LCB}}{\rho_{LCB} * t} \qquad (4\text{-}29)$$

The reactor volume V_R is calculated using the reaction volume V_r and reactor volumetric fill level. The reactor diameter D is calculated from the volume and the assumed length to diameter ratio L/D, see equation (4-30).

$$D = \sqrt[3]{\frac{4 * V_R}{\pi * (L/D)}} \qquad (4\text{-}30)$$

The minimum reactor wall thickness s_{min} is determined using Barlow's formula (equation (4-31)). This formula is universal and independent of specific construction methods. Here p is the design pressure, which is 1.5 times higher than the water vapor pressure at the regarded reaction temperature and $R_{p0.2}$ is the 0.2% offset yield

strength. This formula results in similar values to the description in the technical guideline AD2000 [97].

$$s_{min} = \frac{p * D}{2 * R_{p0.2}} \quad (4\text{-}31)$$

To calculate the reduced solid dry mass at the outlet of a reactor, the mass flow of dry biomass M_{dryBM} is corrected by using the DS and the severity factor compare equations (4-32) and (4-33).

$$M_{dryBM,out} = M_{dryBM,in} * (1 - DS) \quad (4\text{-}32)$$

$$DS = 0.184 * S_0 - 0.438; for\ 3.0 < DS < 4.7 \quad (4\text{-}33)$$

The mass of the reactor jacket M_{jacket} is determined to enhance the understanding of the calculated reactor dimension, see equation (4-34). Here ρ_{steel} is the steel density.

$$M_{jacket} = \rho_{steel} * 0.25 * \pi * ((D + 2s_{min})^2 - D^2) * L \quad (4\text{-}34)$$

Model parameter of the steel 1.4571 with 0.2% offset yield strength $R_{p0.2}$ equals 157 MPa at 250 °C according to DIN EN 10028-7 and a density of 8000 kg/m^3. For the scaling of the screw conveyor reactor, a volumetric fill level of 40 vol% was assumed. The bulk density inside the reactor is difficult to examine; it is affected by the compaction in the screw feeder, the plug break up in the reactor, and changes with pretreatment progress. Here a density of 100 g/L based on the dry solids is used.

5. Results and discussion

The results of this work have partially been published in papers [6,44,71,98], and a patent was filled [99].

5.1. Autohydrolysis kinetics

In this chapter, two kinetic models are compared and evaluated for the use for autohydrolysis process development, namely pseudo-homogenous Arrhenius rate models and the severity factor based model, compare fundamentals section 2.1.4 and method section 4.4.2. For this purpose, LHW experiments in a batch screening plant were conducted, compare section 4.3.1.2. The resulting solids and liquids were evaluated according to section 4.2. Furthermore, it was investigated how the reaction conditions, in terms of temperature, residence time, and pH, affect the maximum pentose yield and hydrolysate composition.

5.1.1. Arrhenius rate models

The solid mass fraction for hemicellulose after the pretreatment in the LHW batch can be found in Tab. 5-1. The experiments are conducted single fold; the analytical error for this analysis and material is typically less than 10 %.

Tab. 5-1: Hemicellulose mass fraction in solids after LHW pretreatment in 0.03 L batch.

	T [°C]				
time [min]	**170 °C**	**185 °C**	**200 °C**	**215 °C**	**230 °C**
0	0.280	0.280	0.280	0.280	0.280
10	0.273	0.208	0.138	0.034	0.008
20	0.258	0.195	0.069	0.014	0.005
30	0.241	0.152	0.036	0.010	0.003
45	0.211	0.112	0.030	0.008	0.003
60	0.189	0.078	0.022	0.006	0.002
90	0.162	0.057	0.014	0.004	0.001

The hemicellulose content is an essential factor regarding the enzymatic digestibility of lignocellulose. Additionally, the hemicellulose fraction in the solid is regarded as a potentially valuable product. In state-of-the-art pseudo-homogeneous Arrhenius models, see section 2.1.4, the hemicellulose concentration is defined as homogeneously distributed across the reaction mixture, including the water content.

This way, the concentration and thus the reaction rate depends on the reactor's solid content; this behavior is not found in LHW experiments. This work compares reactors with different solid content; therefore, a new, more appropriate model is required. Instead of a pseudo-homogeneous concentration, the solid hemicellulose mass fraction in the lignocellulose material will be used. It is independent of the amount of water surrounding it. In order to predict the solubilization or conversion of the solid hemicellulose, a kinetic model describing the change in the solid hemicellulose composition w_{HC} was set up, as described in section 4.4.2.1. A fit of the Arrhenius constants to the experimental data for the first and second reaction order was conducted.

In Fig. 5-1 experimental data points and the model results are represented. In Tab. 5-2 and Tab. 5-3, the Arrhenius constants, the RMSE, and the resulting rate constants are displayed. The initial hemicellulose solid fraction is $w_{HC,0} = 0.28$. The first reaction model describes the experimental data precisely at low temperature (and high mass fractions) but fail at high temperatures (and low mass fractions), compare Fig. 5-1 c) and d). The second order rate model is a precise description of experimental data at high temperatures and (and low mass fractions) acceptable at low temperatures (and high mass fractions). However, the overall RMSE based on the fit of $k_{1,0}^{n}$ and E_A/R shows that, for the tested temperatures, the first order reaction kinetics outperforms the second order kinetics slightly. This is mainly due to the little absolute error at high mass fractions for the first order model.

Tab. 5-2: Arrhenius constants for the hemicellulose conversion step

n		1	2
E_a/R	[K]	16,899	21,505
$k_{1,0}$	[1/s] / [g/gs]	3.6E+12	4.8E+17
RMSE	[-]	0.008	0.010

Tab. 5-3: Rate constants for the hemicellulose conversion step for the investigated temperatures for first and second order and the RMSE.

T	**[°C]**	**170**	**185**	**200**	**215**	**230**
$\boldsymbol{k_1^{n=1}}$	[1/s]	9.8E-05	3.4E-04	1.1E-03	3.3E-03	9.3E-03
$\boldsymbol{k_1^{n=2}}$	[g/(gs)]	4.0E-04	2.0E-03	8.8E-03	3.5E-02	1.3E-01

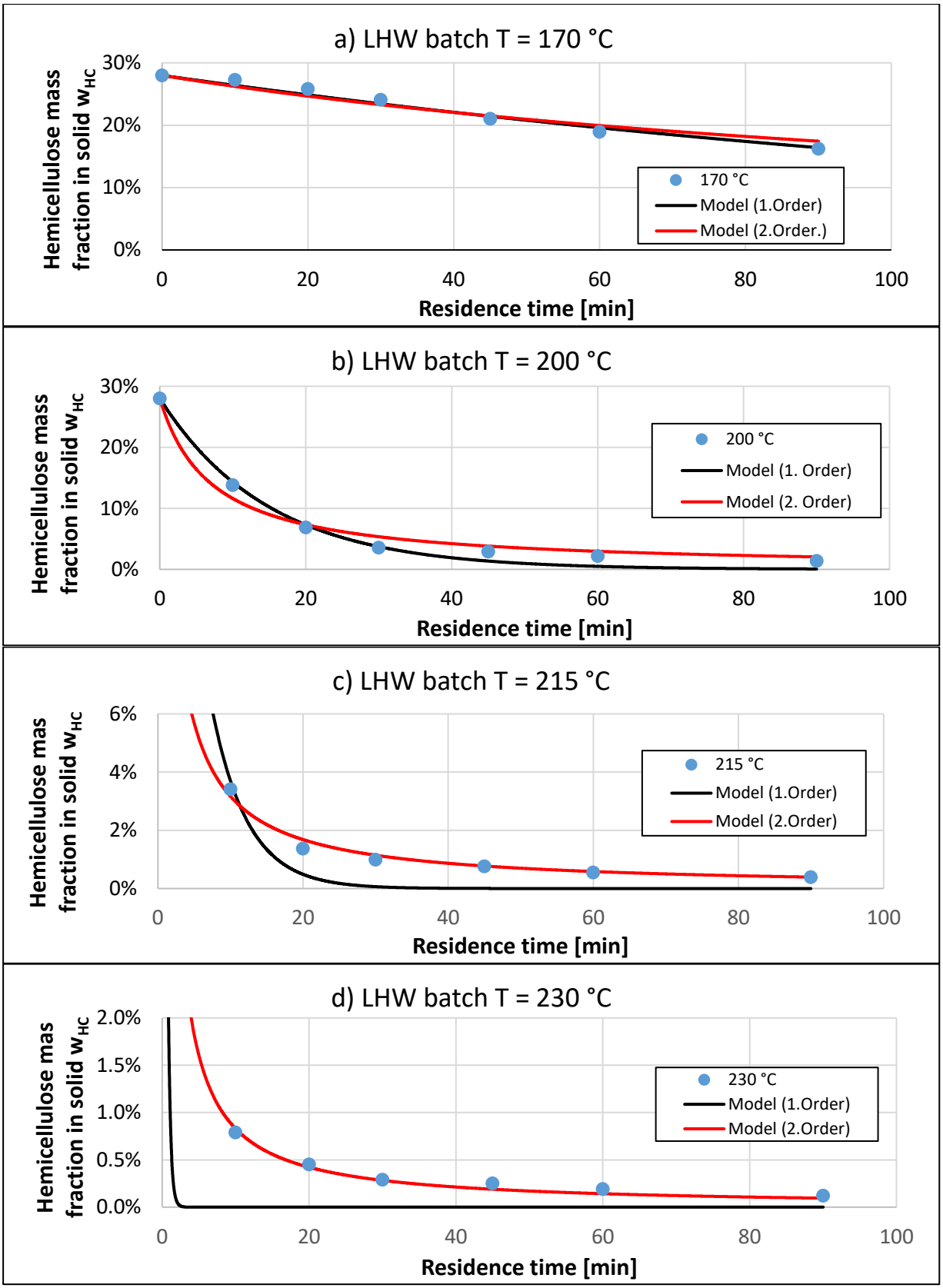

Fig. 5-1: Hemicellulose mass fraction in lignocellulose solid phase profil in a LHW batch reactor during autohydrolysis at, **a)** T = 170 °C, **b)** T = 200 °C, **c)** T = 215 °C, **d)** T = 230 °C

The model for $n = 1$ will be used to determine the hemicellulose conversion X_{HC} for the presented plant concepts, compare section 5.2.5. It is assumed that the calculation of the hemicellulose conversion with the batch model serves the purpose of this work to identify and evaluate promising reactor types and plant concepts suitable for an industrial process. It has be noted, that the calculated energy of activation is apparent and not comparable to the energy of activation that describes the molar concentration change.

However, the prediction of the amount of remaining solids after pretreatment will requires the modelling of other biomass constituents, e.g., cellulose, lignin and inorganics. This is expected to be difficult, since these components show significant but small variations during pretreatment and the natural variation in biomass composition are relatively large. In the following it is investigated, whether a rate model based on the severity factor allows to describe the pretreatment with more precision and less effort.

5.1.2. Severity Factor

The severity factor S_0, compare section 2.1.4, is used to analyze the reaction kinetics in the solid and liquid phase and describe other chemical phenomena. This approach aims to find a pretreatment strategy to fulfill the expected product and process requirements. The degree of solubilization of experimental data points according to equation (4-2) is displayed in Fig. 5-2 as a function of S_0. It can be seen that the different temperatures result in data that resemble a nearly linear dependency, compare equation (5-1), with a small plateau between $4.5 < S_0 < 5.0$.

$$DS = (0.1841 * S_0 - 0.4378) \pm 0.03, \qquad R^2 = 0.940\,, \qquad for\ 3.0 < S_0 < 4.7. \tag{5-1}$$

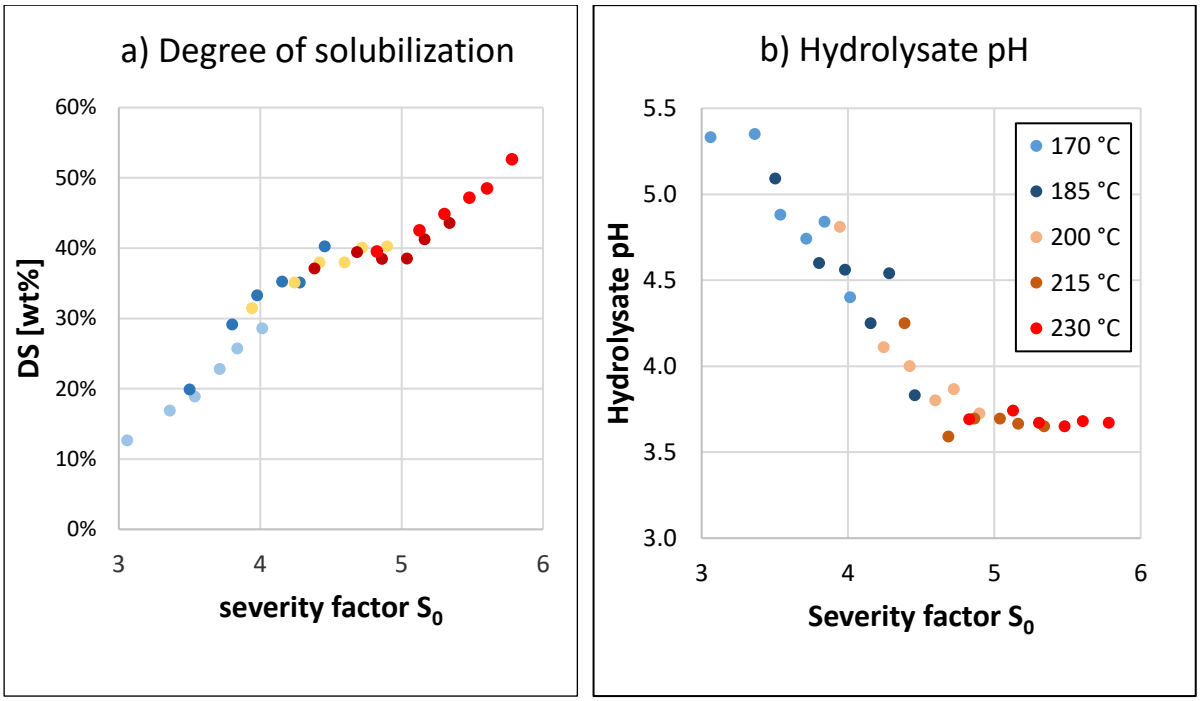

Fig. 5-2: Autohydrolysis experimental data for temperatures from 170 °C to 230 °C versus S_0, **a)** Degree of solubilization (DS). And linear fit between $3.0 < S_0 < 4.7$, **b)** Hydrolysate pH.

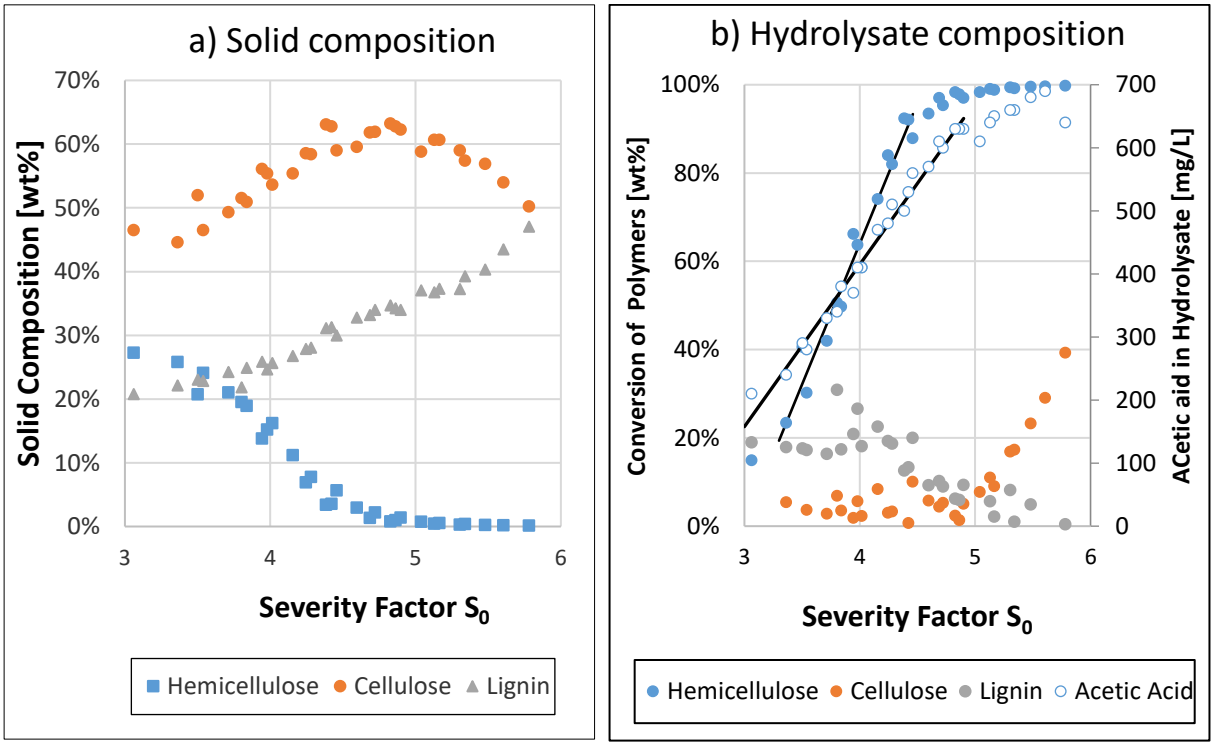

Fig. 5-3: **a)** Solid mass fractions of the lignocellulose components hemicellulose, cellulose, and lignin as a function of S_0, **b)** Experimental data for the solid polymer conversion versus S_0 and a linear fit between $3.3 < S_0 < 4.46$. for the hemicellulose conversion. Released acetic acid concentration and linear fit between $3.0 < S_0 < 4.9$.

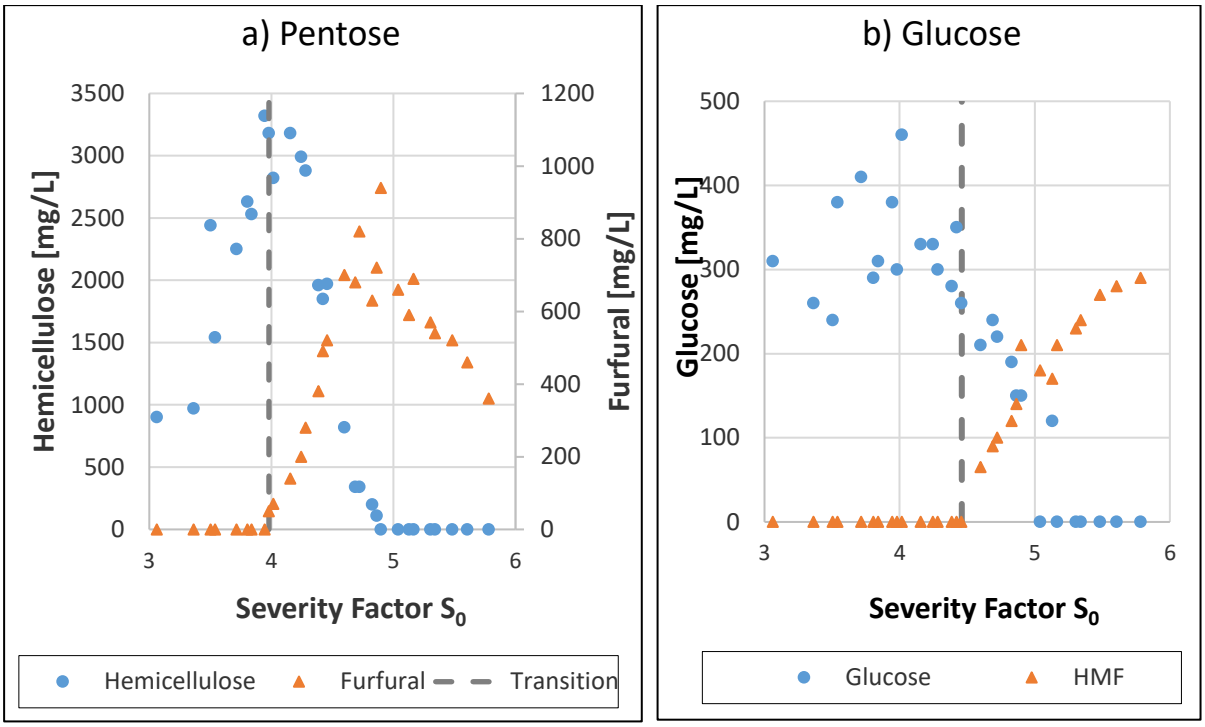

Fig. 5-4: **a)** Fluid phase composition versus S_0 for overall hemicellulose content (monomers and oligomers) and furfural, **b)** Fluid phase composition versus S_0 for overall glucose content (monomers and oligomers) and HMF.

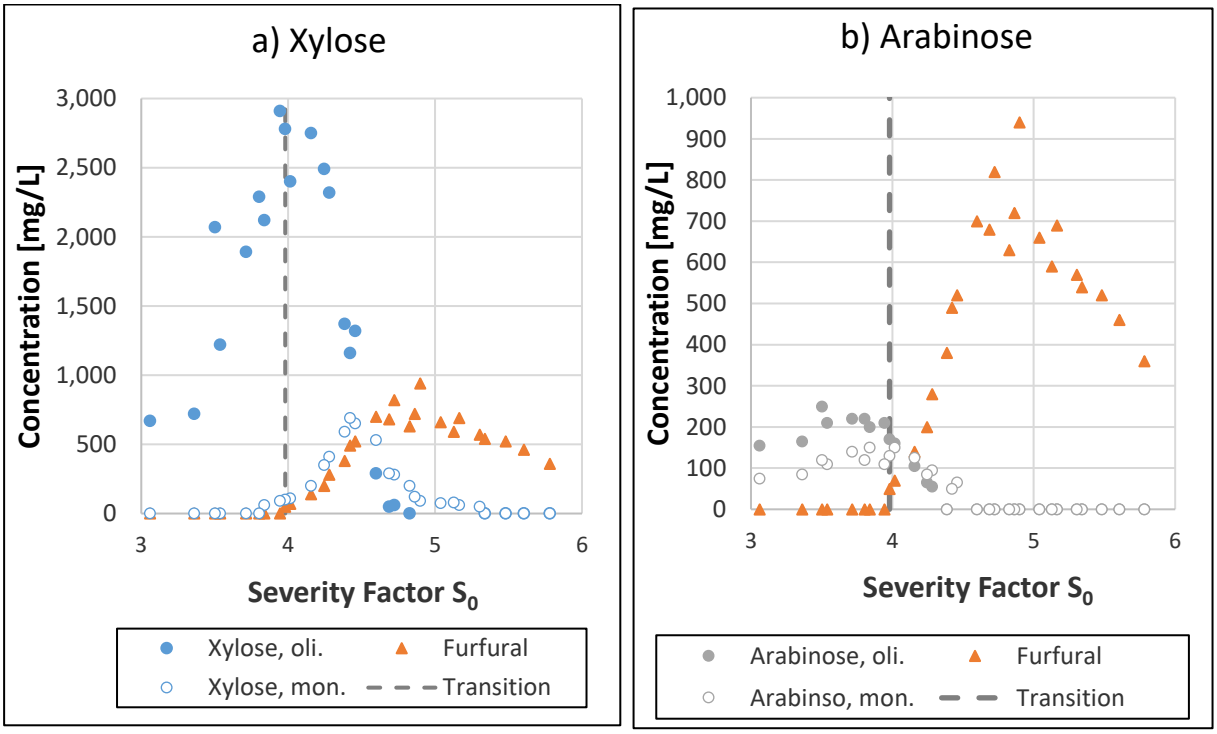

Fig 5-5: Fluid phase composition versus S_0 for monomers and oligomers and furfural, **a)** Xylose, **b)** Arabinose.

Also, the solid mass fraction of the main lignocellulose constituents results in continuous curves when plotted against S_0, see Fig. 5-3a. The courses of the curves are in good agreement with the theory of solubilization during autohydrolysis discussed in chapter 2.1.3. Hemicellulose is hydrolyzed to water-soluble oligomers, and it is vanished at $S_0 = 5.0$, while the inert cellulose remain in the solid, thus its mass fraction rises. The cellulose mass fraction is reduced at a severity factor greater than 5.0 since the cellulose is party hydrolyzed under these harsh conditions. The lignin mass fraction with an initial 22.4 wt% follows a continuous increase at 20.8 wt%. In the linear part of the hemicellulose conversion X_{HC} , see Fig. 5-3b, a polynomial of first degree was fitted to calculate a function of the severity factor S_0, see equation (1).The cellulose conversion of less than 10 wt% is constant until it increase at $S_0 > 5.0$. Lignin conversion of app. 20 wt% is constant until it drops at $S_0 > 4.5$. The plateau in Fig. 5-2 corresponds to the sum of conversion change at $4.5 < \mathrm{S_0} < 5.0$, as can be seen in Fig. 5-3b. The formation rate of acetic acid in the hydrolysate, Fig. 5-3b, shows a linear dependency to the severity factor, thus following the first-order rate. The weak acid is released early and catalyzes the hydrolysis of hemicellulose.

$$X_{HC} = (0.5839 * S_0 - 1.7027) \pm 0.06,\ R^2 = 0.965\,,\ for\ 3.3 < \mathrm{S_0} < 4.46 \qquad (5\text{-}2)$$

$$C_{AA} = (277.26 * S_0 - 614.03) \pm 14,\quad R^2 = 0.984\,,\quad for\ 3.0 < \mathrm{S_0} < 4.9 \qquad (5\text{-}3)$$

The hemicellulose and furfural concentrations in the hydrolysate are plotted against $\mathrm{S_0}$, see Fig. 5-4a. With increasing severity, it can be seen that hemicellulose (monomers and oligomers) accumulates in the liquid phase. At $\log(R_0) = 4.0$ the presence of furfural is detected (detection limit of 100 mg/L), its concentration increases with the severity, whereas the hemicellulose concentration declines since furfural is formed from hemicellulose. Thus, using the severity factor, the transition between solubilization-dominant $(\mathrm{S_0} < 4.0)$ and degradation-dominant $(\mathrm{S_0} > 4.0)$ conditions regarding hemicellulose can be identified. Once no hemicellulose is left in the hydrolysate at $S_0 = 5.0$, the furfural concentration starts to drop with the severity. The significantly lower rate of furfural formation than hemicellulose degradation and the furfural conversion at $S_0 > 5.0$ indicate the high reactivity of furfural in degradation reaction like furfural resinification and condensation [38]. The conditions under which furfural degrades correspond to lignin's “formation” (negative conversion rate). Since

lignin is not detected but measured as solid residue after acid hydrolysis, the solidified furfural degradation products may explain the observed formation of lignin which can also be called pseudo-lignin. Similar considerations for soluble hemicellulose formation and degradation apply to glucose and its reaction product HMF at a much smaller concentration level, as shown in Fig. 5-4 right. The glucose content (oligomers and monomers) derived from cellulose, compare cellulose conversions, in the hydrolysate stays constant until $S_0 = 4.5$; at higher severity HMF is formed and accumulates, and a substantial decline of the glucose content is detected. Glucose degradation and HMF formation occur at the same rate; thus, HMF is regarded stable and not react further.

The hemicellulose in the hydrolysate consists of xylose and arabinose in oligomeric and monomeric form. Despite the oligomers consist of both monomers, the xylose and arabinose are plotted separately in Fig 5-5 to investigate their hydrolysis rates. Xylose shows an apparent reaction cascade characteristic with the concentration peak location increasing in S_0 from oligomers to monomers to furfural, agreeing with their educt and product relationship. The arabinose occurs in a lower frequency and degrades at lower severity factors, and its monomers' and oligomers' peak locations are close to each other thus, arabinose is thermally more labile than xylose. Due to the coincidence of the arabinose monomers' peak location with the start of furfural occurrence, it is postulated that the first furfural detected is derived from arabinose.

Comparing the hemicellulose concentration peak location in the hydrolysate at $S_0 = 4.0$ and the solid hemicellulose conversion at the same condition ($X_{HC} = 63\ wt\%\ at\ S_0 = 4.0$) it is apparent that a full recovery of the hemicellulose in the liquid phase is not possible in a batch extraction. Assuming the selectivity to hemicellulose is 100%, the ratio of the reaction constants of product degradation to product formation is 0.25, compare equation (2-11). It is concluded that the activation energies of product formation and product degradation are similar, since several temperatures resulted in the same maximal yield of hemicellulose.

To gain the cellulose-derived glucose in enzymatic hydrolysis, the cellulose accessibility, affected by the particle size and the remaining hemicellulose content [100], is one purpose of the pretreatment. Since, at complete hemicellulose conversion, a glucose yield of less than 100% is reached, it is suspected that the pseudo-lignin formation decreases the cellulose accessibility. Thus, batch autohydrolysis pretreatment does not allow a full glucose recovery.

The rate-based kinetic does not show a clear reaction order and is more complex to apply without gaining more information. Due to the severity factor's simplicity in application, (linear) dependencies of parameters on the severity factor make it a powerful tool in developing autohydrolysis reaction processes of lignocellulosic materials. Thus, this approach will be used in the following chapters.

5.1.3. Constant pH (pH-Buffers)

As concluded above, a full-fractionation in batch conditions is not possible. Since the reaction sequence involves different components and different types of reaction – deacetylation, hydrolysis, dehydration, and further – their dependency on the pH cannot be assumed to be similar. Moreover, product formation and degradation rates may be affected by the pH differently, which would affect the maximum product yield, compare to fundamental section 2.2.5. Hydrothermal pretreatment in 0.03 L LHW was conducted with and without pH buffers to test this hypothesis. The reaction conditions can be found in Tab. 4-3. In this section, a wide range of acidic pH values are investigated to clarify its effect on pentose recovery in oligomers and monomers and the furfural formation simultaneously.

Each pH condition results in data sets similar to Fig. 5-4. The peak of each component can be characterized by its peak concentration and its location on the S_0 axis. To display the effect of the pH, the components' peak heights are plotted versus this location in Fig. 5-6. The components' peak height corresponds to the heights concentration detected. The peak location change with the pH describes whether the production of this compound is accelerated or delayed.

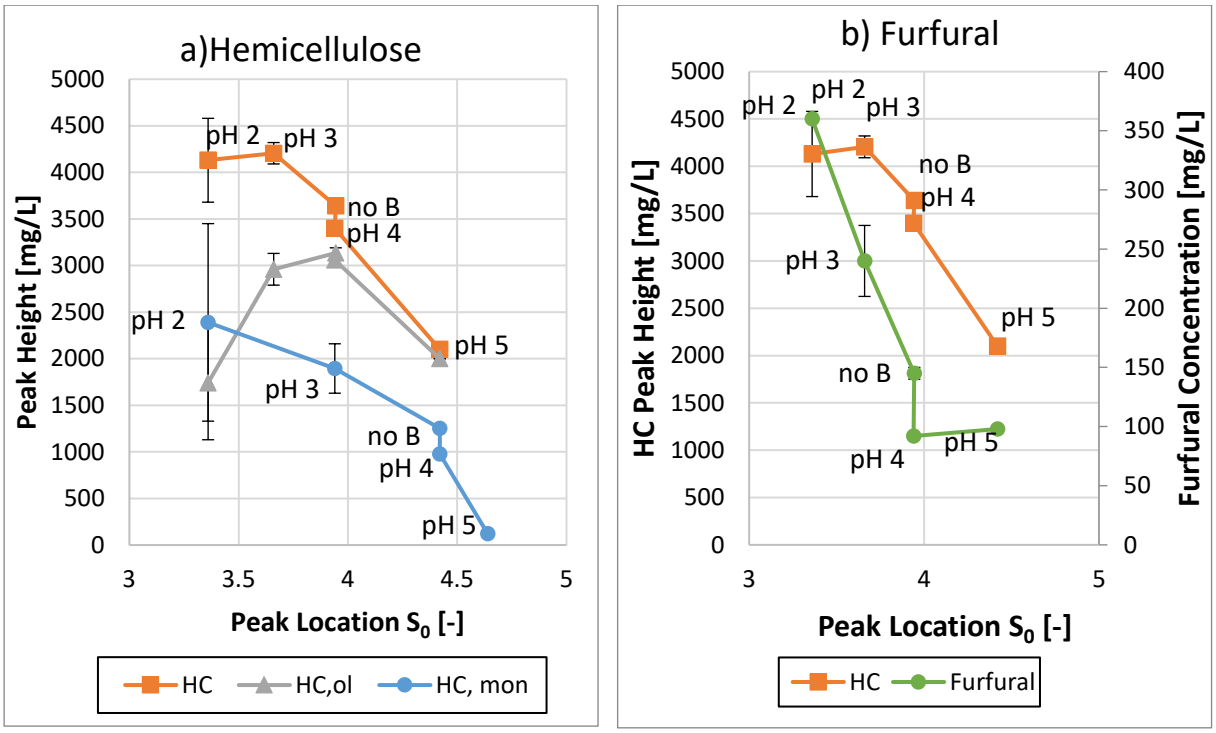

Fig. 5-6: Peak heights (Concentrations) and peak locations (Severity factor) of hemicellulose derived substances under different constant pH values in the reaction mixture, **a)** Individual components peak locations, **b)** HC Peaks and furfural concentration at this severity factors. **HC:** Hemicellulose total. **HC,ol:** oligomer hemicellulose, **HC,mon:** monomer pentoses. **No B:** no Buffer used. Error bars for pH4 and pH5 are not available. Lines are for graphic clarity only.

In Fig. 5-6a, the components' peaks are mapped for different pH values. It can be seen that the locations and height of the peaks depend on the pH. Moreover, the conditions without buffer are between pH three and pH four for all components. The monomer peaks are higher and "earlier", at lower S_0, the lower the pH. In contrast the oligomer peaks run through a maximum at pH 3-4. The sum of the monomers and oligomers is the total hemicellulose concentration. Its peak map shows that increasing pH results in decreasing heights and increasing locations. Due to the uncertainty of the results at low pH (see error bars) the concentration difference from pH 2 to no buffer used is unclear. Assuming a solid's hemicellulose content of 28 wt%, at pH 3 a hemicellulose recovery of 75 wt% is reached, and without buffer, the hemicellulose recovery is 65 wt%. Thus, a full-fractionation is impossible with a constant pH between 2 and 5. Nevertheless, a low pH allows to operate the reactor at a lower temperature and thus pressure, which is beneficial for the investment and operation costs.

In Fig. 5-6b, the total hemicellulose peak map is plotted with the respective furfural concentration at the same severity factor. A strongly declining furfural concentration

with the pH is observed. At a pH value of 2 and 4, the hemicellulose concentration increases, but the furfural concentration increases even more substantially. The hemicellulose to furfural ratio is lowest at pH 2. The use of no buffer results in relatively low furfural concentrations. The highest hemicellulose to furfural ratio can be found at pH four. Both the hemicellulose and furfural concentrations at pH five are almost the lowest. Here all reactions step rates are significantly reduced.

To increase the total hemicellulose yield or increase the hemicellulose to furfural ratio, the low pH of 2-3 or pH 4 are relevant, respectively. It seems that by coincidence, the absence of buffers results in beneficial performances regarding hemicellulose recovery and furfural production. Thus, the benefits of a modified pH on hydrolysate quality are minor, and it is uncertain whether the costs for chemical purchase, storage, mixing – and neutralization units would be justified.

5.1.4. Conclusion

The Arrhenius rate-based models are suitable for describing the hemicellulose autohydrolysis with sufficient precision. The proposed model is independent of the reactor's solid content. Thus, it is expected that it can be used for a wide range of solid contents. However, other pretreatment characteristics, e.g., the degree of solubilization and concentration profiles in hemicellulose sequential reaction, are complicated to describe.

The severity factor is a simple model designed to analyze the hydrothermal processing of lignocellulose and allows a fast and deep understanding of the underlying mechanism of hydrothermal pretreatment and allows the reactor's design at a reasonable velocity.

It was shown that the severity factor is an appropriate tool to describe the residence time and temperature combination that results in a maximum yield of the desired intermediate product. Additionally, it was found that the reaction temperature does not affect the maximum product yield in batch. Thus, there is no single optimal temperature regarding the product yield.

The hemicellulose recovery is limited to 60-65 wt% in a suspended autohydrolysis pretreatment due to the thermal lability of the gained products. The maximal yield depends on the formation and degradation constants ratio in a sequential reaction,

compare to section 2.2.3. This ratio could not be affected towards a higher hemicellulose yield by the pH in an acetic region of pH 2-5. The absence of pH modifying agents resulted in a maximal hemicellulose oligomer recovery.

For each sequential reaction, the maximum yield of the intermediate product can be found at an optimal residence time for each temperature. Thus, aiming at a maximal yield, the used chemical reactor must have a sharp residence time distribution as in a batch or a plug flow reactor. A continuous stirred tank reactor is to be avoided [75].

5.2. Reactor selection and plant design

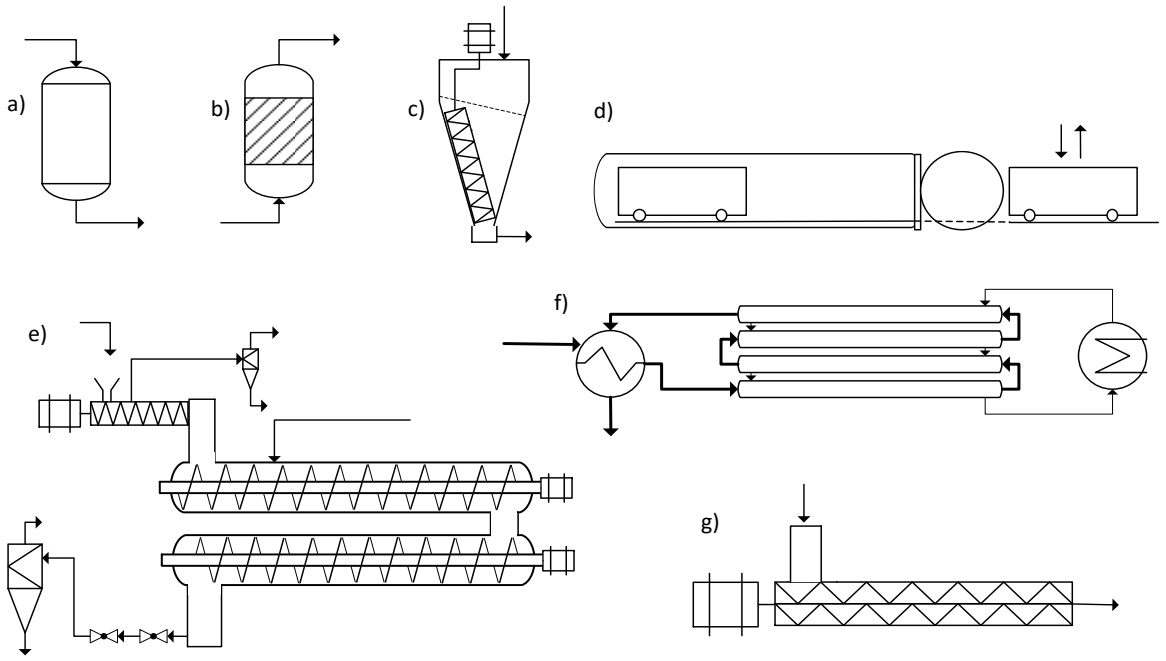

Fig. 5-7: Reactor types evaluated for the autohydrolysis process in a production scale, **a)** LHW or Steam Batch reactor, **b)** flow-through reactor, **c)** solids mixer (batch), **d)** horizontal batch reactor with rails **e)** screw conveyor reactor, **f)** plug flow reactor, **g)** extruder.

In literature, various reactor types and configurations are elevated individually for an industrial full fractionation approach, compare sections 2.2. This work systematically reviews all relevant reactor types to evaluate strengths and drawbacks and clarify improvement potential. The most promising reactor type will be selected based on a method that allows the use of available data with high uncertainty, compare section 4.4.3. The method reviews reactor concepts for industrial application and development demand based on water consumption, heat demand, handling, scalability, complexity, and operation mode. Based on the reactor selection, a processing concept is proposed, and a basic design study is carried out to investigate the scalability to production scale.

5.2.1. Batch reactors

A batch reactor shows a fast heat transfer if direct steaming is used for heating and can operate at several L/S ratios. It is cheap to design, scale, and relatively simple to operate. The heat consumption is substantial, the challenging heat recovery, and the hemicellulose yield is limited to the degradation reactions.

Vertical batch reactor

The LHW batch is based on conductive heat transfer, and its stirrer is a complex part, compare section 4.4.3.1. No stirrer is needed for the steam batch reactor, but the loading and unloading procedure is regarded as one complex part since the flowability of the moist bulk material is challenging.

The solids mixer is a steam-based batch reactor with improved heat transfer. The loading and unloading and the solid agitation under pressure are two complex parts.

Horizontal batch reactor with rails

A horizontal direct steamed reactor with rails to load and unload the biomass on a wagon-like construction is often used for impregnation or thermal modification of timber. The loading can be realized very time-efficient, and steam can be used for a fast heat transfer. A considerable length to diameter ratio allows for thin walls. The mass transport and the volumetric reactor loading are poor. The latter is due to the biomass's uncompressed nature and the reactor's poor volume usage. Its design is complex regarding the wagon construction, the high-pressure reactor opening across the diameter, and the rail system outside the reactor. The material handling outside the reactor also is complex since the biomass and water must be premixed and loaded onto the wagons. The necessity of unloading the material from the wagons adds to the plant's complexity. This reactor shows complex parts at the diameter-wide fast closing system, the rails, and the unloading technique.

5.2.2. Semi-batch reactors

Flow-through reactor

In the flow-through reactor, water is pumped through the biomass bed to solubilize products and remove them from the reaction zone. The inherent solid-liquid separation is the reactor's strength, resulting in a solid treatment time and a shorter liquid residence time. Thus, degradation reactions in the hydrolysate may be limited. The heat transfer based on saturated steam is fast and heats the bed homogeneously [22]. Cooling the outflowing hydrolysate to preheat the inflowing water can reduce heat consumption significantly [22]. Further issues are the convective heat transfer based on liquid water, the residence time distribution of the hydrolysate, the inhomogeneous solid pretreatment (temperature profile), and the usually high L/S.

Additionally, the loading and unloading process might be challenging in a commercial process due to the poor flowability of the biomass. The biomass bed's compression depends on the water velocity, which increases at larger scales. Thus, stabilizing mechanisms are necessary. The biomass is loaded into a cartridge to be loaded and unloaded; thus, a heavy-duty crane is required. The design has low scalability and is prone to a numbering-up for large industrial scales. The complex parts are the crane, the cartridge with bed stabilizers, the diameter wide opening, and the unloading techniques.

5.2.3. Continuous reactors

Extruder reactor

The combination of thermal and mechanical treatment using an extruder has been intensively studied for biorefinery processes in the past years [23]. The strength of this continuous process is the operation at very low L/S, and it possesses fast conductive heat transfer properties. Due to the small diameters, high pressures and temperatures can be applied, which shortens the residence time. Therefore, a potentially high degree of controllability and an expected process intensification is expected. However, it is challenging to contain high steam pressures inside the machine. It could be done with a dynamical sealing and temperature zone in the extruder or external pressure barriers.

Additionally, the size reduction is beneficial for the subsequent enzymatic hydrolysis. Downsides are the large consumption of electrical energy and the small reaction volumes. Furthermore, residence times of 10 minutes and more are hardly realizable, requiring high temperatures and pressures. The high equipment costs make an extruder cascade or numbering up economically challenging. The extruder-based pretreatment is promising for lignocellulosic ethanol production since a full-fractionation of the sugars, and the lignin is not required. In multi-step processes, biomass washing and solid-liquid separation become critical units, technically challenging with finely ground particles produced by an extruder. In unpublished experiments, it was shown that dry and wet extrusion of wheat straw yields 80% of particles smaller than 50 µm.

On the one hand, this is challenging for washing and solid-liquid separation; on the other hand, it is promising for enzymatic digestibility. This size reduction could also be

achieved with much cheaper equipment. Concluding a pretreatment plant aiming at a full-fractionation may not be feasible by only using extruders, but it might be a suitable apparatus to combine with other units. The challenging parts are the two pressure barriers for the biomass injection and release from the pressurized zone.

Screw conveyor reactor

A horizontal pressure reactor with an internal screw conveying mechanism is called a screw conveyor reactor (SCR). It possesses a top opening at one side and a bottom opening at the other side. This reactor type can be operated with several tubes stacked on top of each other and is equipped with a solids pressure feeder and a solids release system. For both, different machine types or solutions are available, see section 3.6.5. The screw conveyor reactor is designed for industrial pulping of annual lignocellulose but is rather difficult to scale down. Operation at low but flexible L/S ratios is possible; heat transfer usually is realized with saturated steam. The steam pressure can also be used to control the reactor temperature. The moving action of the screw and the use of saturated steam allow for fast heat transport. The screw elements move the material through the reactor and presumably reduce the residence time distribution significantly compared to an extruder. The material is processed in an uncompressed manner and takes approximately 40 vol% of the reactor volume. The length to diameter ratio is typically around 9, which allows for thin reactor walls. The number of stacked tubes for a reactor (compare section 3.6) allows even for a further reduction of the diameter. Also, the residence time and throughput are not directly coupled due to the possible stacking of the reactors. A disadvantage is the coupling of solids and liquid residence time. A fiber washing step is applied to separate the inhibitors prior to enzymatic hydrolysis. The complex parts are the feeding and the release system and the operation of the augers under varying conditions of the bulk materials.

Plug flow reactor

Finely ground lignocellulose can be conveyed into pressure reactors in the form of a slurry. Solid concentrations of 13.5 wt% can be realized [27], which equals a L/S = 7. This allows the use of a plug flow reactor (PFR), which is promising due to its very low complexity, low investment costs, and good scalability. The heat transfer can be realized with external heating/cooling fluids that allow easy heat recovery and integration. Cooling the reaction medium provides heat to preheat the medium before the high-temperature zone. The residence time of the solid and liquid phases are

coupled. The particle size reduction is potentially energy-intensive and beneficial for the subsequent enzymatic hydrolysis. Low water consumption in this reactor type cannot be realized. The required solid/liquid separation with very fine particles is the main process limitation in a full fractionation approach. Complex parts are the pressure release of the pretreated slurry and the extraction/ solid-liquid separation of finely ground particles.

5.2.4. Reactor type evaluation

The reactor evaluation regarding their performance parameters can be found in Tab. 5-4. Here, the original and normalized scale alongside the evaluation product, compare section 4.4.3. Here the original and the normalized scores are presented. The normalization scales the original score to a scale from one, for the poorest performance, to ten, for the best performance for each performance criterion. The reactor evaluation on the normalized scale allows comparing their characteristics. The product of all six elevation parameters on this scale allows to rank the reactors, with the best possible score of 1,000,000 (10E6) points.

Tab. 5-4: Reactor performance evaluation. Original and normalized scale. **B:** Batch. **SB:** Semi-Batch. **C:** Continuous. **SCR:** Screw Conveyor Reactor.

	LHW [B]	Solids Mixer [B]	Horizontal [B]	Steam [B]	Flow-through [SB]	Extruder [C]	SCR [C]	Plug Flow [C]	x_a (worst)	x_w (best)
					original					
Water consumption	15	5	2	1	7	0.8	1	6	15	0.8
Heat demand	18	7	4	3	7	0.8	1	7	18	0.8
Handling	2	2	2	2	6	1	1	1	6	1
Scalability	1	5	5	5	1	1	10	5	1	10
Complexity	1	2	3	2	4	2	3	2	4	1
Continuous	1	1	1	1	5	10	10	10	1	10
					normalized				y_a (worst)	y_w (best)
Water consumption	1.0	7.3	9.2	9.9	6.1	10.0	9.9	6.7	1	10
Heat demand	1.0	6.8	8.3	8.8	6.8	10.0	9.9	6.8	1	10
Handling	8.2	8.2	8.2	8.2	1.0	10.0	10.0	10.0	1	10
Scalability	1.0	5.0	5.0	5.0	1.0	1.0	10.0	5.0	1	10
Complexity	10.0	7.0	4.0	7.0	1.0	7.0	4.0	7.0	1	10
Continuous	1.0	1.0	1.0	1.0	5.0	10.0	10.0	10.0	1	10
Product	82	14,228	12,615	25,074	205	70,000	390,797	158,524	1	10

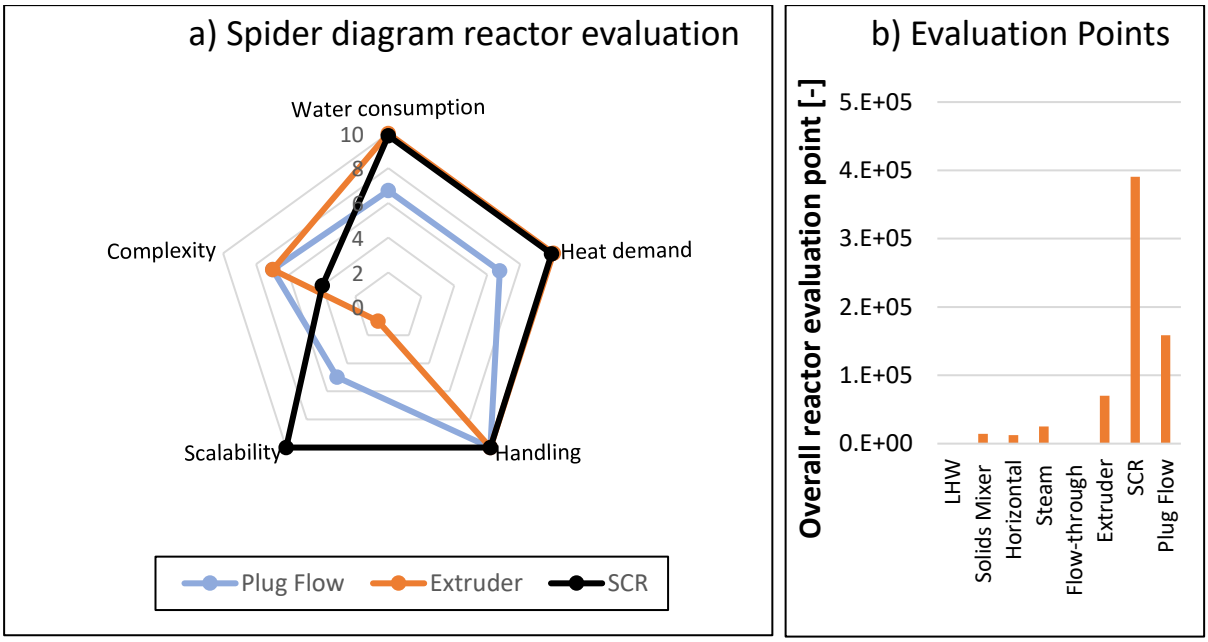

Fig. 5-8: Continuous reactor performance evaluation, **a)** Spider reactor diagram for continuous processes, **b)** Overall evaluation of all investigated reactor types.

The intensively studied flow-through pretreatment reactor scores worst in the performance criteria handling, scalability, and complexity. It gets only intermediate scores in the three remaining performance criteria water consumption, heat demand and operation mode. It is concluded that the process develop for the flow-through pretreatment must be improved on all performance aspects. An improvement on a single criteria will not be enough to compete with other reactor concepts. Thus, it is not likely for this reactor type to reach an industrial readiness in the near future.

In Fig. 5-8, the three continuous reactors' characteristics are displayed in a spider diagram. The weakness of the extruder concept is the poor scalability due to the small reactor volumes and limitations in residence time, resulting in rank 3. The plug flow reactor's highest rating is the handling; other parameters, besides the continuous mode, are seven points or lower; thus, it reaches the second rank. The SCR lowest score can be found in the complexity due to the number of parts that need to be investigated with special care, namely the continuous feeding and release of biomass to/from the pressurized reactor and the biomass transportation with auger screws. All other parameters are at the scale maximum. Thus, the SCR is evaluated as the most promising reactor type and used for further concept development.

Using a SCR does not allow to increase the hemicellulose yield to a higher value than 60-65 wt%, compare section 5.1. In the next chapter a novel processing concept is

presented that is based on two sequential SCRs, in an approach similar to the in-situ product removal.

5.2.5. Plant design: Two-step pretreatment

To overcome the limited hemicellulose yield in a single reaction step due to the sequential reactions, compare sections 2.2.3 and 5.1.2 is a central task in the plant design. The reactor should have a sharp residence time distribution; thus, a twin-screw extruder is excluded.

The flow-through pretreatment is an relevant approach applying a in-sito product separation increase the yield, unfortunately it ahows many hurdles in the process development.Other published methods to deal with a sequential reaction, compare section 2.2.3, are not applicable to lignocellulose hydrolysis: The reaction temperature does not affect the maximal product yield, compare section 5.1.2. The recycling of unreacted xylan, compare Fig. 2-7, is not applicable eighter. The inert inputs to the reactor - lignin and cellulose – cannot be separated from the educt xylan; thus, the separator in the secept cannot be used. Recycling unreacted xylan along with the remaining solids, would radically increase the reactor input (inert compounds). The large inert content in the feed would require a large purge stream, therefore ejecting unconverted educt and lowering the yield.

The proposed process combines the findings from the kinetics investigation in section 5.1, namely a pentose recovery of 60 -65 wt% is possible in a single step, but the xylan hydrolysis needs to be continued to achieve good enzymatic hydrolysis performance and the principles to deal with sequential reactions, namely to remove the product before it can degrade but simultaneously continue the conversion of the educt.

A two-step pretreatment strategy with an intermediate hemicellulose extraction unit is proposed to overcome the challenges above; see Fig. 5-9. It is estimated that no more than two reaction steps are required to reach a pentose recovery above 80 wt%. Both sequential SCRs hydrolyze and dissolve the hemicellulose partly. The first reaction is stopped just before the formation of furfural takes place. At this reaction condition, the hemicellulose concentration in the liquid phase is maximal. Following hemicellulose extraction makes it available for further processing and unavailable for degradation and unwanted side reaction in the next reactor. The second reactor further increases (i) the hemicellulose conversion required for a high glucose yield in the following enzymatic hydrolysis of the cellulose to glucose and (ii) the hemicellulose yield. Based

on the two-step pretreatment concept, the batch reaction kinetics, the reactor design, and reactor scaling are investigated regarding:

- Parameters affecting the reactor dimensions,
- Effect of reaction temperature on the reactor dimensions,
- Effect of the tube number per reactor on the dimensions, and
- Reactor dimensions for relevant scales.

For the dimensioning of the screw conveyor reactor (SCR), equations (4-29) - (4-34) in section 4.4.5 are used; the causal connections between the factors are displayed in Fig. 5-10. One parameter's effect strength and influence on another are evaluated, keeping all other factors constant.

The reactor steel mass, which can be used to estimate the investment costs, here the jacket mass, is affected by the reactor's length, diameter, and wall thickness. The reactor volume is the main parameter, connecting the kinetic and reactor capacity with the reactor dimensions. For a fixed material and throughput, the temperature affects the reactor size in two ways. On the one hand, high temperatures reduce the residence time and thus the reactor volume; on the other hand, it leads to an increase of the corresponding vapor pressure and thus the minimum wall thickness and the reactor mass.

The throughput can be affected by the reactor dimension in the design phase. For an existing reactor set-up, the throughput is affected by the feeder screw speed. It will not increase the internal flow rate, instead increase the reactor filling degree. The rector filling degree must not be too low of too high, due to negative effects in the residence time distribution. Therefore the throughput can only be varied slightly, once the reactor is built. The reactor fillage is also effected by the mixture bulk density, which mainly depends on the biomass type and particle size. This behavior might not be intuitive to chemical engineers, since in liquid or gas phase reactors the input flow rate does increase the throughput and lower the residence time. The SCR throughput cannot be effected by the reactor screw speed, only the linear traveling velocity of the biomass and the residence time will be affected.

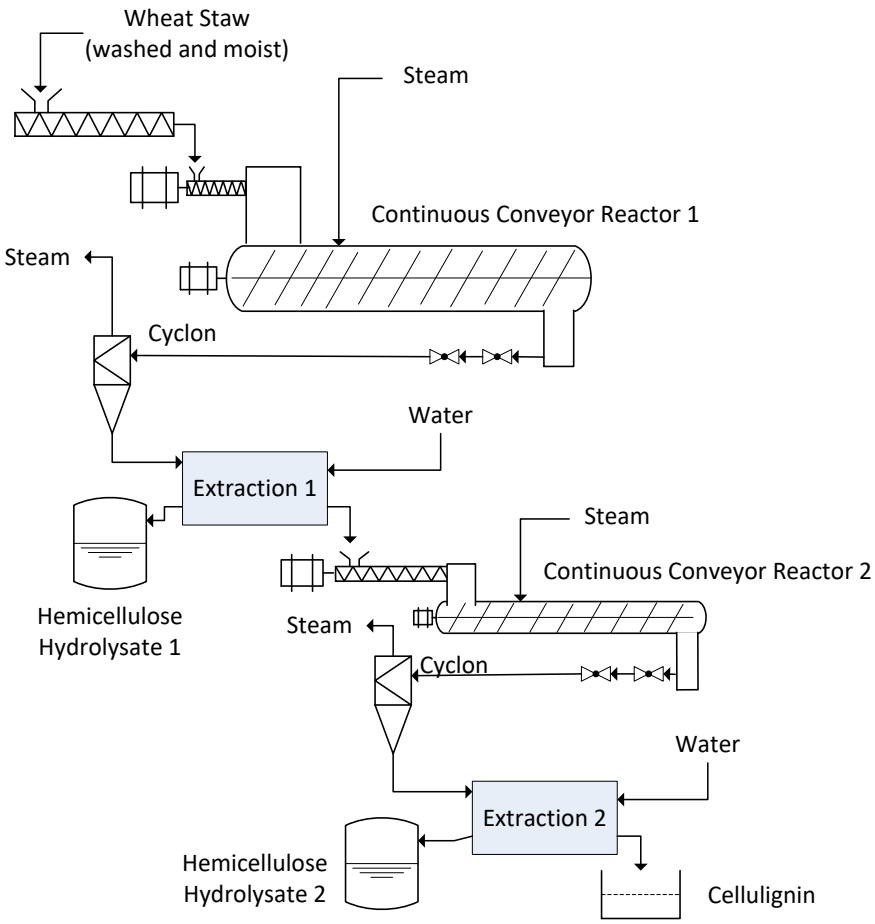

Fig. 5-9: Two-Step pretreatment concept with intermediate extraction.

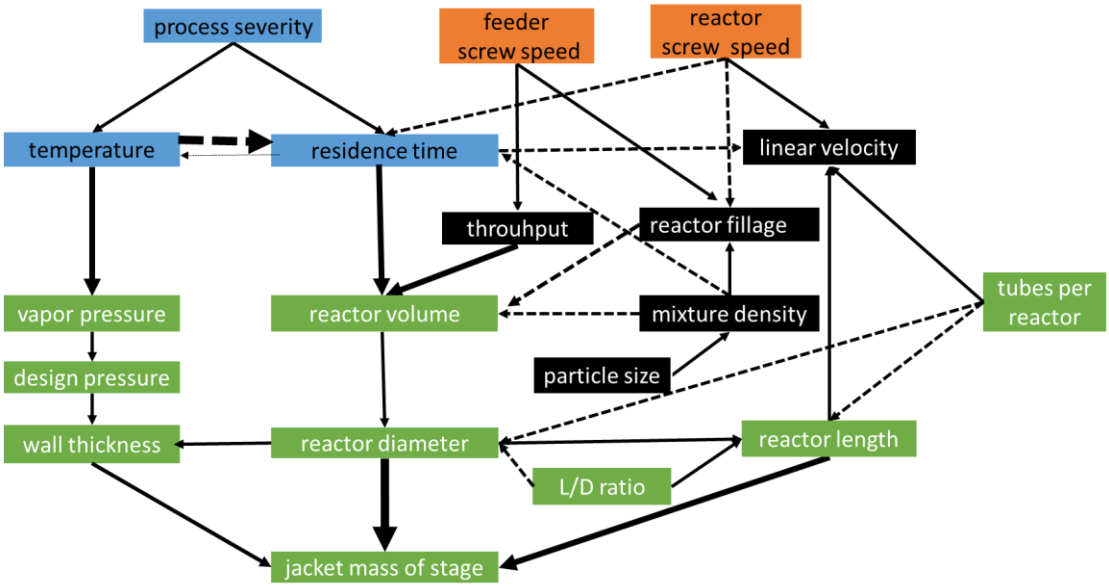

Fig. 5-10 Causal diagram of factors relevant for the dimensioning of screw conveyor reactors (SCR); blue boxes: Kinetics-related factors; black boxes: reactor capacity-related factors; green boxes: Reactor dimension and design-related factors; red boxes: operational parameters. Solid line arrow: Positive effect; dashed line arrow: Negative effect: arrow thickness: effect strength.

The temperature's effect on the reactor's mass is calculated to select the optimal one. Fig. 5-11a shows that an increase in temperature leads to a substantial decline in reactor mass. Dividing the reactor volume up into two, three, or any number of reactor tubes does not affect the overall reactor jacket mass. The temperature effect on the steam pressure, and thus the design pressure, is small compared to the reduction in residence time. Each 10 °C step, the residence time drops by 50%, compare Fig. 2-4. Fig. 5-11b shows the expected hemicellulose conversions for one, two, and three consecutive reactors according to the batch kinetics, compare section 5.1, and the proposed two (or multi-) step pretreatment, compare Fig. 5-9.

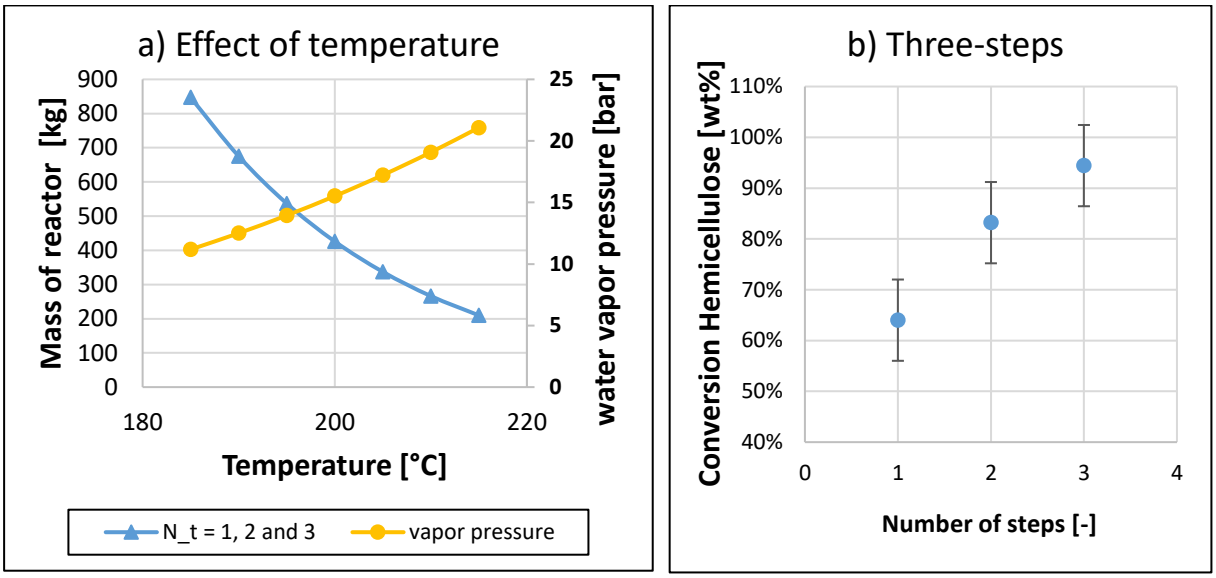

Fig. 5-11: **a)** Mass of reactor jackets versus the treatment temperature; The severity of the each step is $S_0 = 4.0$; Design pressure is vapor pressure times 1.5; Calculations are done for one, two, and three tubes per reactor; The results for a 3 cases are the same, **b)** Hemicellulose conversion versus the number of reactors in a cascade; each reactor step possesses a severity of $S_0 = 4.0$; Error bars indicate $X_{HC} \pm 0.06$ wt%, derived from experimental data.

Tab. 5-5: Reactor volumes in [m³] in dependence of the throughput and reaction temperature. S_0 = 4.0. A operation time of 8000 h/a is assumed.

M_{dryBM}		T [°C]			
[t/a]	[t/h]	180	190	200	210
3,000	0.4	7	4	2	1
30,000	3.8	69	35	18	9
150,000	18.8	346	176	89	45
300,000	37.5	692	351	178	90
600,000	75.0	1,383	702	356	181

The size of the first step reactor is evaluated for different throughputs and reaction temperatures to evaluate the feasibility of the two-step pretreatment plant concept, see Tab. 5-5. The throughputs represent the full scale of commercial production facilities. The Quaker Oats Furfural plant, based on three parallel SCRs with each a throughput of 60 t/h and four reactor tubes was reported with 1.8 m diameter and 16 m length resulting in 163 m^3 reactor volume [65]. Thus a 600,000 t/a scale is possible with a single reactor. In the Quaker Oats process and an NREL study [21], three reactors are built parallel with two permanent in operation and the third for maintenance. Thus three 181 m^3 reactors can reach a plant capacity of 1,200,000 t/a of annual lignocellulose. The second reaction step will possess an essentially smaller reactor due to the reduced mass input and the enormously increased bulk density of the mildly pretreated annual lignocellulose.

5.2.6. Conclusion

The screw conveyor reactor shows the very high fulfillment of all reactor design criteria and the overall best evaluation with great distance to the second-best reactors. The sequential reaction problem cannot be tackled with a single reactor. Thus, the combination of two reactors with intermediate extraction is proposed in this work. The reactor design was investigated using the kinetic data derived from LHW experiments. A high operation temperature was identified as an effective method to reduce the reactor size and investment costs. The two-step autohydrolysis pretreatment of annual lignocellulose was not yet tested experimentally; also, the extraction process needs to be investigated experimentally and designed to validate this concept, which will be the content of the next chapter.

5.3. Two-step autohydroysis

The autohydrolysis pretreatment was investigated in one and two consecutive steps to evaluate the two-step autohydrolysis concept, designed is section 5.2.5, regarding the recovery of pentose, glucose, and lignin and reduced furfural formations. The concept validation is carried out in different reactor types, sizes and operation modes. First, process behavior is to be investigated and described using the severity factor. Second, the transferability of liquid hot water hydrosis (pretreatment in suspension) to a reaction environment with little liquid but mainly gaseous water (steam pretreatment) is of interest. Also, the effect of the reactor scale and the transfer from batch to continuous processing is investigated. In the beginning, the focus is on the understanding of the reactions pathways. Later, the focus is on the process development that shows economically relevant traits, such as high pentose recoveries, the use of small specific amounts of energy and technical enzymes, the operation of a continuous reactor, and the separation of unwanted substances such as fines and furfural in the hydrolysate.

5.3.1. Liquid hot water

The LHW two-step autohydrolysis pretreatment and consecutive enzymatic hydrolysis were investigated in 50 individual experiments, and the solid and liquid phases were analyzed, compare sections 4.3.1.2 and 4.2. The pH and DS profiles versus the severity factor of the reproduced first and second steps agree with the analyzed data in section 5.1, see Fig. 5-15 and Fig. 10-2. In the following graphs, the first hydrothermal pretreatment step is marked with full symbols, and the second steps are marked with hollow symbols. The full diamonds are experimental data from Reynolds et al. generated for reactions kinetics investigations [55,101] using the same set-up. These data are used to compare the single-step and two-step hydrothermal pretreatment of wheat straw. The experiments for the first step are analyzed six-fold and conducted more often for the second step. The experiments of the second step are conducted and analyzed in duplicate, and every single data point is shown, which allows a graphical representation of the experimental and analytical uncertainty.

5.3.1.1. Autohydrolysis

In Fig. 5-12, concentrations and recoveries of pentoses and recoveries of furfural are plotted versus the overall severity factor. Fig. 5-12 shows the bell-shaped concentration profile of the first step autohydrolysis, already discussed in section 5.1. The optimized conditions for the first step regarding pentose yield, glucose yield, and

lignin purity, called Opt1, can be found on the degrading part of the curve. The tested first step conditions A1 and B1 match the reference data on the formation side of the curve. The second step curves A2 and B2 form a bell-shaped curve, with a higher overall severity factor than their predecessors (A1→A2, B1→B2) and show a lower concentration than the first step curve. B1 is located closer to the bell top than A1, and B2 shows, in turn, a lower maximum concentration. The highest overall pentose yield can be found at the maximum concentration of the second step. While A1 and A2 show similar concentrations, B1 shows a much higher concentration than B2. Thus, a considered selection of the process conditions for both pretreatment steps will influence the applicability of the resulting streams.

Next to the concentrations, the pentose yield demand consideration. In Fig. 5-12b, the pentose recovery in the first pretreatment step (unpublished raw data from Reynolds) shows a maximum of 50 - 60 wt% at S_0 = 4.0 - 4.2. At severities larger than S_0 = 5.0, the pentose yield tends towards zero. Both A2 and B2 possess a maximum of (65 ± 8) wt% at S_0 = 4.2. The Opt1 condition is a tradeoff between the criteria of a high hemicellulose removal from the solids, > 95 wt%, and a high pentose recovery, 33 - 47 wt%. The two-step hydrothermal pretreatment avoids a tradeoff between pentose removal and recovery but allows fulfilling both.

In Fig. 5-12c, furfural recoveries are displayed versus the overall severity factor. All first step pretreatment conditions follow the same curve, which increases from zero at S_0 = 3.9 - 4.1 and does not exceed $R_{Fur,th}$ = 20 wt%. At a severity of $4.6 > S_0$, there is no significant accumulation of furfural, which indicates further furfural degradation reactions. Furfural resinification or re-polymerization with other dissolved components are possible degradation reactions. As discussed above, this may explain the constant DS at $4.6 < S_0 < 5.2$.

Regarding the highest pentose recovery and lowest furfural recovery, the optimal conditions for the second pretreatment step, now called OptA2 and OptB2, are observed at an overall severity factor of S_0 = 4.1 – 4.3. Tab. 5-6 shows the first and optimal second step conditions tested in this work. The pentoses, furfural, and glucose recoveries are displayed, respectively.

In Opt1, the furfural recovery is: $R_{Fur,\mathrm{opt1}}$ (9.8 ± 1.6) wt%. The furfural recovery of the two-step approach is $R_{Fur,\mathrm{optA2}}$ = (1.8 ± 0.2) wt% and $R_{Fur,\mathrm{optB2}}$ = (4.2 ± 0.5) wt%. Thus, the two-step pretreatment reduces the furfural formation massively.

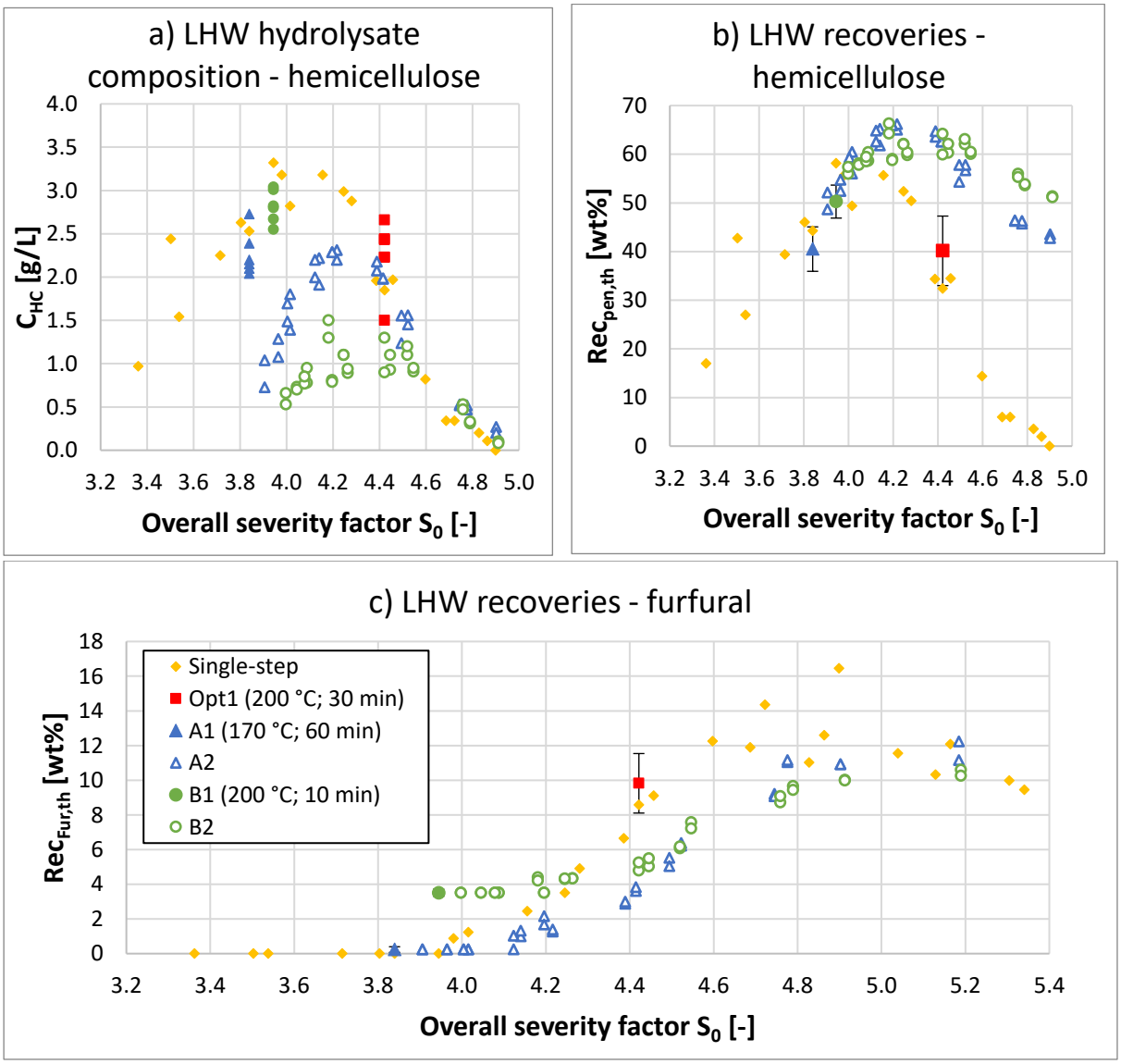

Fig. 5-12: **a)** Concentration of pentose **b)** Pentose recovery **c)** Furfural recovery in the first (full symbols) and second step (hollow symbols) hydrothermal pretreatment. Opt1 (full square), A1 (full triangle), B1 (full circle), A2 (hollow triangle) and B2 (hollow circle). The error bars indicate the standard deviation for the first step hydrothermal pretreatment experiments (six repetitions). For the second step, all experimental results (duplicates) are shown.

Tab. 5-6. First and second step pretreatment experiment. Experimental conditions and recoveries.

# [-]	T [°C] a)	t [min] a)	S_0 [-]	DS [wt%]	Rec_{HC} [wt%]	Rec_{Glu} [wt%]	Rec_{Fur} [wt%]	Rec_{Rest} [wt%]
A	170	60	3.84	38 ± 3	40.5 ± 4.2	1.8 ± 0.1	0.2 ± 0.5	9.1 ± 0.8
B	200	10	3.94	40 ± 2	50.3 ± 3.1	2.2 ± 0.2	3.5 ± 0.8	12.2 ± 1.9
Opt1	200	30	4.42	48 ± 2	40.1 ± 6.5	6.5 ± 0.5	9.8 ± 1.6	13.0 ± 3.0
OptA2	170; 200	60; 10	4.20	52 ± 5	65.9 ± 7.1	2.8 ± 0.3	1.8 ± 0.2	10.0 ± 1.1
OptB2	200; 185	10; 20	4.18	48 ± 5	65.3 ± 7.0	3.5 ± 0.4	4.2 ± 0.5	12.8 ± 1.4

a) Temperatures and residence time in chronological order

5.3.1.2. Enzymatic hydrolysis

The enzymatic hydrolysis was conducted to investigate the effect of the single and two-step pretreatment on the enzymatic digestibility, compare sections 4.3.2.1 and 4.2. The reducing sugar content in the EH hydrolysate represents glucose, xylose, and arabinose.

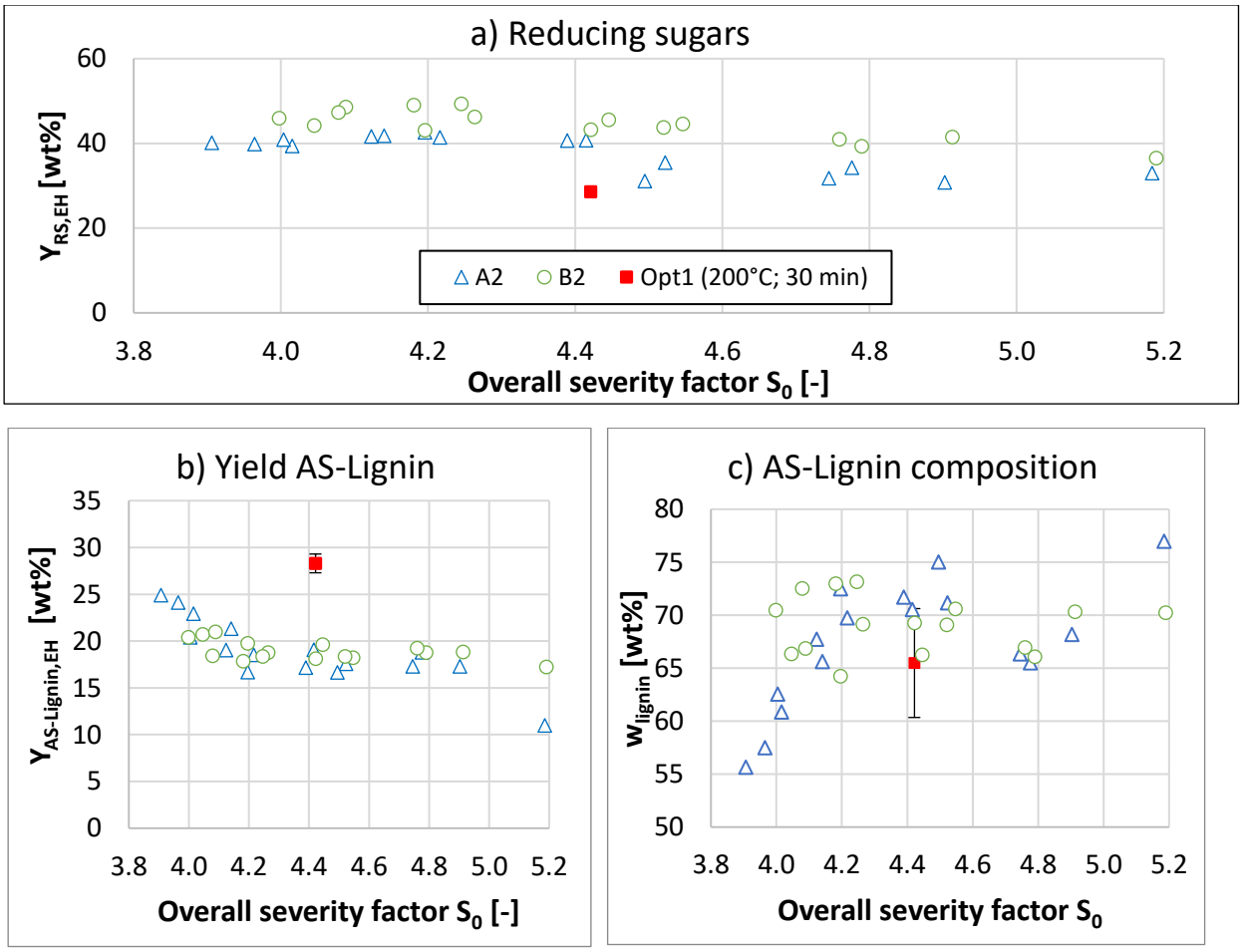

Fig. 5-13: **a)** Reducing sugar yield, **b)** AS-lignin yield, and **c)** AS-lignin composition versus the overall severity factor. The first (full symbols) and second step (hollow symbols) hydrothermal pretreatment are displayed. Opt1 (full square), A2 (hollow triangle) and B2 (hollow circle). The error bars indicate the standard deviation for the first step hydrothermal pretreatment experiments (three repetitions). For the second step, all experimental results are shown.

Fig. 5-13 shows the enzymatic hydrolysis results versus the overall severity factor applied in the hydrothermal pretreatment. Fig. 5-13a shows the reducing sugar yield, which is not affected by the pretreatment conditions in the relevant range $4.0 < S_0 < 4.4$. The highest yield was observed for B2 conditions, which is (47 ± 5) wt%. A2 conditions result in (40 ± 4) wt%. The yield of the Opt1 condition being lower is (29 ± 1) wt%. More reducing sugar can be obtained after EH using the two-step pretreatment. The ratio of glucose and pentoses in the hydrolysate was not measured here. Since the pentose recovery in the hydrothermal pretreatment remained below 90 wt%, it is suspected that some pentoses are released during the enzymatic hydrolysis, as was observed by Ertas et al. [102].

Fig. 5-13b shows the yield of the remaining solid called AS-lignin. A2 and B2 conditions show a similar yield of 16 - 20 wt% for an overall severity greater than 4.1. The AS-lignin yield for Opt1 is (26.1 ± 0.9) wt%. The differences in yield between the single-step and two-step hydrothermal pretreatment can be explained using the lower recovery of reducing sugars and the assumed re-polymerization involving furfural, which are suspected to reduce the enzymatic digestibility [39].

In Fig. 5-13c, the lignin content in AS-lignin is plotted versus the overall severity factor. A2 shows an increasing lignin content until $S_0 = 4.2$; it stagnates until $S_0 = 4.5$, then it goes through a minimum at $S_0 = 4.7$ - 4.8. A2 shows the highest lignin content of (72 ± 4) wt% at the severity of $S_0 = 4.2$ - 4.5. Even though there is a tendency for the two-step AS-Lignin purity to be higher than a single-stage autohydrolysis of (65 ± 5) wt%, there is no significant increase regarding the uncertainty of the measurement.

5.3.1.3. Fractionation performance

The pretreatment in second-generation biorefinery aims to fractionate the biomass components fully. For its evaluation, the product yields are used. The reference mass is the dry, untreated biomass, see equation (4-13) - (4-15). In Fig. 5-14a, the composition of the used wheat straw pellets is shown. Here the fraction $Rest$ is the deviation to a closed mass balance and represents inorganics, proteins, waxes, and the analytical error.

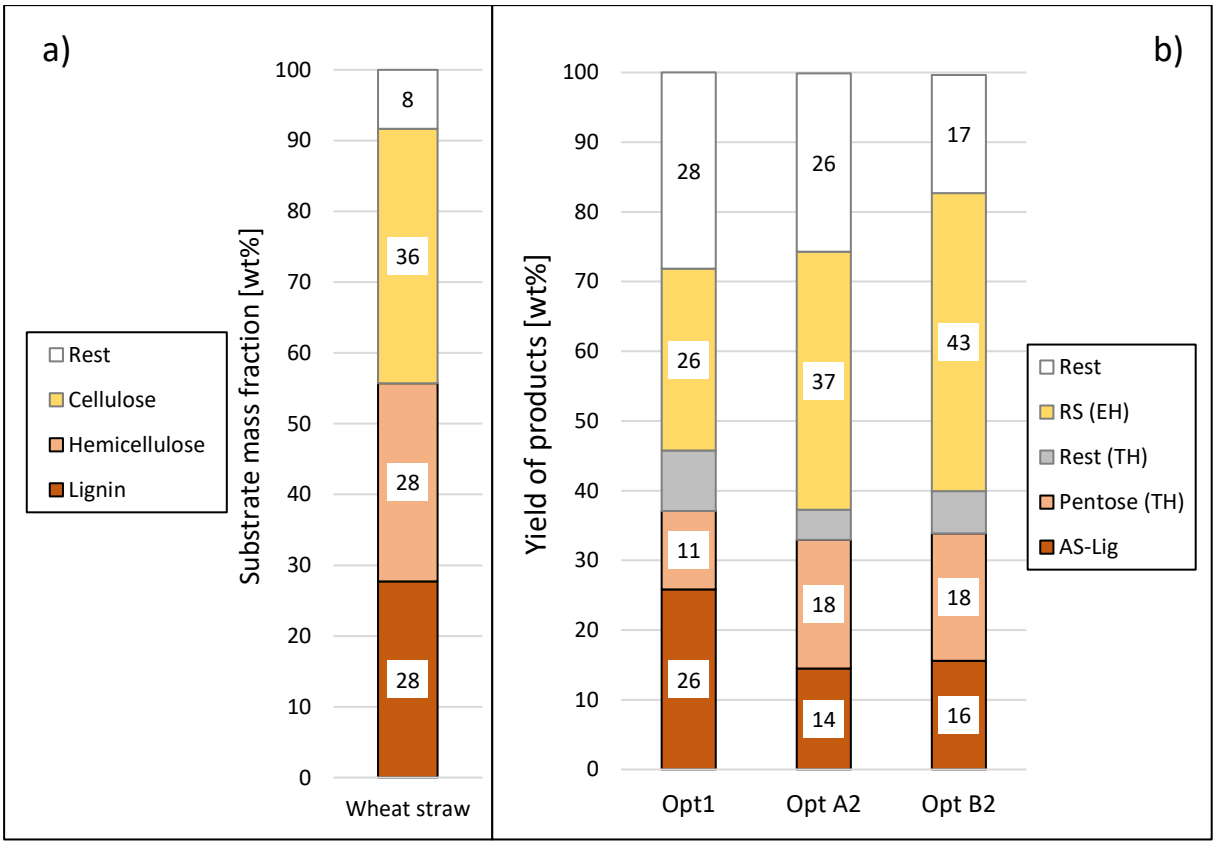

Fig. 5-14: **a)** Composition of wheat straw used in this work; **b)** Fractionation yields for optimized conditions for a single-step (Opt1) and two-step (OptA2 and OptB2) pretreatment. (TH) yield in hydrothermal hydrolysate; (EH) yield in enzymatic hydrolysate; Pentose: xylose and arabinose, Rest (TH): glucose, furfural, acetic acid, and formic acid; RS: Reducing sugars after the enzymatic hydrolysis.

Tab. 5-7: The yield of components in mass percentage for the optimized condition in single-step and two-step pretreatment in mass percentage.

#	Y_{AS-Lig}	$Y_{Pentose,TH}$	$Y_{Glucose,TH}$	$Y_{Fur,TH}$	$Y_{Acids,TH}$	$Y_{RS,EH}$	Y_{rest}
Opt1	25.8 ± 0.9	11.2 ± 1.8	2.3 ± 0.2	2.8 ± 0.4	3.6 ± 0.9	26.1 ± 1.0	28.2 ± 3.1
OptA2	14.5 ± 3.6	18.5 ± 1.8	1.0 ± 0.1	0.5 ± 0.1	2.8 ± 0.3	37.0 ± 3.2	25.6 ± 2.8
OptB2	15.6 ± 3.9	18.3 ± 1.8	1.3 ± 0.1	1.2 ± 0.1	3.6 ± 0.4	42.8 ± 3.7	16.9 ± 1.9

Fig. 5-14b and Tab. 5-7 display the product yields obtained using the optimized conditions for the single-step pretreatment (Opt1) and the two-step pretreatment (OptA2 and OptB2). For the autohydrolysis pretreatment, four yields are denoted with (TH). The first yield with (TH), $Y_{pen,TH}$, is the yield of pentoses, namely xylose, and arabinose. The second $Y_{fur,TH}$ is the furfural yield. The third is $Y_{Acids,TH}$ and represents the acetic acid and formic acid. The fourth $Y_{Glu,TH}$ is the glucose yield in the hydrothermal hydrolysate. The fraction Y_{Rest} is the deviation to a closed mass balance and represents undetected dissolved components, like aromatic components and other degradation products. Fig. 5-14b the yields $Y_{fur,TH}$, $Y_{Acids,TH}$, and $Y_{Glu,TH}$ are

presented combined as $Rest\ (TH)$. The pentose yield is the same in conditions OptA2 and OptB2. For the other performance parameters, not only the overall severity factor is decisive, but also the severity factor of the first step. OptB2 results in higher furfural yield, reduced sugars yield, and higher mass balance closure than OptA2. However, the two-step autohydrolysis (OptA2 or OptB2) is superior in the fractionation performance than the single-step autohydrolysis Opt1. The pentose yield increases by 65 %, from 11.2 wt% (Opt1) to 18.5 wt% (OptA2). The furfural yield is sharply decreased; for OptA2, it is below 1 wt%. The reducing sugar yield is increased from 26.1 wt% (Opt1) to 37.0 wt% (OptA2) and 42.8 wt% (OptB2), which is an increase of 42 % and 64 %, respectively. The overall sugar yield is increased from 39.6 wt% (Opt1) to 56.5 wt% (OptA2) and 62.3 wt% (OptB2), which is an increase of 43 % and 57 %, respectively. A lower AS-lignin recovery in the two-step pretreatment compared to the single-step pretreatment is apparent. The reason for this might be increased lignin solubilization or an increased lignin removal during analytical hydrolysis, but it remains unclear and should be further researched.

5.3.1.4. Catalyst exploitation

In autohydrolysis, water and organic acids are catalysts for xylan hydrolysis. The best use of the weak acids is achieved by avoiding pH buffering by biomass inherent components. In Fig. 5-15a, pH values of the hydrolysates are displayed versus the overall severity factor. All data points follow the same decreasing trend. The single-step pH curve shows higher values and ends on a stagnating pH of 3.65. In contrast, the lowest two-step pretreatment pH values are 3.50 and 3.25 for B2 and A2, respectively. A similar or even lower pH profile in the two-step pretreatment is unexpected since all dissolved organic compounds are removed in the extraction stage after the first pretreatment step. Thus, lower acetic acid and higher pH profiles are expected.

In Fig. 5-15b, pH values are displayed versus the acetic acid concentration of the hydrolysate. The detection limit is 50 mg/L; the values below are set to zero. Here, two different curves can be distinguished for the first and the second pretreatment step. For the first step pretreatment, a three-times higher acid concentration results in the same pH values compared to the second step pretreatment.

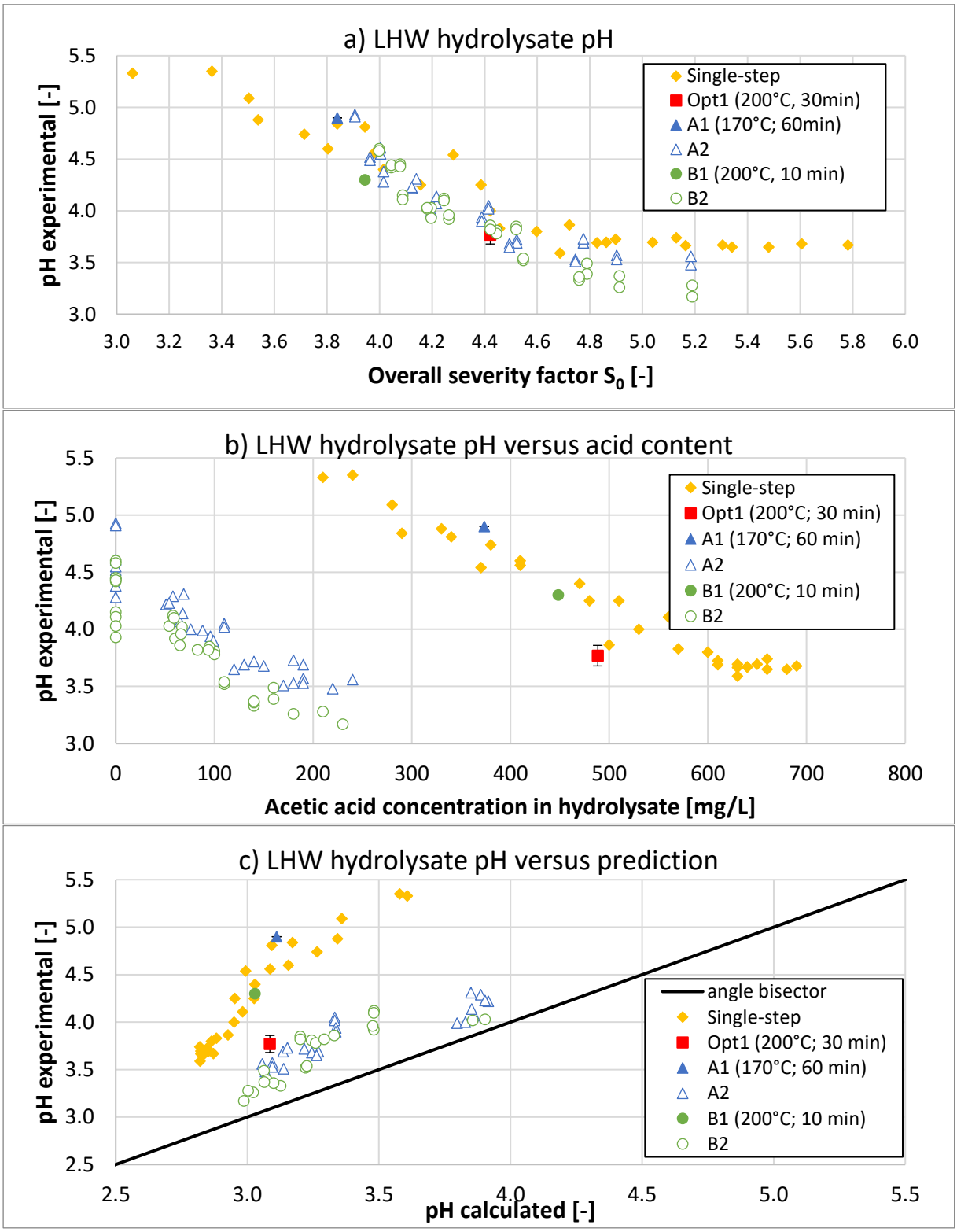

Fig. 5-15: **a)** Hydrolysate pH value versus the overall severity factor. **b)** Hydrolysate pH value versus the acetic acid concentration. **c)** The Hydrolysate pH value versus the calculated pH value. The first (full symbols) and second step (hollow symbols) hydrothermal pretreatment are displayed. Opt1 (full square), A1 (full triangle), B1 (full circle), A2 (hollow triangle) and B2 (hollow circle). The error bars indicate the standard deviation for the first step hydrothermal pretreatment experiments (six repetitions). For the second step, all experimental results (duplicates) are shown.

In Fig. 5-15c, experimental pH values versus the calculated pH, based on the law of mass action using the weak acids concentrations, are displayed. All experimental data points show a higher pH than the calculated one, indicating the neutralization capacity of the biomass. The first step data show a more substantial deviation from measured to calculated pH than the second step data.

These observations can be explained with a biomass-inherent neutralizing. The neutralization of acids via cation exchange with mineral salts in the biomass was reported several times in literature [17,18,103]. It is assumed that acetic acid is partially neutralized, and more acetic acid is required to lower the pH. Since acetic acid is released throughout the autohydrolysis, a pH drop is delayed in the single-step pretreatment. This may already occur in the mild first pretreatment before the neutralized acetic acid is removed in the filtration and washing step. In the second step, the released acetic acid can induce a fast pH drop with a reduced neutralizing capacity.

It is concluded that the extraction after the first pretreatment step does not lower the catalyst exploitation but improves it. Additionally, it is suspected that some inorganic compounds that possess a pH buffering capacity, as described above, are water-soluble and are removed via extraction after the first reaction step.

This theory is supported by the increased DS in the second step, compare to Fig. 10-2, since these DS values can otherwise only be achieved at higher severities. The higher severity in B1 presumably leads to a decline of buffer capacity in the first step than A1, thus lowering pH values of B2 experiments compared to A2 and the lower pH value in the two-step autohydrolysis compared to the single-step autohydrolysis.

Based on these observations, a washing step prior to the first reaction step or washing with slightly acetic process water might remove some pH buffering capacity and accelerate the hydrolysis reaction rate.

Nevertheless, the two-step pretreatment approach was validated experimentally in an LHW environment, meaning with an excess of water, but needs to be tested in a saturated steam environment and on a larger scale to simulate the conditions in the screw conveyor reactor.

5.3.2. Steam batch

5.3.2.1. Proof of concept in 3 L reactor

A 3 L high-pressure autoclave was set up with a steam generator and a condenser to collect the vapors formed during the depressurization, compare section 4.3.1.3. Thirty-six individual steam experiments were performed with cut straw particles to investigate the first and second reaction step. The pretreated solids were pressed with a piston press to analyze the concentrations in the liquid phase without dilution, called pressate.

In Fig. 5-16, the pressate concentration and yield can be found. The concentration of 50 g/L and more can be achieved in the first step, which is around 20 times higher compared to LHW experiments, compare section 5.3.1.1. Only the top section of the bell-shaped curve was of interest for the two-step pretreatment; thus, a narrow parameter window was chosen. The maximum is in the range of $3.8 < S_0 < 4.2$. The second step concentration are found in the same relation to the first step, as in LHW experiments.

In Fig. 5-16b, the yield is expressed based on the initial total dry mass. Both second step conditions, A'2 and B'2, achieve a greater yield than the single-step experiments. A'1 with a severity factor of 3.66 was chosen as very mild to achieve a similar concentration. This was successful, but the maximum yield of A'2 is significantly lower than B'2. From A'1 to B'1, the hemicellulose conversion can be increased essentially without the degradation of pentoses. Concluding, the first step condition should be severe as possible on the formation side of the bell-shaped curve to gain the highest overall yield with two steps. The maximum yield, 17.3 ± 0.3, was archived at $S_0 = 4.2$. Again, the location of the maximum is identical to the LHW experiments. An excellent transfer of the data from LHW to steam experiments, both in batch mode, is possible.

Fig. 5-16c and Fig. 5-16d show the furfural yield in the pressate and the condensate; please note the scale. The steam pressate of the first and second steps contains essentially no furfural. OptB'2 contains one g/L furfural in the pressate. Around 90 wt% of the furfural can be found in the condensate. Due to the azeotropic behavior of a water-furfural mixture, furfural becomes more volatile than the water below specific concentrations. Thus, it evaporates selectivity depressurizing the reactor after the reaction time. This way, most of the furfural is removed from the liquid adhered to the pretreated biomass.

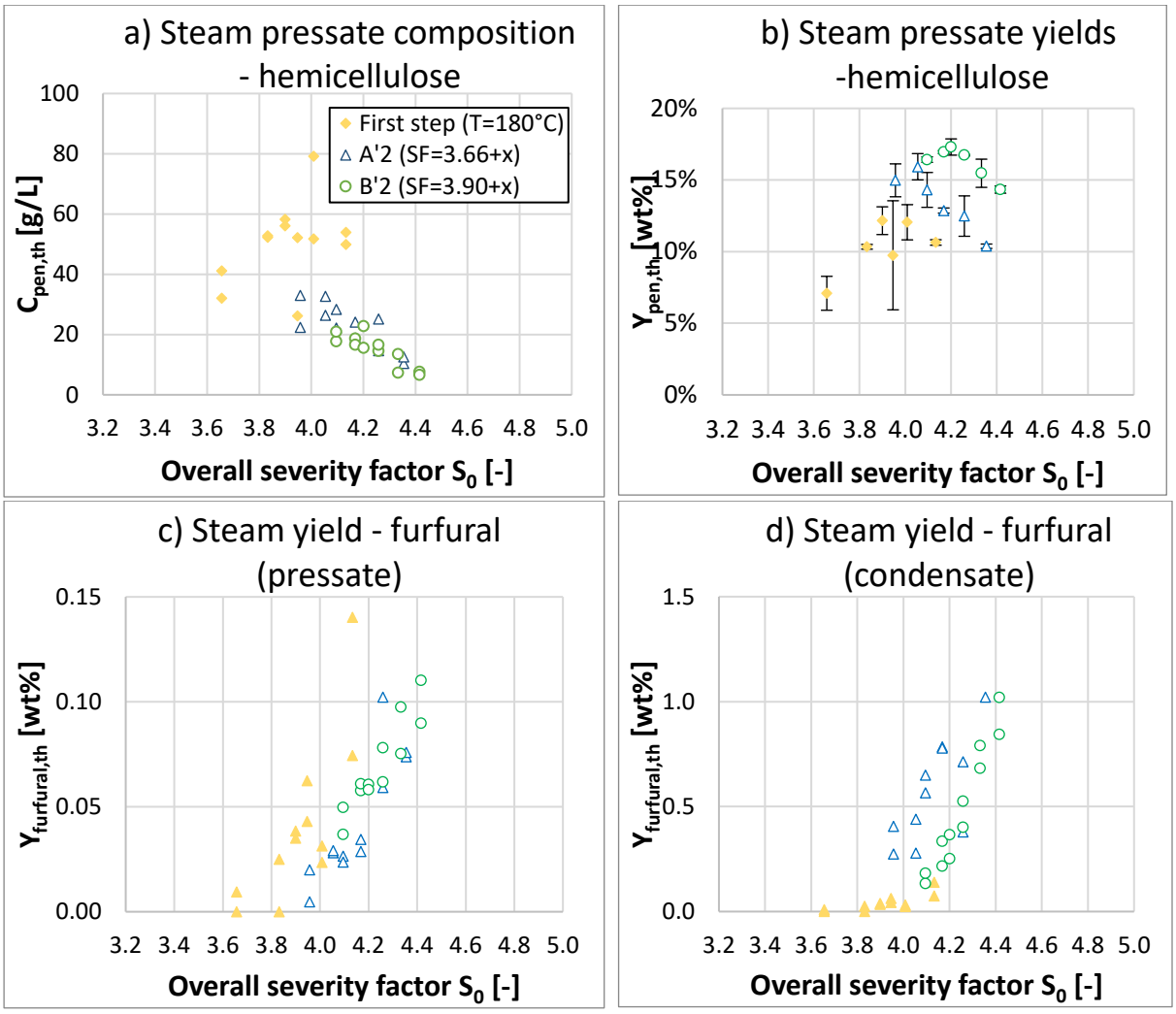

Fig. 5-16: 3 L steam pretreatment at 180°C experiments for a single-step process (yellow diamonds) and two-step pretreatment based on 20 minutes (blue hollow triangles) and 30 minutes (hollow green circles) treatment time in the first step, expressed against overall severity factor during steam pretreatment. **a)** pentose concentrations, **b)** pentose yields, **c)** furfural yield in steam hydrolysate, **d)** furfural yield in the steam condensate.

The subsequent enzymatic hydrolysis was carried out in 50 mL tubes in a water bath shaker. In Fig. 5-17, the resulting liquid and solid compositions are analyzed. Carbohydrates yield after EH based on the total initial dry matter shows that a single-stage process can reach values of 39 wt% to 60 wt%, increasing with the steam pretreatment severity. The two-step processes show values greater than 55 wt% and are under most conditions above 60 wt%, with the highest value at 69 wt%. All second step carbohydrates yields after EH show similarly high values. The mass fraction of xylose in the carbohydrates (xylose and glucose) show a decreasing trend starting from 33 wt%, represented by a single curve for all tested conditions. Using the two-step pretreatment lower values of down to 10 wt% can be reached. This is equivalent

to a glucose purity of 90 wt%. Thus, the two-step process can obtain a slightly purer glucose stream.

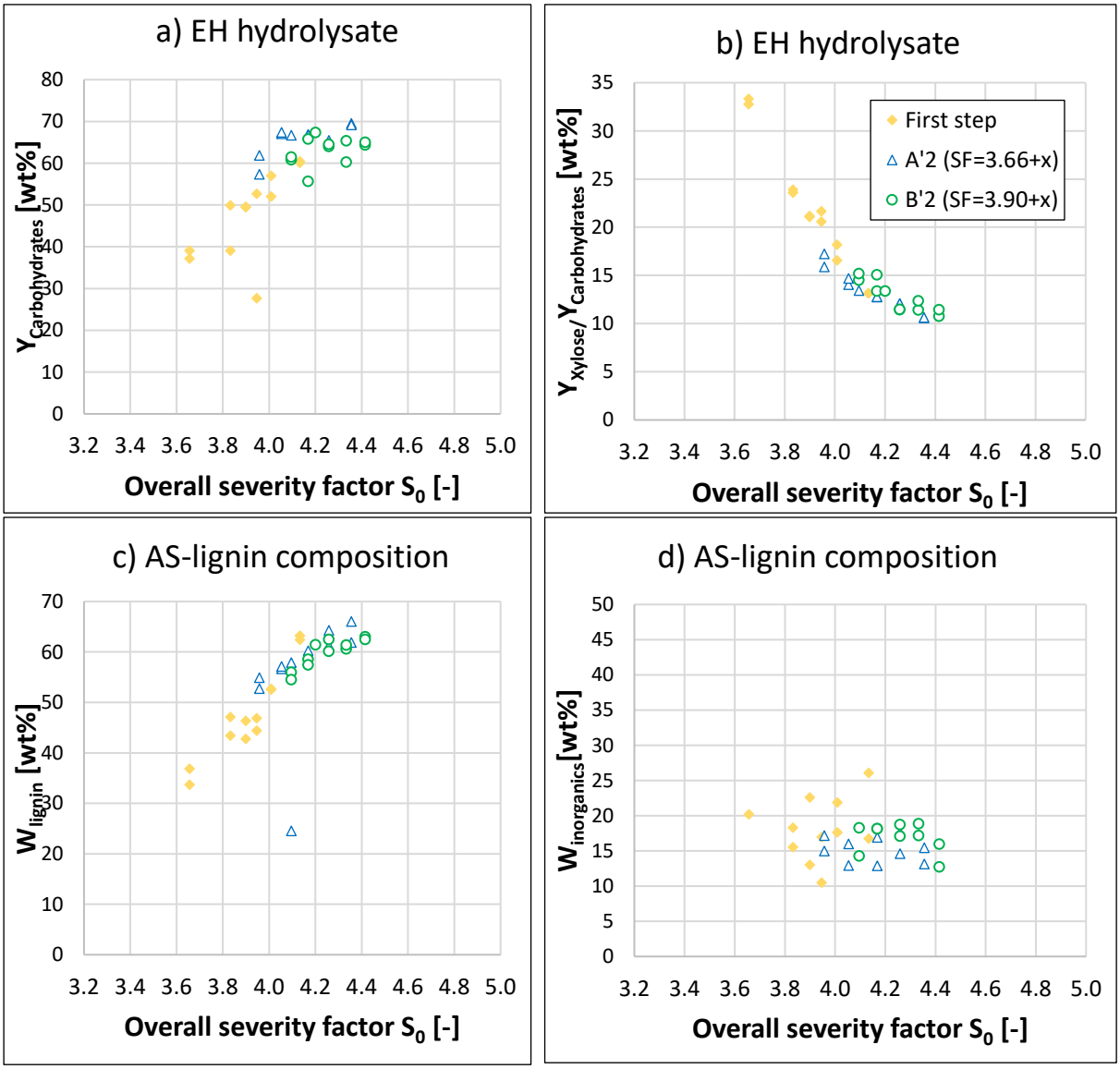

Fig. 5-17: Enzymatic hydrolysis (EH) experiments of 3 L steam (180°C) pretreated materials for a single-step process (yellow diamonds) and two-step pretreatment based on 20 minutes (blue hollow triangles) and 30 minutes (hollow green circles) treatment time in the first step, expressed against overall severity factor during steam pretreatment. **a)** carbohydrates yield and **b)** xylose mass fraction after EH. **c)** lignin mass fraction (Klason and acid-soluble Lignin) and **d)** inorganics mass fraction in solids residue after EH (AS-Lignin).

The solid obtained after EH was analyzed on its composition. The lignin content shows an increasing curve against the severity factor, with all data points on a single curve. All three tested processes can achieve the highest lignin purity of 63 - 66 wt%.

Based on these results, the steam pretreatment severity can be chosen. The two-step processes are superior performance considering the goal of high lignin purity and high pentose recovery. Achieving a lignin purity of 63 wt%, the single-step pretreatment

solely reaches a pentose recovery of 10-11 wt% and a carbohydrates recovery after EH of 60 wt%. For the two-step pretreatment, recoveries of 63 wt%, 18 wt%, and 68 wt% are achieved, respectively. Applying the two-step pretreatment process, the pentose recovery is improved by 70 - 80 %. For the first and second step autohydrolysis, 35 min and 180 °C or S_0 = 3.9 was chosen, resulting in overall severity of S_0 = 4.2 [44]. The autohydrolysis mechanism and reaction rates are in excellent agreement with the LHW experiments.

The method used in the 3 L steam study is analytical, and the results need to be validated in a more extensive setup with conditions more relevant for an industrial process. The use of a piston press is appropriate to prove the presence of high concentrations in the liquid phase after steam pretreatment and to calculate the yields. A method with a higher extraction yield is required on an industrial scale. Thus, the hydrolysate is extracted in a water suspension from the pretreated solid material in the following. The condenser of the 3 L plant is connected to the bottom of the reactor. This allows a small amount of sugars to be washed into the condensate stream. Thus, the condenser is connected to the top of the reactor in the following. The EH should also be reproduced in a stirred tank for validation, as done in the following.

As discussed above, it is suspected that pH buffering compounds can be removed with water washing. Since this is a wanted effect, it was tested before the steam pretreatment.

5.3.2.2. Feedstock washing

Feedstock washing was performed in batch mode to determine the inorganic mass that could be removed prior to autohydrolysis pretreatment, compare section 4.3.3.2. The removal of organic materials, such as dissolvable compounds and fine particles, is investigated. Experiments are conducted in sized wheat straw sources, each in triplicates. After filtration, the remaining moisture content was in the range of 80 wt% water or L/S=4.

Fig. 5-18 displays the masses of organics and inorganics for a 100 kg initial dry biomass scenario. The amount of water (L/S) used increases from left to right, wherein the most intensive washing is a cross-flow with fresh water each time. In Tab. 5-8, the results are reported. The more water is used, the more inorganics and organics are removed from the biomass. It can neither be determined to what extent the removed

inorganics are dissolved or bound to fine particles nor the state (particles or dissolved) of the removed organics. As expected, the washing yield of organics (and inorganics) is greater for the milled straw since a greater fraction of fines is present in the feedstock. It is assumed that no dissolved compounds are present in the remaining washing liquid after the most intensive washing. Thus, the remaining compounds (organic and inorganic) are regarded as structural. The structural content of the cut and milled straw inorganics are 6.1 ± 0.2 wt% and 4.9 ± 0.1 wt%, respectively. For cut straw, the most intensive washing resulted in a removal of 29 ± 3 wt % of inorganics and 5.3 ± 0.9 wt of organics. Even though the relative removal of organics is small, the total removed mass is high compared to inorganics. This is observed for both tested raw materials. Structural inorganics remain in washed solids.

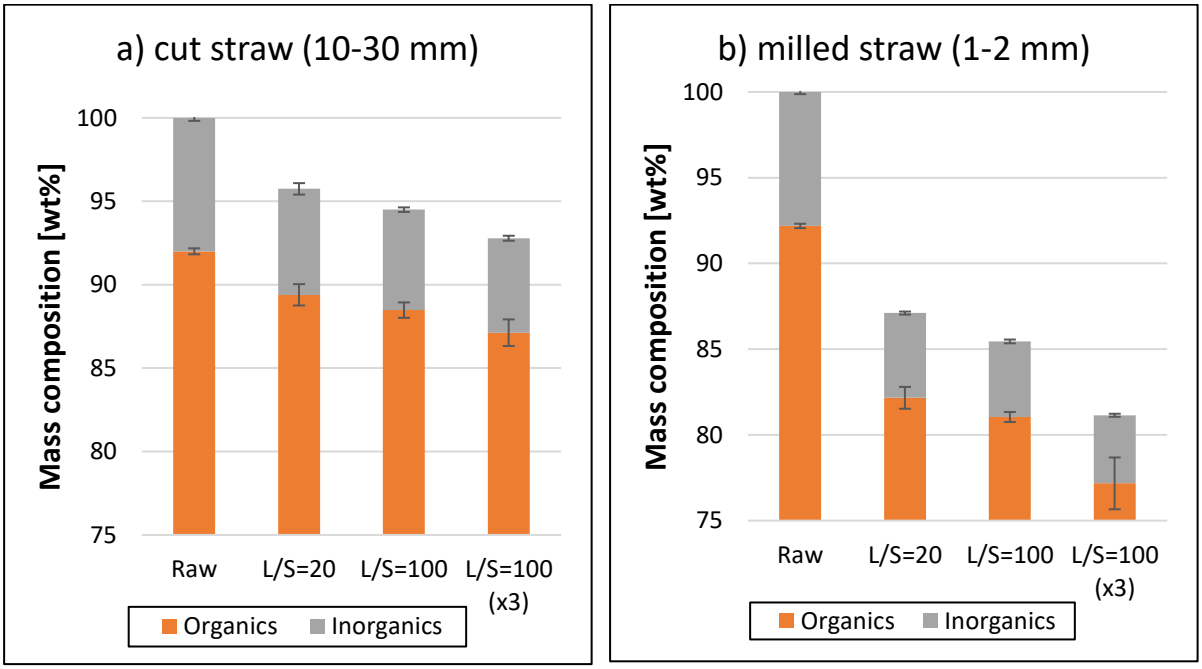

Fig. 5-18: Biomass composition and total mass in feedstock washing. A) cut straw, b) milled (pelleted straw). L/S= Liquid to solids mass ratio in the washing experiment. Triplicates.

Tab. 5-8: Feedstock washing experiments. Masses normalized to 100 kg initial dry biomass. **L/S:** liquid to solid mass ratio during extraction. $\boldsymbol{Y_{W,i}}$**:**Yield of washing of compound i. error reported as the standard deviation of triplicates.

Material	value	unit	Raw	L/S=20	L/S=100	L/S=100 (x3)
Cut straw (Q-Mehl)	M_{total}	[kg]	100 ± 0	95.7 ± 0.5	94.5 ± 0.4	92.8 ± 0.8
	$w_{inorganics}$	[wt%]	8 ± 0.2	6.6 ± 0.4	6.4 ± 0.1	**6.1 ± 0.2**
	$M_{inorgnics}$	[kg]	8 ± 0.2	6.4 ± 0.3	6 ± 0.1	5.7 ± 0.2
	$M_{organics}$	[kg]	92 ± 0.2	89.4 ± 0.6	88.5 ± 0.5	87.1 ± 0.8
	$Y_{W,inorganics}$	[wt%]	-	21 ± 5	25 ± 3	**29 ± 3**
	$Y_{W,organics}$	[wt%]	-	2.8 ± 0.7	3.8 ± 0.5	**5.3 ± 0.9**
Milled straw (Bioneto)	M_{total}	[kg]	100 ± 0	87.1 ± 0.6	85.5 ± 0.3	81 ± 2
	$w_{inorgnics}$	[wt%]	7.8 ± 0.1	5.7 ± 0.1	5.2 ± 0.1	**4.9 ± 0.1**
	$M_{inorganics}$	[kg]	7.8 ± 0.1	4.9 ± 0.1	4.4 ± 0.1	4 ± 0.1
	$M_{organics}$	[kg]	92.2 ± 0.1	82.2 ± 0.6	81 ± 0.3	77.2 ± 1.5
	$Y_{W,inorganics}$	[wt%]	-	37 ± 2	44 ± 2	**49 ± 2**
	$Y_{W,organics}$	[wt%]	-	10.9 ± 0.7	12.1 ± 0.3	**16 ± 2**

An L/S=20 washing of milled straw is conducted before the autohydrolysis experiments on a 40 L scale. For a commercial process, 20 tons fresh water per ton dry substrate is not feasible. In section 5.3.5, different techniques are investigated to improve the relevant washing parameters to find a feasible washing/extraction process for the industrial scale. Besides removing potentially pH buffering or degradable substances, washing the feedstock has the advantage of achieving a more homogeneous moisture distribution in the straw (water holding capacity of app. 4-5), compared to spraying water over the substrate while mixing. In other words, to achieve homogenous and reproducible moisture destitution in the substrate prior to autohydrolysis, some inorganics are washed already. Thus, developing a process that achieves both tasks with desirable performance is meaningful. The effect of the feedstock washing is evaluated using data from 3 L and 40 L reactors in the following.

5.3.2.3. Mass balance in 40 L Reactor

To close the mass balance of the two-step pretreatment and reproduce the results on a larger scale, a 40 L steam pretreatment plant, compare section 4.3.1.4, and a 10 L enzymatic tank, compare section 4.3.2.2, were used. The entire processing sequence was conducted three times independently.

In Fig. 5-19, the effect of feedstock washing is displayed for the extract pH and the degree of solubilization. The hydrolysates pH is significantly lower for washed wheat straw. Thus the hypothesis that feedstock washing can remove buffering capacity is

supported. The measured difference in pH is equivalent to a twofold increase in the concentration of hydronium ions. Due to the acid-catalyzed hemicellulose hydrolysis, it is suspected that feedstock washing can accelerate the pretreatment.

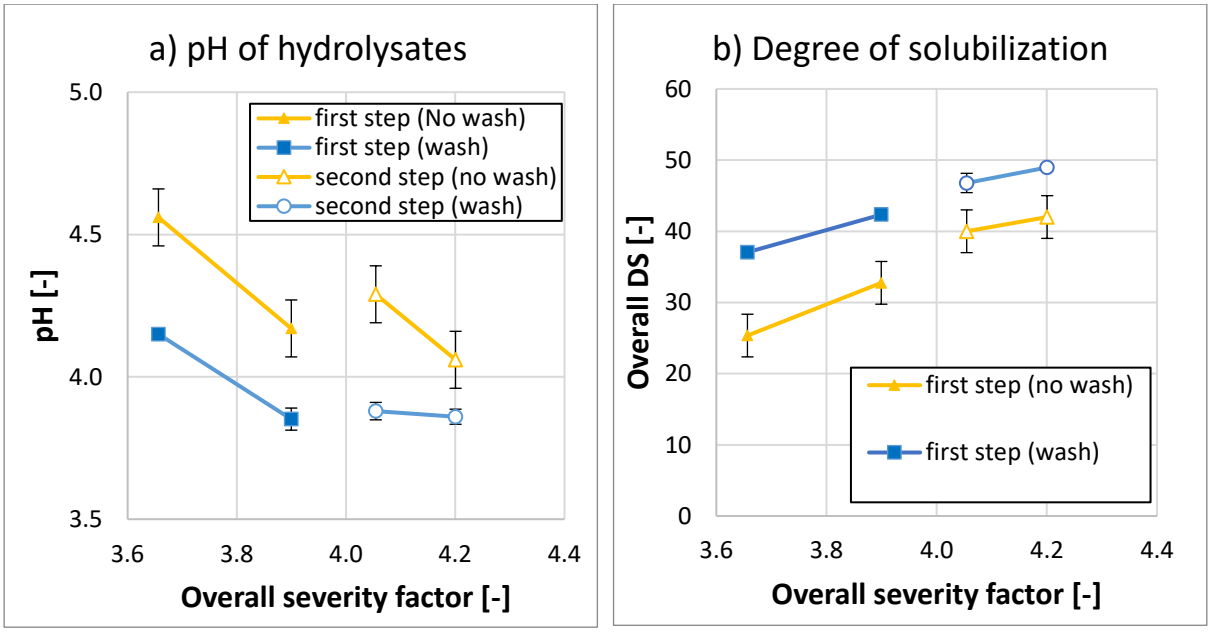

Fig. 5-19: Effect of feedstock washing in steam pretreatment. No wash: 3L reactor, Wash 40 L reactor a) extract pH, b) Degree of solubilization (DS).

The DS evaluates the autohydrolysis progress. This parameter is also affected by the removal of mass via washing. After pretreatment (with and without feedstock washing), the overall DS was determined after extraction and washing to remove the influence of dissolvable substances. Thus, all fines and soluble components should be removed after the first pretreatment step and not affect the overall DS, assuming the autohydrolysis rate is not affected. In Fig. 5-19b, it can be seen that the overall DS is significantly larger for washed substrate in the first and second pretreatment steps. Thus, the DS data support the pretreatment accelerating effect of the feedstock washing.

The hemicellulose and furfural concentration in the extract after steam pretreatment of washed straw in the 40L rector can be seen in Fig. 5-20. The pentose yield in the first step is similar and high concerning the dilution with water for extraction. Regarding the water content change, the concentration before the extraction (after steam pretreatment) is around 3.3 times higher. In these extracts, the furfural concentration is insignificant. The second step extract shows low concentrations. For condition A'' a similar concentration in the first and second steps are expected, compare Fig. 5-16. Comparing A'' and B'', a more extended treatment in the first step does not increase

the furfural concentration. In the second step, the concentration drops at smaller severity factors as expected, compare Fig. 5-16. This observation further shows that washing the material accelerates the autohydrolysis rate. Thus the near bell-shaped curve of the first step cannot be assumed to be identical to not washed material but is shifted towards lower severity factors. The two-step pretreatment conditions are thus not chosen optimally and the effect of the second step for conditions B'', see Fig. 5-20c, is still large compared to a single-step approach to remove all hemicellulose to increase the cellulose digestibility, compare section above. Conditions A'' is considerably mild and shows a great improvement in hemicellulose yield in the second step. Based on the unwashed substrate, the hemicellulose lost in the wash water is below one percent.

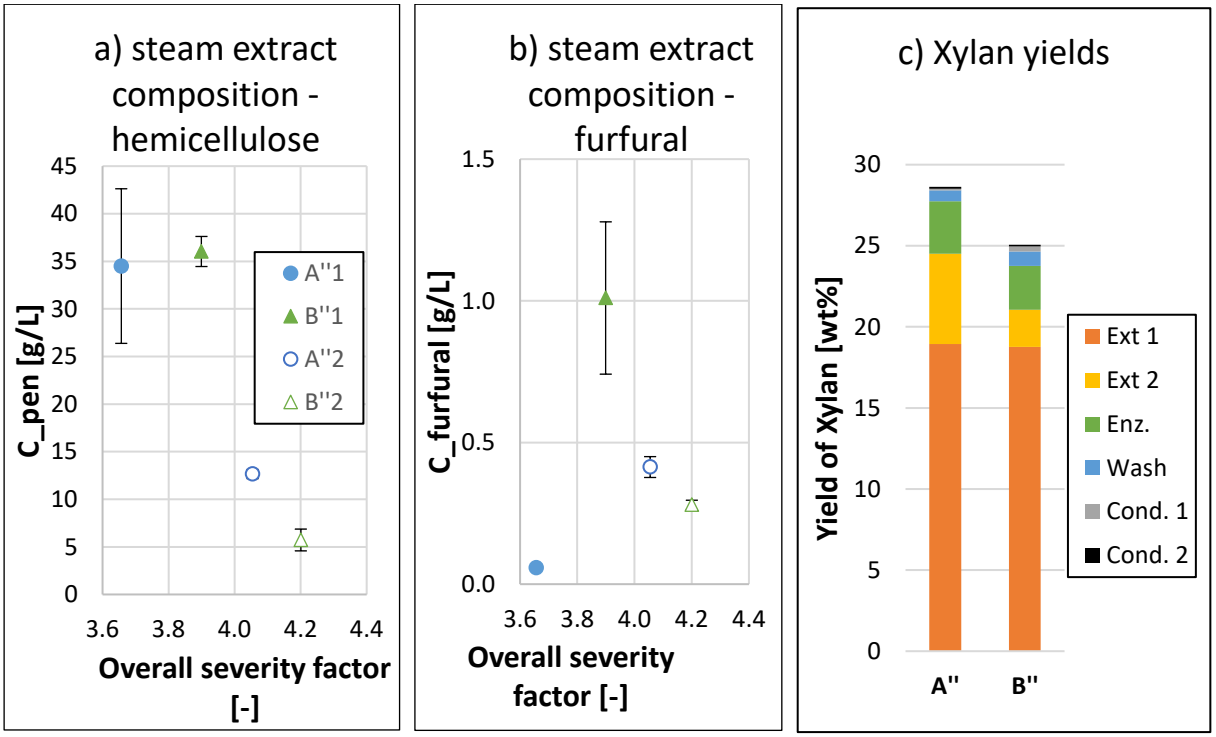

Fig. 5-20: 40 L steam pretreatment at 180°C experiments, with washed straw for two-step pretreatment based on A''1 (20 min, blue circle) and A''2 (35 min, hollow blue circles) and B''1 (20 min, green triangle) and B''2 (30 min, green hollow triangle) **a)** pentose concentrations, **b)** furfural concentrations, **c)** yield of hemicellulose (based on the unwashed substrate) in different streams, in the condensates only furfural is regarded.

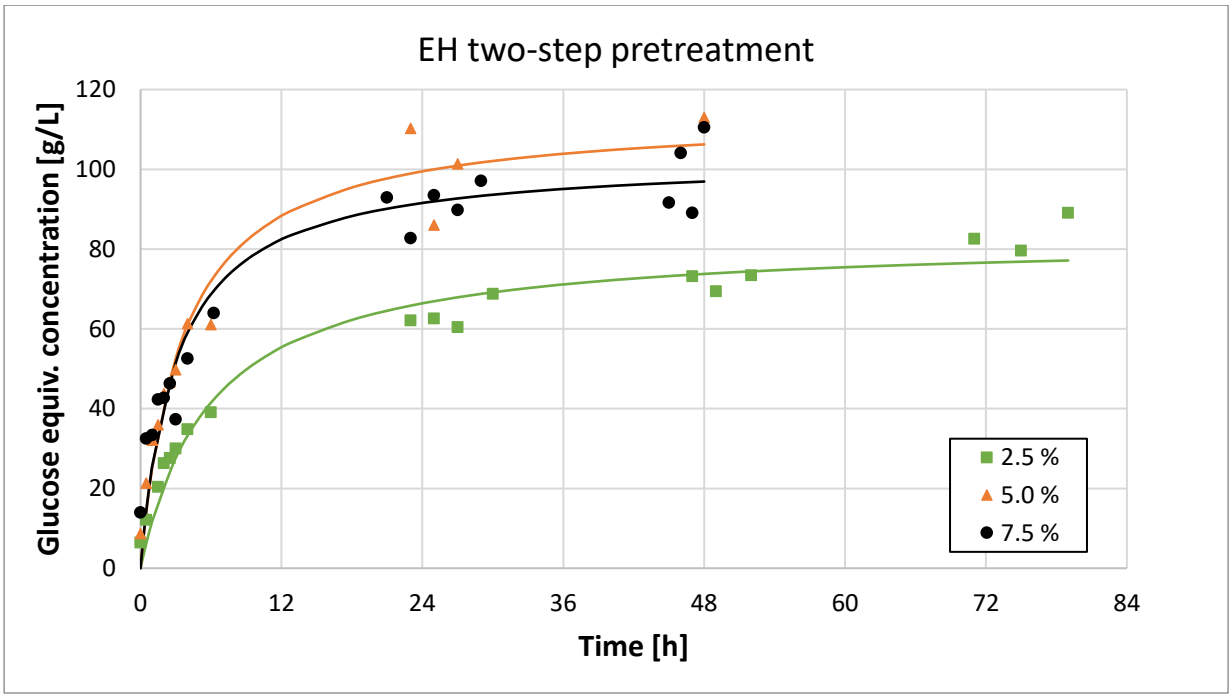

Fig. 5-21: Enzymatic Hydrolysis in 10 L stirred tank with pretreated wheat straw with Enzymes CtecIII. 14 wt% of cellulignin, solid feeding via fed-batch in the first 60 minutes. 50 °C, pH 5, DNS test for reducing sugars. Varied enzyme dose in $mL_{CtecIII}/g_{drymass}$. Curves for graphical orientation.

The pretreated solids of condition B'' are treated in enzymatic hydrolysis in scalable conditions in a 10 L stirred tank with three different enzyme loadings, see Fig. 5-21. A loading of 2.5 mL / 100 gram of dry mass showed the slowest conversion rate, whereas the loading 5.0 and 7.5 cannot be differentiated from each other. For the last cases, a nearly complete conversion is reached after 24 hours with a final reducing sugar concentration in the range 80-110 g/L. The concentration increase after further 24 hours is insignificant.

The mass flows of all relevant components from raw feedstock to all side- and product streams for condition A'' are displayed in Fig. ***5-22***. Here water is neglected to remain clarity. The mass balance shows only tiny errors. The fractionation of hemicellulose, cellulose, and lignin with 24.5 wt%, 29,6 wt%, and 19 wt%, respectively, in the desired stream, based on the substrate, is achieved. The solid mass composition gap, called "rest" is presented as a component. It can be partly undetected biopolymers as xylan or not regarded compounds as proteins and waxes. In the first steam pretreatment step, it disappears, and more hemicellulose is found than expected; thus, it is suspected that it was mainly undetected hemicellulose. The found HC content of 20.7 wt% is lower than the usual value of 25-28 wt%, compare Fig. 5-3. The degree of solubilization in all first steps of autohydrolysis pretreatment is higher than the yield of

hemicellulose; thus, another substance is made soluble in the pretreatment. In future work, it is recommended to analyze the hydrolysate for proteins, waxes, and inorganics to identify the “rest” in the hydrolysate. The unknown compound is dissolved since the hydrolysate is essentially particle-free (turbidity < 250 NTU).

A fraction of the inorganics can be removed via washing; the remaining inorganic content in the solid phase can be found in the AS-Lignin. The pentose loss to furfural in hydrolysates or condensate is neglectable. Tiny lignin fractions seem to be removed via washing and pretreatment, but they can be found again in the final solid residue. The “rest” could be party undetected, thus explaining the deviation. However, the presence of lignin-derived compounds should be searched for in the liquid streams.

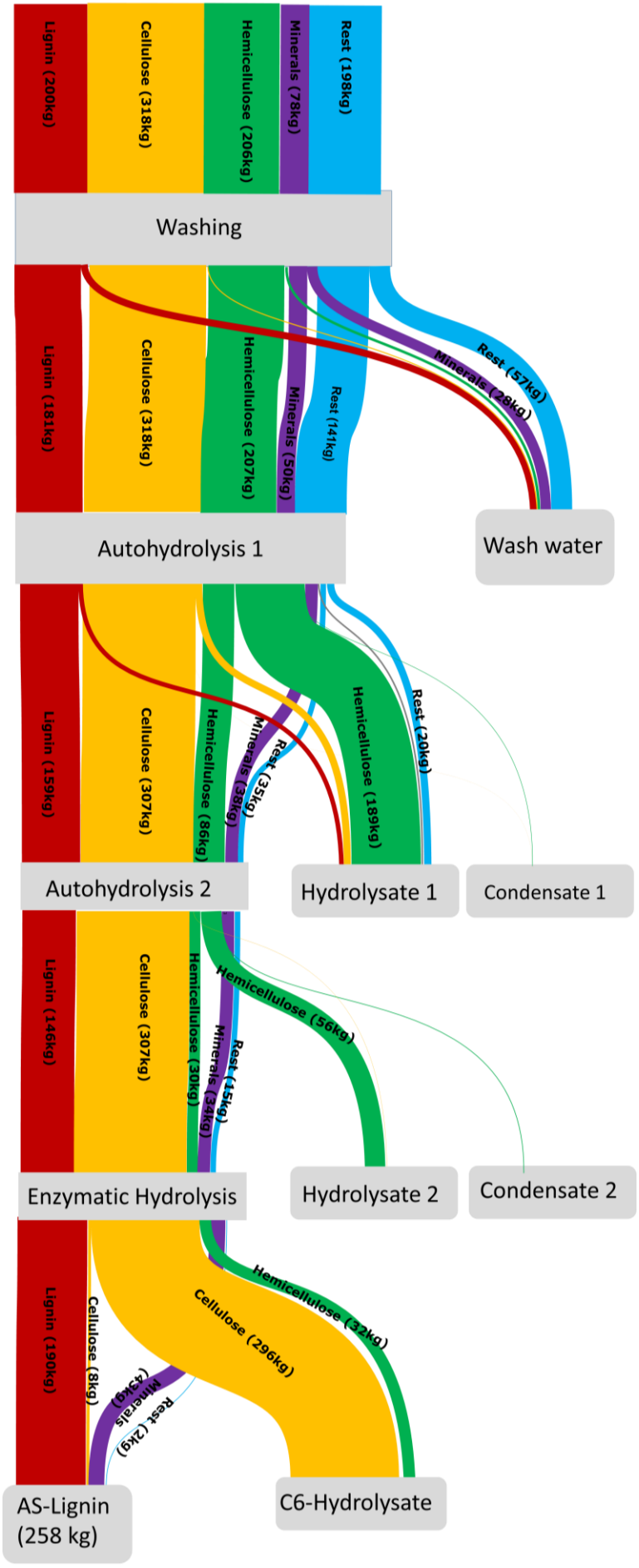

Fig. 5-22: Sankey diagram for the two-step autohydrolysis pretreatment and enzymatic hydrolysis. Component flow mass corresponds to its width. Lignin, cellulose, hemicellulose, minerals (inorganics) and rest are determined in the solid; component mass removal is regarded to fluid effluent. Hemicellulose, furfural and cellulose are derived from measurement in the hydrolysates and condensate.

5.3.2.4. Scale-up in 400 L reactor

The two-step autohydrolysis pretreatment, followed by enzymatic hydrolysis of the liquid fraction and solid fraction, separately, and product purification (AS-lignin filtration and drying; and C5 and C6 hydrolysate filtration and vacuum distillation) were tested in a two weeks trial with 18 kg dry wheat straw at Fraunhofer CBP in Leuna, Germany, compare section 4.3.1.5. The fractionation took place with the desired quality of the hydrolysate streams. The yield of pentose (C5) and glucose (C6) and the lignin purity was below expectation, see Tab. 5-9. The pentose yield in the C5 hydrolysate in total is 7.8 wt%, but more than 20 wt% is expected, see Fig. 5-20.

Tab. 5-9: Masses and Yield of AS-lignin, glucose (C6), and pentose (C5) of the 400 L pretreatment reactor sequential processing following the two-step autohydroysis approach.

i **[-]**	**stream** **[-]**	**M_i** **[kg]**	**Y_i** **[wt%]**
AS-Lignin	40 wt% Lignin	5.4	**30.0**
C6	in C6 stream	2.73	15.2
	in C5 stream	0.08	0.4
	total recovered	2.81	**15.6**
	in AS-Lignin	3.24	18.0
C5	in C6 stream	0.94	5.2
	in C5 stream	1.40	7.8
	in wash liquors	0.46	2.6
	total recovered	2.34	**15.6**
	Sum	16.6	**79.2**

After the pretreatment of the first step, the pentose is recovered via percolation with 200 L of 90 °C water for 23 minutes. The recovery on 400 L scale was lower than in the suspended batch extraction at the 40 L scale. Thus, the percolation did not achieve an equilibrium of pentose concentration in the wheat straw pore and the flowing water. Consequently, the remaining pentose attached to the straw can be easily degraded in the second pretreatment step. Additionally, tiny particle size reduction was achieved; it was impossible to have a steam explosion release to reduce the particle size, but the reaction was quenched with water. The used mill after first and second pretreatment is not designed for wheat straw and did not allow to reach the particle size required for the enzymatic hydrolysis. As a result, the lignin content was only raised to 40 wt% in the AS-lignin.

The scale-up experiments successfully identified critical processing steps that need careful consideration in further process development, such as particle size reduction and temperature-dependent protein precipitation and filtration. Additionally, the importance of dedicated equipment selection and testing was demonstrated. It was impossible to transfer the knowledge made with one material type and equipment to another material, e.g., milling and dewatering the suspension after pretreatment. For a batch process with batch milling, as conducted here, either different processing parameters, e.g., solid content, milling duration, screw speed of the press, or a different type of wet milling, must be tested.

5.3.3. Steam continuous

Screw conveyor reactors at Fraunhofer WKI in Braunschweig, Germany, compare section 4.3.1.6, and Lund University in Lund, Sweden, compare section 4.3.1.7, are tested with wheat straw for two days each to investigate the operational behavior and validate the two-step autohydrolysis pretreatment approach. In both pieces of equipment, the two-step pretreatment was operated stably with desired quality of the solid and liquid fractions.

In Braunschweig, the washed lignocellulose was fed into the reactor via a look chamber. Material of any density and moisture can be fed as long as the biomass does not adhere to the look chamber wall blocking the chamber. Wheat straw is especially prone to adhere to metal surfaces due to its low particle density and high water holding capacity; thus, the feed moisture content must be below a certain threshold. Additionally, a high-pressure screw feeder was tested that facilitates a volumetric compression of the straw to form a gas and pressure-tight plug. The drainage drill allowed pressed liquid to escape radially. At a constant screw speed, the screw motor power consumption, which is a measure for the torque exerted on the plug, was used to evaluate the plugging quality. This particular machine was designed for wood chips requiring different volumetric compression and did not reach the required torque.

The high-pressure screw feeder in Lund did not make volumetrically compact the straw in the screw, but the plug was formed in the annular plug zone without screw flights. Here the biomass also acts as a bearing for the screw. The plug is compressed by a jacket section in the plug zone that can move radially toward the plug. The compaction force is controlled with hydraulic oil; thus, the plug diameter is flexible with constant radial pressure. Here the plug quality is not affected by the required volumetric

compaction of the raw material. Additionally, this system possesses more operations parameters, thus more degrees of freedom to find a suitable parameter combination for the desired material. Finally, when pushed through the plug zone, the plug is conveyed into the reactor with screw flights. The limitations of this system are the moisture content of the material since it needs to be dry enough to be conveyable in the high-pressure screw. It was observed that the feeding conditions that are stable for room temperature wheat straw resulted in an undesirable plug opening when only the straw temperature was raised to 40 °C. It is suspected that the stiffness of the fibrous straw particles is reduced with increasing temperature. Thus a new set of feeding parameters had to be found. It is evaluated that the feeding parameter needs to be set regarding the substrate type, moisture and temperature, and the feeding rate and reactor pressure. The steam-exploded wheat straw (190 °C, 14 bar, 18 min, S_0 = 3.9), massively defibrillated and reduced particle size was fed against 14 bar with stable parameters for one hour. Here, it was demonstrated that pretreated material could be fed into the reactor with the same high-pressure feeder used for raw straw and wood chips.

The transportation of the biomass in the reactor was achieved for straw with varied moisture content. When straw with the moisture of L/S= 1.5 was used, no material adhering to the inner walls and screw was found when the reactor was opened, whereas, at a moisture content of L/S = 2.3, a certain amount of particles were found on walls, the screw shaft. Thus it is recommended to work with a low moisture content to maintain a narrow residence time distribution.

It was observed that the straw particle size is not affected by the high-pressure screw feeder but by the material release technique. Opening the reactor, pretreated material was recovered next to the outlet; thus, it was thermally pretreated and still intact. The material was released via steam explosion during the operation, resulting in an intense defibrillation and particle size reduction.

The temperature control in the reactor is facilitated by pressure control. In the two investigated reactors, two different pressure control systems were used. The first is a ball valve controlled by a PID controller, and it leads to long drifts of the pressure around the set point. The second is a mechanically controlled pressure reducer, resulting in a highly stable reactor pressure and thus temperature. In this system period, drops were detected caused by the discontinuous feeding. A discontinuous

discharge of the pretreated material leads to small periodic fluctuations in the reactor. Regarding the volatile behavior of furfural, it is suspected that the pressure drops, leading to boiling of the liquid at reaction temperature and evaporation of volatiles into the vapor phase. Furfural does not degrade in steam and can be purged via discontinuous discharge.

5.3.4. Overall evaluation

In Fig. 5-23, compare Tab. 5-10, the pentose yield after pretreatment at a severity factor of $S_0 = 3.9$ is plotted versus the initial moisture content of the wheat straw. The pentose mass is determined after analytical extraction for the steam pretreatments. Extremely low moisture content leads to a decrease in yield and increase in concentration for the same reactor type. The use of the 3 L reactor leads to a substantial increase in the water content, compared to the 40 L reactor, induced by the heat loss. This result is expected since water is a reaction partner that needs to access the hemicellulose. The LHW experiments result in extremely poor concentrations but comparable yields as the 3 L steam pretreatments. The 40 L steam data is generated with washed straw; here, the highest yields and resulting loading were achieved. It is unclear to which extent the initial moisture content, the wheat straw source, and the prewashing contribute to this result. It is suspected that water saturation is reached at a moisture content of 50 wt% or L/S=1; otherwise, the LHW experiments should also show higher yields. Regarding Fig. 5-6 and Fig. 5-19, the change in pH is not large enough to explain the increase in yield. The observations result in the hypothesis that the prewashing does remove organic acid pH buffering inorganics and positively affects the ratio of xylan hydrolysis and pentose degradation rates.

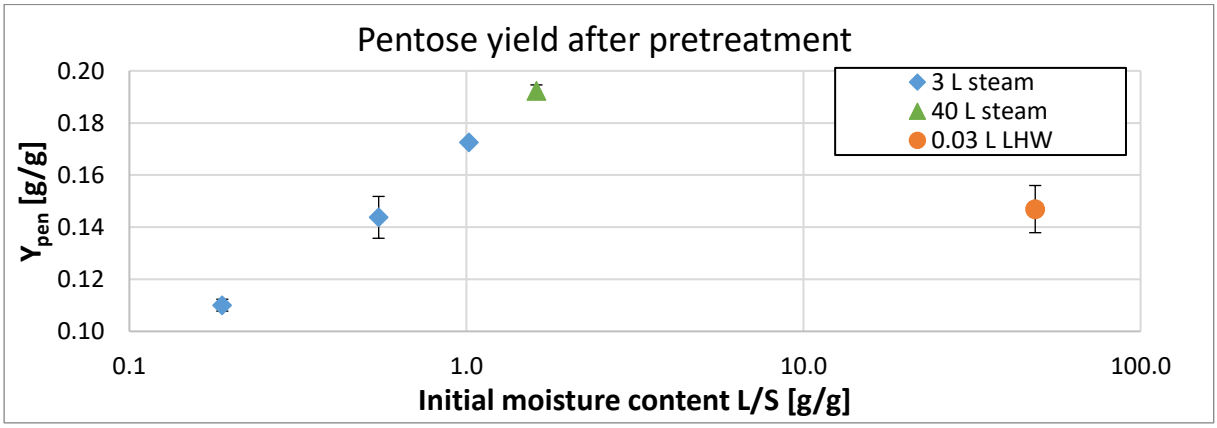

Fig. 5-23: Pentose yields versus the initial moisture for at S_0 = 3.9. 40 L steam experiments in triplicate others in duplicate, error are the standard deviation. Yield in 40 L reactor based on washed material.

Tab. 5-10: Pentose yields for different initial moisture content in different reactors.

Reactor	**Initial moisture**		**Final moisture**		**Concentration**	**Y_{HC} ($M_{HC,f}/M_0$)**	
	w_{water}	L/S	w_{water}	L/S	C_{HC}	Value	st. Dev.
[-]	[wt%]	[g/g]	[wt%]	[g/g]	[g/L]	[g/g]	[g/g]
3 L steam	15.9	0.19	52.8	1.12	86.5	0.110	0.002
	35.4	0.55	67.6	2.09	60.5	0.144	0.008
	50.4	1.02	72.1	2.58	58.9	0.17256	0.00003
40 L steam	61.7	1.61	68.4	2.20	106.0	0.192	0.009
0.03 L LHW	98.0	48.67	98.0	48.67	2.816	0.147	0.009

The two-step autohydrolysis pretreatment approach was tested and validated in batch and continuous operation mode in several reactor sizes. Compared to a single-stage autohydrolysis pretreatment, this approach generates improved

- recoveries of the xylan fraction in the hydrolysate,
- reaction rates,
- purity of xylans in the hydrolysate,
- the concentration of xylans in the hydrolysate,
- suppression of fine particle presence, and
- suppression of degradation reactions.

The stream quality is improved regarding the essential absence of fine particles that are difficult to remove, allowing a concentration and processing in membrane-based processes and does not show a problem with fouling in pipes and tubes.

Furthermore, it was shown that feedstock washing help to increase the purity and quality of the hydrolysates and can reduce the buffering capacity on the biomass and thus increase the reaction rate.

This research also posed new questions regarding the

- presence and fate of proteins, waxes, and non-structural carbohydrates in the feedstock,
- the effect of inorganics on the xylan hydrolysis and pentose degradation rate, and
- the use of wash water in a biorefinery concept.

5.3.5. Product quality evaluation

Another part of the process evaluation is the product evaluation. In the frame of the project “ELBE-NH” funded by the German Federal Ministry of Education and Research, the applicability of the product stream of proposed two-step autohydrolysis pretreatment were evaluated. Technical results from ELBE-NH that allow the product quality evaluation are summarized in this section.

The wash water, condensates, and cellulignin are tested for the biogas potential, compare section 4.2.1. The wash water and condensate are produced in batch and show a small concentration; thus, they could not be analyzed directly but as a co-substrate and resulted in high conversions. The cellulignin biogas potential, see Fig. 5-24, is 433 norm cubic meters per ton of organic dry matter after 11 days. The yield and conversion based on the present carbohydrates in the cellulignin are comparable to microcrystalline cellulose.

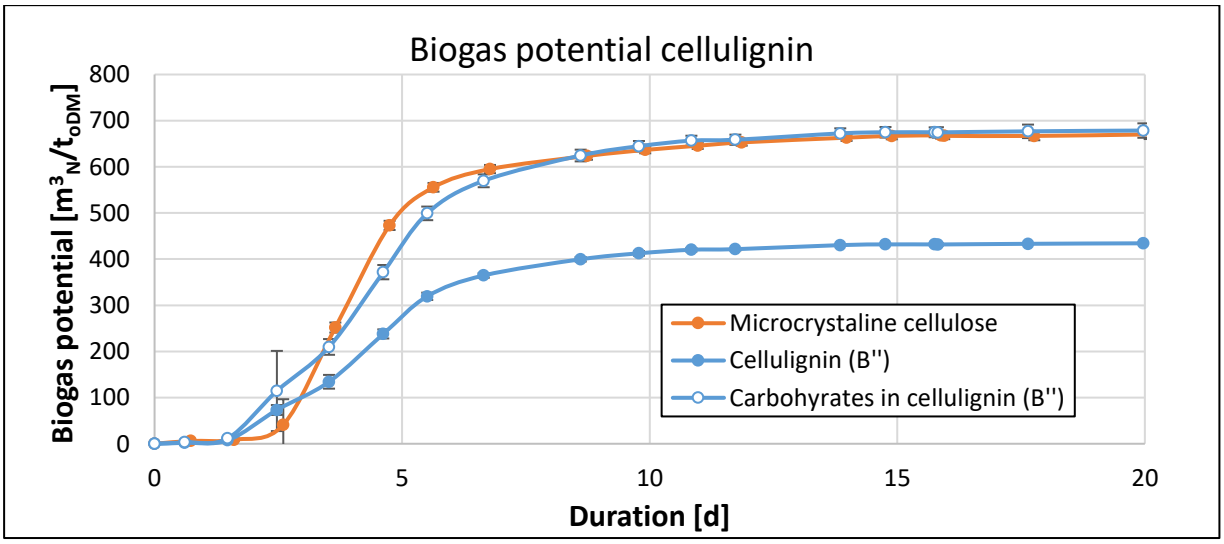

Fig. 5-24: Biogas potential of cellulignin (B’’) from 40 L reactor with a carbohydrates mass fraction of 64 wt% (cellulose 60 wt%, hemicellulose 4 wt%). Experiments in duplicate. Lines for graphical orientation.

The hydrolysates possess a low particle concentration measured in drinking water suitable turbidity methods, compare section 4.2.2. The hydrolysate never exceeded turbidity of 250 NTU and could be as low as 14 NTU based on the depth filtration throughput using pretreated wheat straw as a bed filter. The filtered hydrolysate was used in ultrafiltration and reverse osmosis without a detectable effect on the membrane permeability. The hydrolysates must be essentially free of fine particles and contaminants to purify pentose oligomers from it. The TUHH-IUE can produce a white pentose oligomers powder fraction from the steam hydrolysate based on UF and anti-

solvent precipitation without using a further clarification technique after pretreatment. The TUHH-IBB successfully converted the hemicellulose and glucose in the hydrolysate to organic acids with essentially complete conversion. In previous trials based on hydrolysate from a flow-through pretreatment, the solid particle load in the pentose-rich hydrolysate caused clogging in the tubes; there was no such problem with the steam hydrolysate.

The AS-Lignin was washed, dried, and milled to produce a fine powder, see Fig. 10-4 and Fig. 10-5. *Tesa SE* can reliably produce an adhesive tape with 10 wt% lignin and application-relevant properties, e.g., cohesion, adhesion, and optical clarity.

5.4. Solid-Liquid Extraction

The results of this section have been partly published in paper [98], and a patent was filled [99].

The two-step autohydrolysis comprises an intermediate extraction of the pentoses. It should possess a high extraction yield for the plant profitability and avoid the pentose to furfural conversion in the second reaction step. The extract concentration should be high to reduce the demand for a costly concentration step. Also, the specific solvent (water) consumption should be low to simplify the demand for fresh, recycling, and waste-water treatment. There are established counter-current extraction process established for different biomasses, such as pulp, compare Fig. 2-11, and sugar beet extraction, see Fig. 2-14. There is no such established process available for lignocellulosic material. At ENEA a suspension extraction is combined with a belt extractor, this configuration may result in a high extraction yield, but not in a high extract concentration, low water demand, or low space demand, see and Fig. 2-12. Sievers at al. [84], investigated the belt filtration extraction of pretreated biomass, but only achieved high pentose recoveries at high water consumptions of L/S = 10 – 15, compare Fig. 2-13.

This work proposes a process that fulfills the goal discussed above and is operated in a counter-current manner. Data for the design parameters are based on the experimental experience. The proposed process is evaluated by a mass balance and compared to two simpler extraction processes, compare section 4.4.4.

The proposed counter-current extraction process shows similarities to a mixer-settler extraction process in liquid-liquid extraction systems, see Fig. 5-25a. Solid and liquid phase flow in a counter-current manner through a series of suspension extractors (mixers) and mechanical dewatering devices (settlers) organized as stages.

To facilitate a low solvent consumption, the fluid pressed out of the solids, called filtrate, is recycled mainly into the extractor, while only a tiny amount of liquid is fed to the next stage, see Fig. 4-2 and Fig. 5-25b. A conveyor for the transport of pressed biomass to the next extractor may be required in large plants. In this case, it is suggested that the extract of the next stage is not fed directly to the extractor but the conveyor first. It is regarded as means to contact the solids with a lower concentrated fluid stream. Therefore, less solute must diffuse from the particle inside to the surface. The conveyor

is regarded as optional. The wet biomass is transferred directly into the extractor through gravity without a conveyor. To achieve a steady operation of the screw press, the feed tank is kept full at all times by overflowing. The excess amount of suspension is recycled back to the extractor. Additionally, it is a meaningful measure to increase the mixing residence time in a plug flow manner, promoting to achieve an equilibrium. The residence time distribution in the continuous stirred tank is imperfect to reach an equilibrium. The filtrate recycle-stream decreases the extract amount fed to the previous stage and allows for extraction in a suspension similar to the suspension extraction with recycling.

In Fig. 5-26a, the block flow diagram of the extraction process is shown in three stages. Here it is integrated into a two-step pretreatment approach. The first reactor (SCR 1) produces the steam pretreated lignocellulose leached in the discussed process. The pressed material leaves the extractor and is pressed further in the second reactor's high-pressure plug screw feeder (HP screw before SCR 2). The HP screw filtrate is fed to the filtrate tank, while only fresh solvent is fed to the extractor in the last stage. This integration to a high-pressure feeder is beneficial for the extraction process since the pressed out solute can be recovered. Fig. 5-26b shows the exemplary integration of the last stage of the counter-current extraction and the following screw conveyor reactor with 3D symbols.

In the following sections, first, the experimental results of the suspension extraction are presented and discussed, and second, the design calculations for suspension extraction with and without recycling and the counter-current suspension extraction are given.

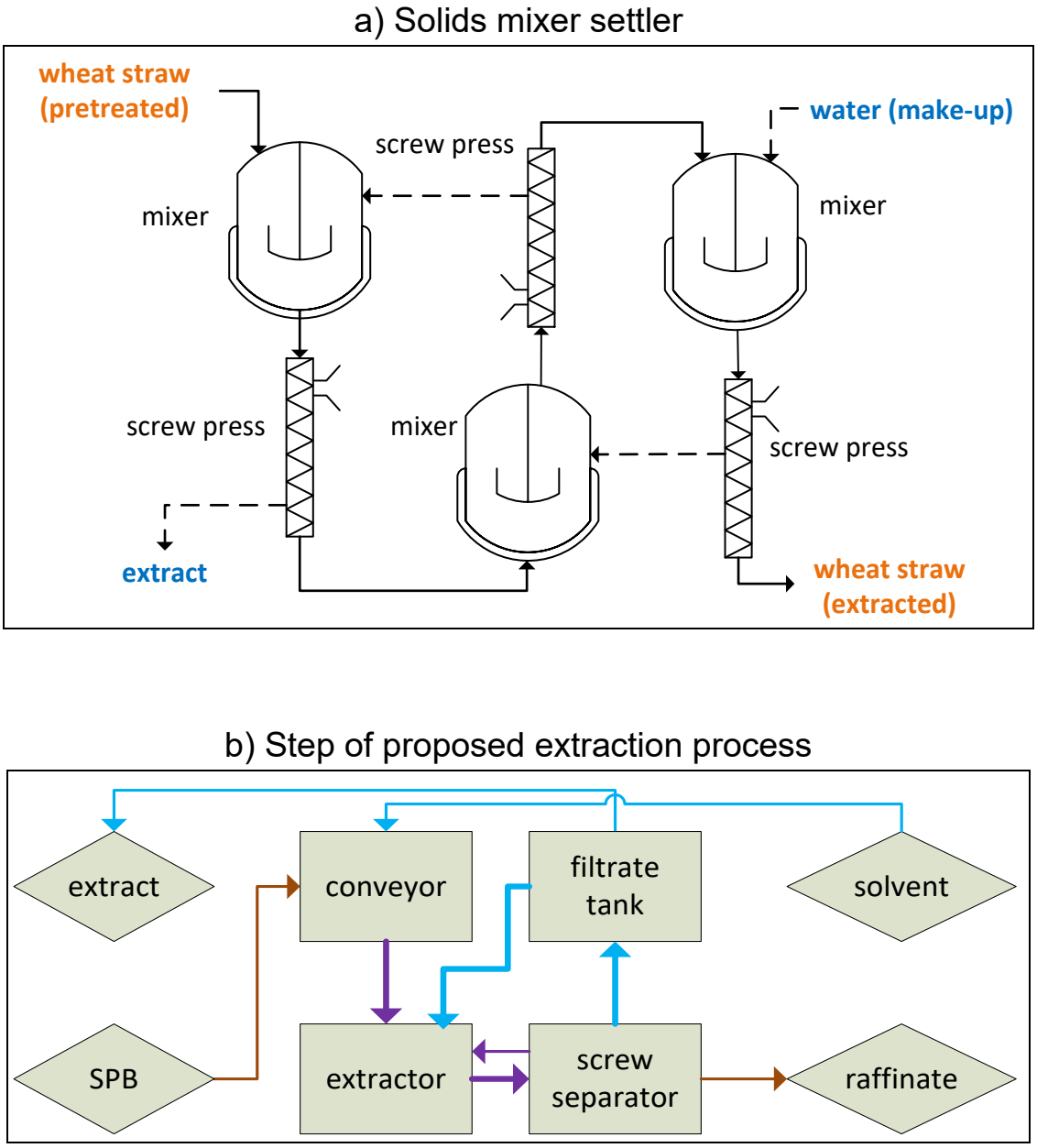

Fig. 5-25: Proposed counter-current solid-liquid extraction process for lignocellulosic material **a)** Simplified process scheme of the proposed counter-current solids-liquid extraction process. Solid containing stream (solid arrows). Mainly solid free stream (dashed arrows). **b)** Block flow diagram of a single stage of the new counter-current extraction process. Diamonds represent overall input and output flows; steam pretreated biomass (SPB), raffinate, solvent, and extract. Rectangles represent the units of each stage, conveyor (optional) with initial mixing of moist solids and solvent, extractor as a continuous stirred tank, screw separator as mechanical dewatering device, and filtrate tank. Recycle streams are overflow from the screw press feed tank (not shown) back to the extractor and fluid from the filtrate tank to the extractor.

a) Two stages of counter-current extractor

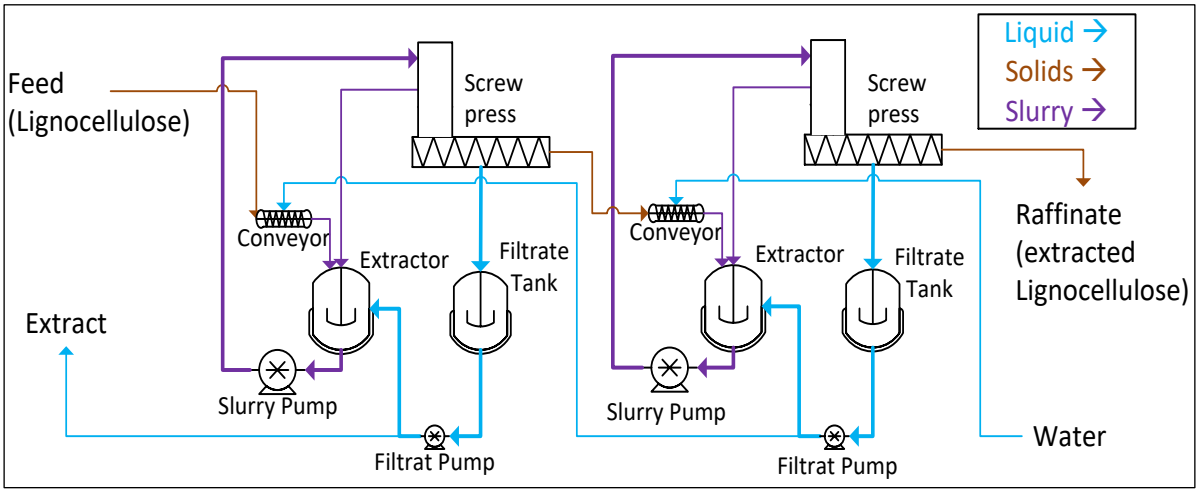

b) Integration of extraction with screw conveyor reactor

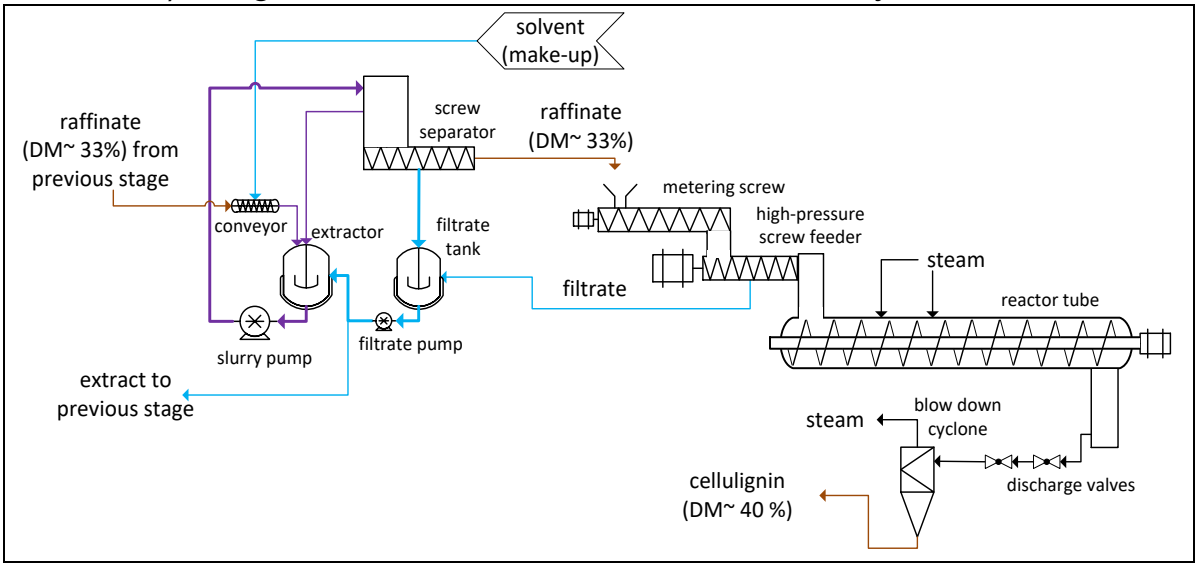

Fig. 5-26: Proposed counter-current solid-liquid extraction process for lignocellulosic material **a)** Graphical representation of counter-current solid-liquid extraction with two stages. Integration into a two-step autohydrolysis concept, including two screw conveyor reactors (SCR). **b)** Graphic representation of the counter-current solids extraction integrated into the subsequent HP screw of the screw conveyor reactor.

5.4.1. Suspension extraction experiments

The solute mass transport rate from the particle interior to the particle outside is essential in an extraction process. The concentration change over time in the bulk phase in a batch suspension extraction was investigated to determine the time to reach the equilibrium concentration for cut and ground pretreated wheat straw, compare section 4.3.3.1. In Fig. 5-27, the total pentose concentration is shown in a dimensionless scale from zero (no solids added) to 100 (equilibrium concentration).

The main difference between the two shown samples is the particle size. The ground particles reach 87 % of the equilibrium after one minute, while 58 % is reached for the larger particles. The ground and coarse samples reach an equilibrium between one and five minutes and between five and ten minutes, respectively.

Smaller particles possess a larger surface area and a shorter average distance inside the particles; thus, mass transfer rates are significantly larger. The oligomer nature of the pentoses after autohydrolysis stream pretreatment and the solute free bulk phase at the beginning of the batch extraction are expected to increase the equilibration time during the suspension extraction. However, the equilibration time is reasonably short for ground particles, which makes a continuous extraction feasible. The residence time distribution of a batch extractor and a continuous stirred tank are not comparable. It is assumed that a bulk concentration close to the equilibrium concentration can be achieved by selecting a hydraulic residence time five to ten times greater than the measured equilibrium time in a batch extractor. Therefore, the assumption to reach an equilibrium in the continuous stirred tank suspension extractor in the proposed counter-current extraction is considered feasible. In a continuous stream pretreatment process, the biomass particle size is reduced through the plug screw feeding, similar to a single screw extruder, and the unloading of the reactor, which can be realized as a continuous steam explosion. The composition of the ground pretreated wheat straw was taken as the feed in the leaching scenario.

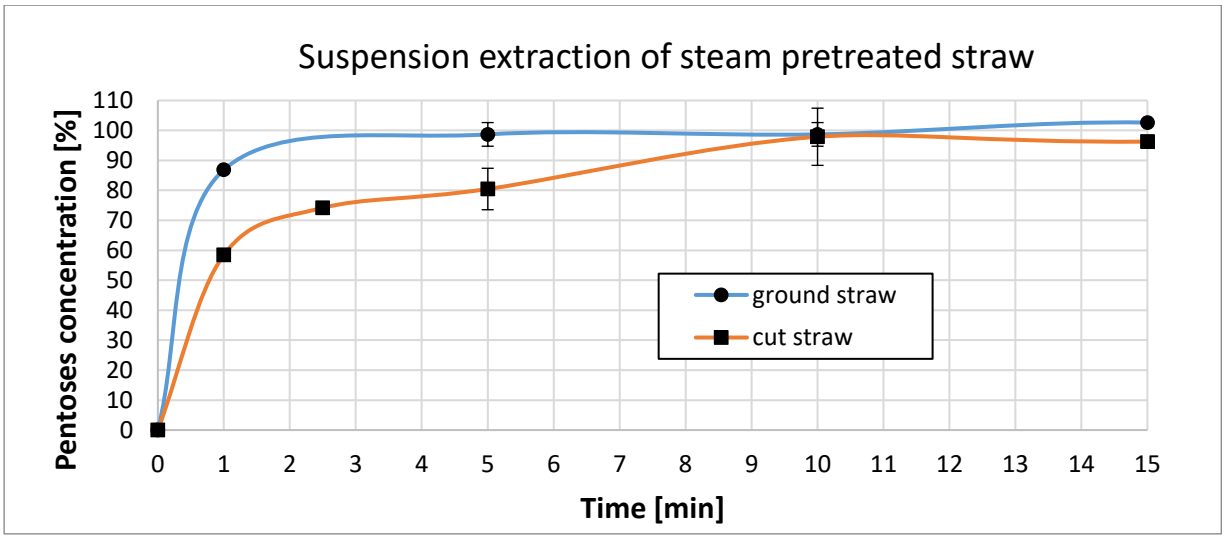

Fig. 5-27: Dimensionless concentration of total pentoses of a suspension extraction of steam pretreated wheat straw (180°C, 35 minutes) in a stirred tank with water at 70 °C. Solid lines are shown for visual orientation only. Experiments in duplicate.

5.4.2. Process simulation and plant scaling

This section presents the process windows for the three discussed extraction processes. Here the process window is the range of the extraction yield Y^E and the extract concentration C^E that can be achieved by the individually selected design parameters. The design parameters range is chosen based on experience. Fig. 5-28 shows the process windows for the three extraction processes and a combined process window for applying the leaching process. Fig.5-29 displays them in an analog manner for the washing process.

The performance targeted design goal for extraction is to reach simultaneously high extraction yield and extract concentration at a low solvent consumption.

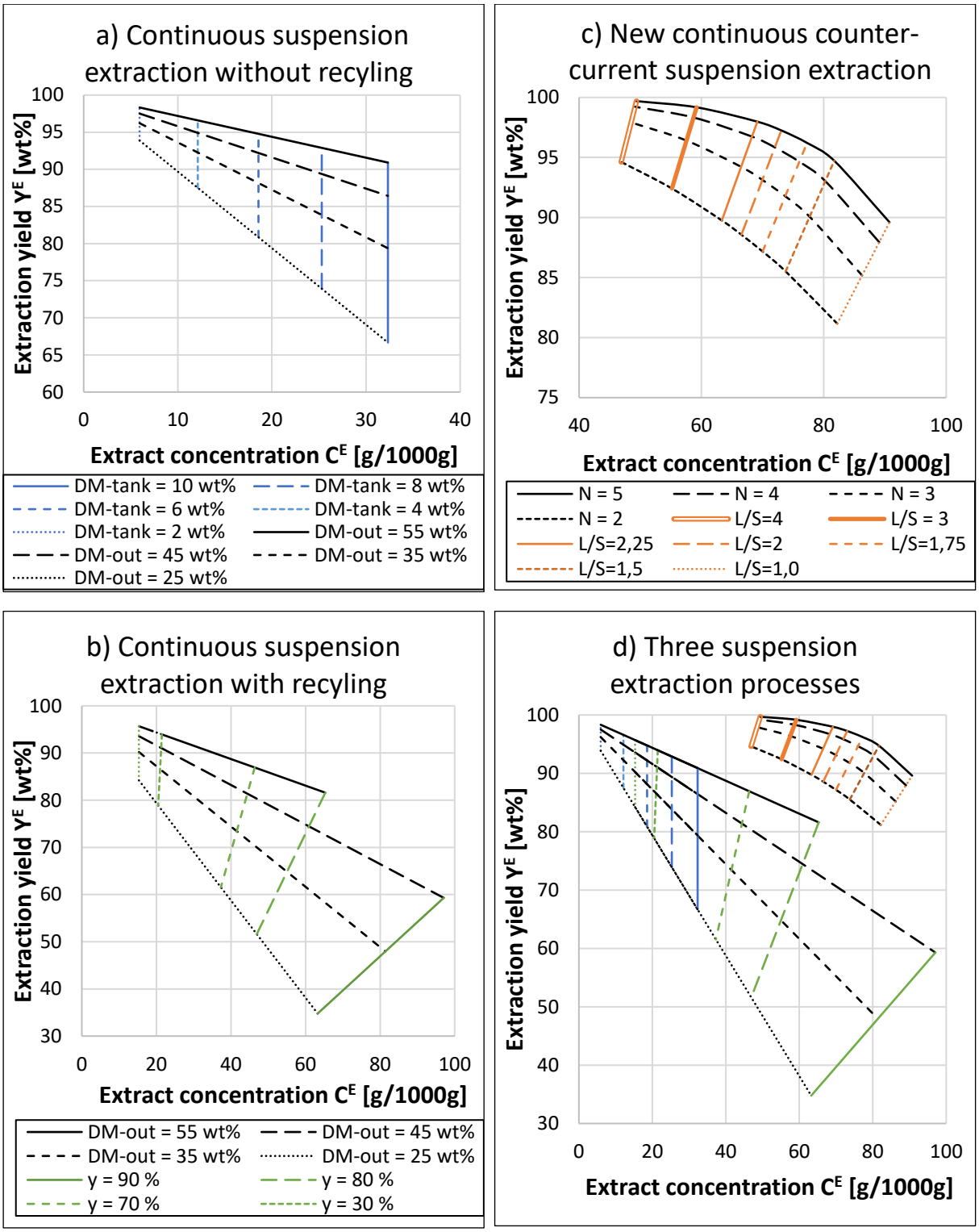

Fig. 5-28: Process windows for the continuous suspension extraction processes for the leaching scenario**. a)** Continuous suspension extraction without recycling. **b)** Continuous suspension extraction with recycling. **c)** New continuous counter-current suspension extraction. **d)** All three suspension extraction processes. DM-tank = dry matter content in the extraction tank. DM-out = dry matter content at the stage outlet (press). y = recycling factor. N = number of stages. L/S = liquid to solid ratio (solvent consumption).

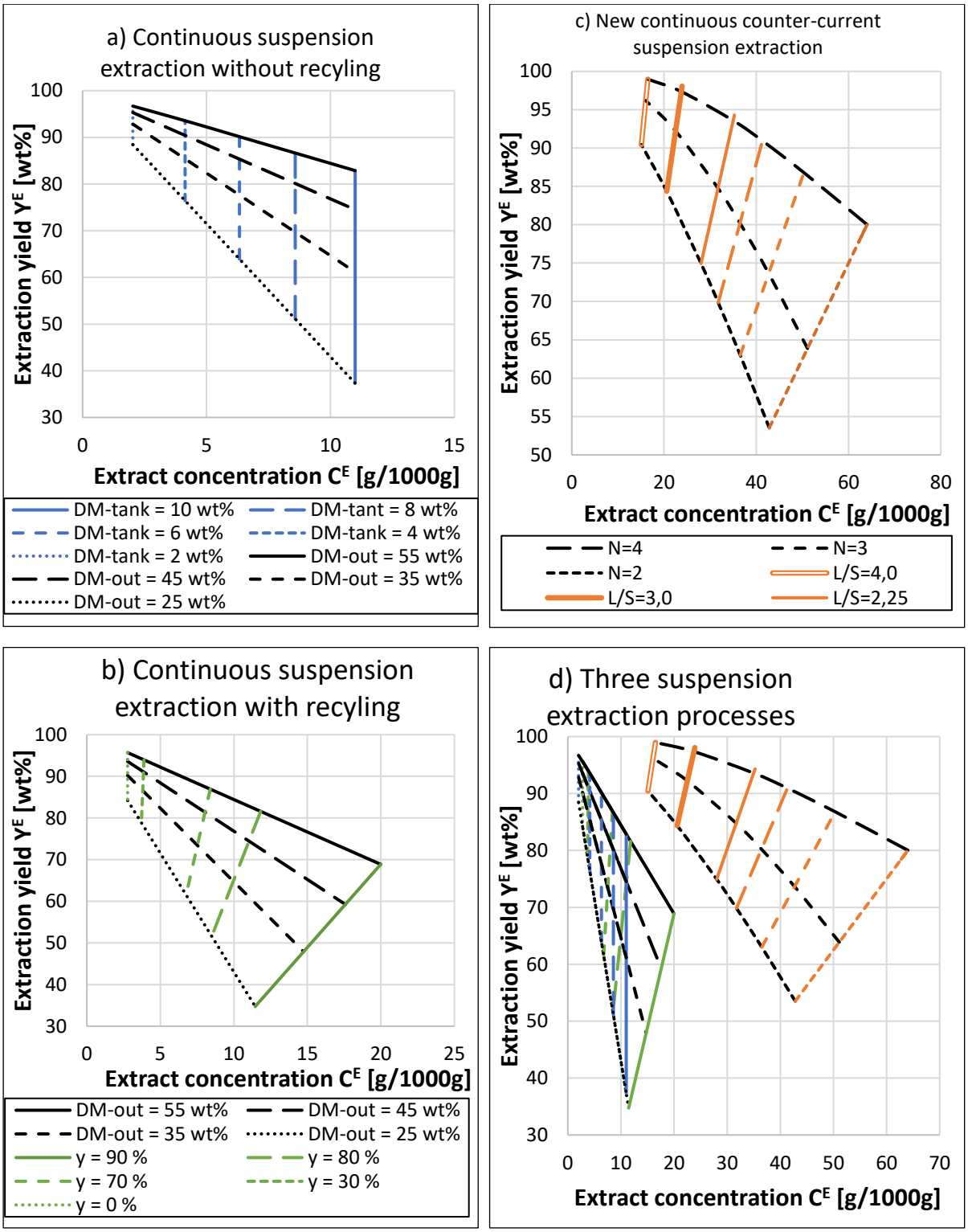

Fig.5-29: Process windows for the continuous suspension extraction processes for the washing scenario. **a)** Continuous suspension extraction without recycling. **b)** Continuous suspension extraction with recycling. **c)** New continuous counter-current suspension extraction. **d)** All three suspension extraction processes. DM-tank = dry matter content in the extraction tank. DM-out = dry matter content at the stage outlet (press). y = recycling factor. N = number of stages. L/S = liquid to solid ratio (solvent consumption).

5.4.2.1. Extraction without recycling

Fig. 5-28a and Fig.5-29a show the process windows for the continuous suspension extraction. The vertical lines refer to the variation in the dry matter content in the tank. As expected, the less the feed is diluted with the solvent, the higher is the extract concentration. The near-horizontal lines represent constant values of DM-out. The dry matter content after the pressing, DM-out, shows no effect on the extract concentration. The dryer the material after the press, the higher is the extraction yield. The slope of the near-horizontal lines is affected by DM-out. The extraction yield is affected by both design parameters. The dilution of the solids in the tank reduces the raffinate concentration. Thus, the remaining solute in the final underflow – liquid in the pressed solid – is reduced. The dry matter content after pressing determines the amount of solute remaining at the solids in the outflow.

The leaching and the washing case differ in the position of the process window and not in its characteristics. The washing case shows a minor maximal concentration, which is expected to result from the lower solute amount in the feed. Also, a more comprehensive range of extraction yields is possible than in the leaching scenario. This is caused by lower solute content and a larger solvent amount in the feed. The solvent consumption is in increasing order of DM-tank: 46, 21, 13, 9, and 6 for the leaching scenario, and 49, 24, 16, 11, and 9 for the washing scenario, compare with supplementary material.

5.4.2.2. Extraction with recycling

Fig. 5-28b and Fig.5-29b display the process windows for the continuous suspension extraction with recycling. Here a dry matter content in the tank was chosen to be 5 wt% and was not varied in this study. The dry matter content at the outlet after pressing and the recycling factor are varied to calculate the process window.

The line for a constant recycling rate is vertical at no recycling, and its slope decreases with rising values of the recycling factor itself. The larger the recycling factor at constant DM-out, the larger the concentration, the lower the solvent consumption and the lower the yield. An increase in DM-out improves the extraction yield and extract concentration at the same time if the recycling is larger than zero. Like the previous process, the lines for constant DM-out are nearly horizontal, and the slope decreases with decreasing DM-out. When increasing the recycling rate, the lines of constant DM-out are extended towards higher concentrations and lower yields. Changing DM-tank

does not affect the position of the lines of constant DM-out but leads to a shift of this line along its direction (not shown).

In Fig. 5-30, the effect of the recycling factor is shown on the extraction yield, extract concentration, and solvent consumption for the leaching scenario at DM-tank = 5 wt% and DM-out = 35 wt%. On the one hand, increasing the recycling factor decreases the solvent consumption linearly and increases the extract concentration, which targets the performance-centered design. On the other hand, increasing the recycling factor decreases the extraction yield progressively. That means that the effect on the yield is small for small recycling factors and large for larger ones. A recycling factor of 100% is not possible since the water input is larger than the water output adhering to the solids. Thus, some amount of extract must be removed from the system. The maximal recycling factor depends on the feed composition and the selected process parameters (not shown).

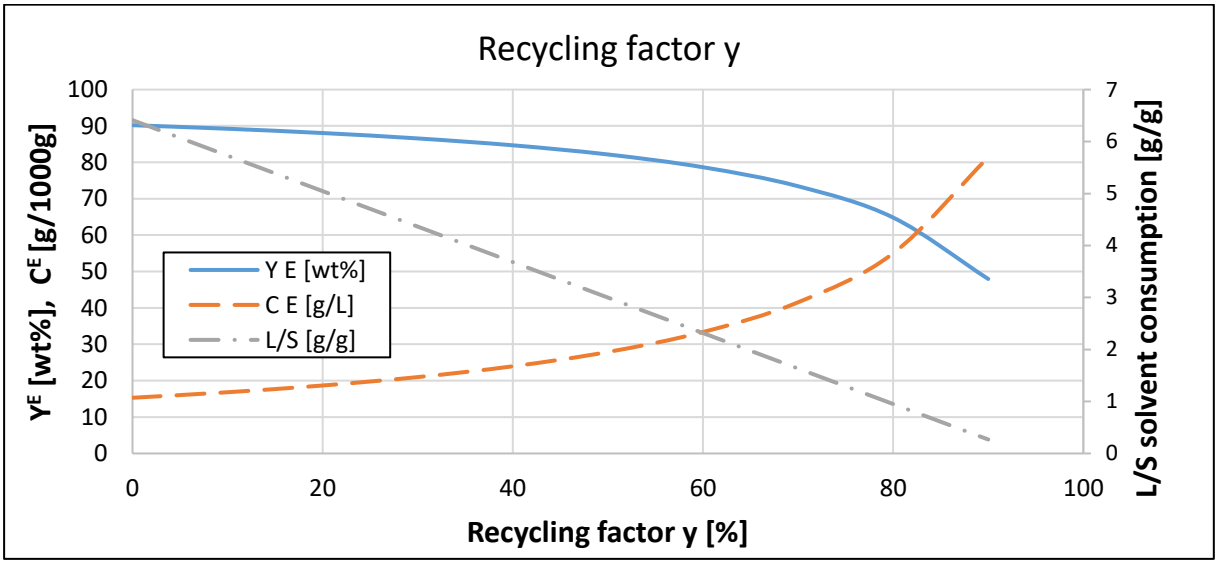

Fig. 5-30: Effect of recycling factor in suspension extraction for leaching scenario. Extraction yield, extraction concentration, and solvent consumption as a function of the recycling factor. DM-tank = 5 wt% and DM-out = 35 wt%.

5.4.2.3. Counter-current suspension extraction

Fig. 5-28c and Fig.5-29c show the process windows for the continuous counter-current suspension extraction. The near-vertical lines represent a constant solvent consumption L/S, while the near-horizontal lines represent the number of stages N. The DM-tank does not affect the process windows (not shown). Increasing the number of stages increases the extraction yield and the extract concentration simultaneously, without affecting solvent consumption. Thus, it becomes evident that many stages are favorable to reach the performance-centered design criteria. The higher the number of

stages, the lower is the effect of another stage on the yield and concentration. This effect is more pronounced with an increasing solvent consumption. By increasing the solvent consumption, the yield increases, and the extract concentration decreases. At low solvent consumption, the effect of further stages on yield and concentration remains large.

For this process, the two regarded process parameters can be selected in a wide range of values. Choosing a stage number higher than five does not seem necessary. However, it is possible. For both scenarios, it can be seen that a high yield, high concentration, and low solvent consumption can be achieved with the regarded dry matter contents after pressing.

5.4.2.4. Comparison of the three extraction methods

Fig. 5-28d and Fig.5-29d show the process windows for the three regarded continuous suspension extraction processes. The lines for constant DM-out are identical for the extraction with and without recycling for both scenarios. Thus, recycling a fraction of the extract opens a larger process window and allows more flexibility in selecting design parameters. Additionally, recycling allows achieving substantially larger extract concentrations. Unfortunately, the yield is reduced at the same time. This effect is more pronounced in the leaching scenario than in the washing scenario. A lower DM-tank or a larger recycling factor (> 90 wt%) can be chosen to expand the lines of constant DM-out for the suspensions extraction with recycling.

The counter-current extraction process can be found further up and right in the process window diagrams, which means that the extraction yield and the extract concentrations are improved simultaneously. In the counter-current process, the combination of extraction yield and extract concentration is not defined by the DM-out but depends on the number of stages. Also, meager solvent consumption is possible with this process, with a comparatively mild decrease in the yield at a constant stage number. In the recycling process, low solvent consumption is possible but with generally worse extraction yields. The yield in the counter-current extraction process is approaching 100 %, and concentrations of up to 90 g/1000g are possible. The high performance is possible because the solvent is used to remain a medium but constant concentration difference to the raffinate in each stage. Thus, the underflow concentration is relatively low at the input to the final pressing device. The extract concentration is enriched and approaches the feed concentration. The extract concentration can be further improved

by choosing a lower solvent consumption and a higher number of stages to compensate for the yield. The limit in yield and concentration is 100 wt% and the feed concentration, respectively.

5.4.3. Overall evaluation

The suspension extraction without recycling possesses low flexibility in selecting design parameters and extraction performance. Very high extractions yields are possible by a substantial dilution of the extract concentration and enormous solvent consumption. It is impossible to reach concentrations in the extract near the feed concentration. However, this process does not require recycling streams; thus, a low effort in the set-up and operation is required.

The suspension extraction with recycling improves flexibility by selecting design parameters from a more comprehensive process window. The advantage of this process is the vastly reduced solvent consumption without a significant increase in the process complexity. Thus, it is suspected that the installation and operational costs are still low. The application for washing and leaching is possible. The application of extreme recycling factors enlarges the process window but is limited by practical constraints. With an increasing recycling factor, the recycling stream increases immensely. A significant reason is that the inflow to the filtrate tank is increased. The amount of liquid recycled at extreme recycling factors becomes a multitude of the process solids mass. Additionally, it is challenging to split a stream into two very differently large streams since fluctuations in all streams may be larger than the small outflow. Thus, it is not easy to maintain a steady operation.

It was demonstrated by Sanchis-Sebastiá et al. [104] that suspension extraction with recycling is a feasible approach to wash straw after it is used as animal bedding to gain a straw-rich substrate for the production of lignocellulosic ethanol and one manure-rich stream for bio-methane production. Here, the advantages are an increased concentration for biogas production and reduced demand for costly wastewater treatment. The application is possible due to the moderate requirements for the extraction yield [105].

The process engineer still has to find a trade-off between concentration and extraction yield for the leaching applications. If the two-step pretreatment process is considered, the valuable solute should be removed before further treatment of the solid to avoid

product degradation. Thus, a high extraction yield is favored. In this case, there is no significant advantage of using a recycling stream.

The continuous counter-current suspensions extraction process proposed in this work allows to reach the three desired extraction performance parameters, namely extraction yield, extract concentration, and low solvent consumption, simultaneously. Thus, this process is favorable for leaching and washing applications over the other two discussed reference processes. Already at two stages, the superiority was shown. An extensive range of values for the process parameters can be chosen; thus, the process can be flexibly adapted to the regarded separation task and processing requirements. An advantage over other counter-current extraction processes is the low solvent consumption and highly concentrated extracts. At the same time, it uses only standard equipment that is widely available and affordable. Furthermore, the spatial arrangement of the plant is flexible, e.g., it can be organized on two or more levels to spare ground area.

A disadvantage is the complexity of the process. The extraction speed is achieved by applying external forces in the mixing and pressing. Here the electrical energy demand must be considered carefully and at best with the help of experiments. Each application's performance and process windows are different and must be evaluated individually. In addition, the screw press must be selected and tested for each material. The throughput, dry matter content in the solids, and the liquid effluent's fines must be investigated experimentally. The mass of fines in the filtrate may be influenced by the dry matter content in the entrance of the screw press and the rotational speed of the screw. The latter also affects the dry matter content at the outlet and the throughput. As a rule of thumb, the lower the screw speed, the higher the dry matter content of the pressed solids, the lower the throughput, and the lower the content of fines in the filtrate. The amount and size of fines in the filtrate are essential for the plant design. Due to many possible (screw) press configurations and the non-predictable behavior of the feed material, the apparatus size and energy demand require individual process development. The process was not realized experimentally in its entirety. Thus, many essential characteristics remain unknown, like the stage efficiency, the energy demand for pressing, the pressing throughput.

The stage efficiency is mainly determined by mass transport in the extractor. Therefore, the assumptions of equilibrium, thus, an efficiency of 100% in every stage

might not be appropriate in every application. The main parameters affecting the efficiency are the solids loading in the tank, the energy input by stirring, the residence time and residence time distribution in conveyor, extractor, piping to the press, and the extract inlet positions. If the efficiency is less than 100 %, the process windows are incorrect. It is suspected that a reduced efficiency and a lower dry matter content after pressing can be compensated by increasing the number of stages. While removing fines in a washing application might be desirable, it may cause the need for additional fines removal, e.g., filtration in the extract before further use.

Overall, this study has shown the favorable characteristics of the newly proposed counter-current solid-liquid extraction process and indicates that the demand for experimental and analytical research is needed. The careful selection of a continuous pressing device and its operational parameters at first and secondly the operation of the entire process is proposed for further investigations. Additionally, the economic effects on the plant-wide cost structure of biorefinery processes through integrating the proposed extraction process can be evaluated with flow sheet models. It would allow the evaluation to which extent the extraction process can improve the economic feasibility for known and new biorefining applications.

5.4.4. Conclusion

If all assumptions of the proposed extraction process can be validated experimentally, this process can improve existing biorefinery processes and allow more complex pathways. The latter can be the washing of straw-based animal bedding to reduce the substrate costs or the leaching of oligomeric pentose after steam pretreatment in the two-step autohydrolysis approach. Regarding the continuous steam pretreatment, the feedstock needs to be washed. Feedstock water impregnation and removal of fines and inorganics can be efficiently combined using the investigated processes.

6. Conclusions and outlook

This work aims to facilitate the chemical industry's feedstock change from fossil to renewable resources. The two-step continuous autohydrolysis pretreatment process was developed in this thesis based on a deeper understanding of sequential pentose hydrolysis, allowing a high fractionation of pentoses, hexoses, and lignin.

1. In this work, a wide processing window was investigated for the autohydrolysis pretreatment in terms of temperature, residence time, pH, solid concentrations, and pre- and post- treatments. A deeper understanding of the solid and liquid phase hydrolysis of hemicellulose-derived substances is achieved.
2. Mathematical descriptions of the conditions leading to characteristic phenomena during autohydrolysis aided the process development and allowed the transfer of lab data to production-relevant conditions in the technical hall and pilot scale.
3. The proposed two-step autohydrolysis substantially increases the recovery of pentose oligomers in a separate steam, enabling a separate valorization. The pentose recovery can be improved by 62 %, compared to a single-step pretreatment. In addition, the formation of fermentation inhibiting furfural is suppressed, and the xylan hydrolysis reaction rate is increased.
4. A method was developed to compare processing concepts based on preliminary data. The process targets in technical and economic terms are defined in the first step. Second, each process is evaluated for each target using a meaningful mathematical estimation. Third, the target scores are normalized to a scale from one, for the worst score, to ten, for the best score. Fourth, the normalized score allows fast comparison of the process characteristics; the product of the normalized scores of each process results in the overall performance score, with low tolerance to a weakness.
5. A new screw conveyor reactor (SCR) two-step autohydrolysis pretreatment process is proposed and validated. Comparing it with a flow-through pretreatment at the same full-fractionation performance, it operates with a massively reduced water and energy consumption, resulting in higher pentose and hexose recovery. Also, the SCR operates continuously and has no trouble

loading and unloading annual lignocellulose with challenging transport properties. A prewashing step allows wetting of the biomass to avoid limiting mass transport processes in the reactor, removes fine particles to avoid hydrolysate purification, and removes water-soluble inorganics to reduce the pH- buffering and accelerate the hydrolysis. A further advantage is that there is no limiting heat or mass transport process in the reactor; thus, scaling can be pursued in enormous steps. This concept was validated in scales from a 30 mL batch-screening reactor to a 230 L continuous pilot reactor, along with equipment for intermediate processing steps.

6. A continuous counter-current extraction process was developed that allows the wetting of lignocellulose and removal of fine particles and water-soluble inorganic compounds with low water demands before the pretreatment. The exact process allows the extraction of water-soluble pentoses (product) after the pretreatment. The extraction process comprises a suspension extractor and presses in an approach similar to the mixer-settler process. The extract on every stage is mainly rerouted to the suspension extractors to facilitate fast mass transport and a small and controllable effluent stream to the next stage. The process allows achieving high extract concentrations and extraction yields and low solvent (water) demand for porous biomass with meager product concentration on little available space. A patent was filed.
7. All objectives are achieved. The thesis contains the foundation for a new advanced full-fractionation process of annual lignocellulose fit for industrial application. The gained understanding of all fundamental aspects allows the implementation to commercial users, which has already begun.

Several questions can be investigated in future work to optimize aspects of the two-step autohydrolysis pretreatment process:

The reaction rate and conversion can be investigated for intensively washed feedstock since the reaction speed is significantly affected by the washing-induced removal of buffering capacity. The proposed extraction shows high potential for washings since fines can be removed easily along with pH buffering inorganics. Critical parts of the extraction process are validated experimentally. Realizing a complete and functional plant is a meaningful next step to validating the mass balances and comparing the operation to other extractors, e.g., a continuous belt extractor.

The heat integration can be further investigated via simulation and experiment. A promising approach is to use the exhaust steam to preheat the feed; special attention is needed for the acetic acid that can affect the reaction rate.

The two-step pretreatment process should be tailored to specific products, and the feedstock basis should be widened to other annual lignocelluloses, such as bagasse, corn-stover, and rice straw.

7. References

1. Verband der Chemischen Industrie e.V. (VCI) Daten Und Fakten Rohstoffbasis Der Chemieindustrie, 2017, Https://Www.Vci.de/Vci/Downloads-Vci/Top-Thema/Daten-Fakten-Rohstoffbasis-Chemieindustrie.Pdf, Downloaded 08.09.2021; 2017;
2. Bundesministerium für Ernährung und Landwirtschaft (BMEL) Ernte 2017 Mengen Und Preise, Https://Www.Bmel.de/SharedDocs/Downloads/DE/_Landwirtschaft/Pflanzenbau/Ernte-Bericht/Ernte-2017.Pdf?__blob=publicationFile&v=4, Downloaded 08.09.2021; 2017;
3. Konvalina, P.; Stehno, Z.; Capouchová, I.; Zechner, E.; Berger, S.; Grausgruber, H.; Janovská, D.; Moudrý, J. Differences in Grain/Straw Ratio, Protein Content and Yield in Landraces and Modern Varieties of Different Wheat Species under Organic Farming. Euphytica **2014**, 199, 31–40, doi:10.1007/s10681-014-1162-9.
4. Bachmann, T.M. Considering Environmental Costs of Greenhouse Gas Emissions for Setting a CO2 Tax: A Review. Sci. Total Environ. **2020**, 720, 137524, doi:10.1016/j.scitotenv.2020.137524.
5. Liu, C.; Wyman, C.E. Partial Flow of Compressed-Hot Water through Corn Stover to Enhance Hemicellulose Sugar Recovery and Enzymatic Digestibility of Cellulose. Bioresour. Technol. **2005**, 96, 1978–1985, doi:10.1016/j.biortech.2005.01.012.
6. Ruiz, H.A.; Conrad, M.; Sun, S.-N.; Sanchez, A.; Rocha, G.J.M.; Romaní, A.; Castro, E.; Torres, A.; Rodríguez-Jasso, R.M.; Andrade, L.P.; et al. Engineering Aspects of Hydrothermal Pretreatment: From Batch to Continuous Operation, Scale-up and Pilot Reactor under Biorefinery Concept. Bioresour. Technol. **2020**, 299, 122685, doi:10.1016/j.biortech.2019.122685.
7. Energie aus Biomasse: Grundlagen, Techniken und Verfahren; Kaltschmitt, M., Hartmann, H., Hofbauer, H., Eds.; 2., neu bearbeitete und erw. Aufl.; Springer: Heidelberg ; New York, 2009; ISBN 978-3-540-85094-6.
8. Azad, Md.A.K.; Islam, Md.S.; Amin, L. Straw Availability, Quality, Recovery, and Energy Use of Sugarcane. In Biomass and Bioenergy: Processing and Properties; Hakeem, K.R., Jawaid, M., Rashid, U., Eds.; Springer International Publishing: Cham, 2014; pp. 275–287 ISBN 978-3-319-07641-6.
9. Biorefineries - Industrial Processes and Products: Status Quo and Future Directions; Kamm, B., Gruber, P.R., Kamm, M., Eds.; Wiley-VCH: Weinheim, 2010; ISBN 978-3-527-32953-3.
10. Schmidt, L.M.; Andersen, L.F.; Dieckmann, C.; Lamp, A.; Kaltschmitt, M. The Biorefinery Approach. In Energy from Organic Materials (Biomass): A Volume in the Encyclopedia of Sustainability Science and Technology, Second Edition; Kaltschmitt, M., Ed.; Encyclopedia of Sustainability Science and Technology Series; Springer: New York, NY, 2019; pp. 1383–1412 ISBN 978-1-4939-7813-7.
11. He, Y.; Fang, Z.; Zhang, J.; Li, X.; Bao, J. De-Ashing Treatment of Corn Stover Improves the Efficiencies of Enzymatic Hydrolysis and Consequent Ethanol Fermentation. Bioresour. Technol. **2014**, 169, 552–558, doi:10.1016/j.biortech.2014.06.088.
12. Alonso, D.M.; Wettstein, S.G.; Dumesic, J.A. Bimetallic Catalysts for Upgrading of Biomass to Fuels and Chemicals. Chem. Soc. Rev. **2012**, 41, 8075–8098, doi:10.1039/C2CS35188A.
13. Alvira, P.; Tomás-Pejó, E.; Ballesteros, M.; Negro, M.J. Pretreatment Technologies for an Efficient Bioethanol Production Process Based on Enzymatic Hydrolysis: A Review. Bioresour. Technol. **2010**, 101, 4851–4861, doi:10.1016/j.biortech.2009.11.093.
14. Hydrothermal Processing in Biorefineries; Ruiz, H.A., Hedegaard Thomsen, M., Trajano, H.L., Eds.; Springer International Publishing: Cham, 2017; ISBN 978-3-319-56456-2.
15. Huang, C.; Wu, X.; Huang, Y.; Lai, C.; Li, X.; Yong, Q. Prewashing Enhances the Liquid Hot Water Pretreatment Efficiency of Waste Wheat Straw with High Free Ash Content. Bioresour. Technol. **2016**, 219, 583–588, doi:10.1016/j.biortech.2016.08.018.
16. Sluiter, A. Determination of Ash in Biomass: Laboratory Analytical Procedure (LAP); Issue Date: 7/17/2005. Tech. Rep. **2008**, 8.

17. Springer, E.L.; Harris, J.F. Procedures for Determining the Neutralizing Capacity of Wood during Hydrolysis with Mineral Acid Solutions. Ind. Eng. Chem. Prod. Res. Dev. **1985**, 24, 485–489, doi:10.1021/i300019a030.
18. Lloyd, T.A.; Wyman, C.E. Predicted Effects of Mineral Neutralization and Bisulfate Formation on Hydrogen Ion Concentration for Dilute Sulfuric Acid Pretreatment. In Proceedings of the Proceedings of the Twenty-Fifth Symposium on Biotechnology for Fuels and Chemicals Held May 4–7, 2003, in Breckenridge, CO; Finkelstein, M., McMillan, J.D., Davison, B.H., Evans, B., Eds.; Humana Press, 2004; pp. 1013–1022.
19. Yeoman, C.J.; Han, Y.; Dodd, D.; Schroeder, C.M.; Mackie, R.I.; Cann, I.K.O. Chapter 1 - Thermostable Enzymes as Biocatalysts in the Biofuel Industry. In Advances in Applied Microbiology; Advances in Applied Microbiology; Academic Press, 2010; Vol. 70, pp. 1–55.
20. Bichot, A.; Delgenès, J.-P.; Méchin, V.; Carrère, H.; Bernet, N.; García-Bernet, D. Understanding Biomass Recalcitrance in Grasses for Their Efficient Utilization as Biorefinery Feedstock. Rev. Environ. Sci. Biotechnol. **2018**, doi:10.1007/s11157-018-9485-y.
21. Zhai, R.; Hu, J.; Saddler, J.N. The Inhibition of Hemicellulosic Sugars on Cellulose Hydrolysis Are Highly Dependant on the Cellulase Productive Binding, Processivity, and Substrate Surface Charges. Bioresour. Technol. **2018**, 258, 79–87, doi:10.1016/j.biortech.2017.12.006.
22. National Laboratory of the U.S. Department of Energy, O. of E.E. and R.E., USA, Chapter 25 - Reducing Enzyme Costs, Novel Combinations and Advantages of Enzymes Could Lead to Improved Cost-Effective Biofuels Production. In Bioenergy; Dahiya, A., Ed.; Academic Press: Boston, 2015; pp. 407–412 ISBN 978-0-12-407909-0.
23. Godoy, C.M. de; Machado, D.L.; Costa, A.C. da Batch and Fed-Batch Enzymatic Hydrolysis of Pretreated Sugarcane Bagasse – Assays and Modeling. Fuel **2019**, 253, 392–399, doi:10.1016/j.fuel.2019.05.038.
24. Larsen, J.; Haven, M.Ø.; Thirup, L. Inbicon Makes Lignocellulosic Ethanol a Commercial Reality. Biomass Bioenergy **2012**, 46, 36–45, doi:10.1016/j.biombioe.2012.03.033.
25. Humbird, D.; Davis, R.; Tao, L.; Kinchin, C.; Hsu, D.; Aden, A.; Schoen, P.; Lukas, J.; Olthof, B.; Worley, M.; et al. Process Design and Economics for Biochemical Conversion of Lignocellulosic Biomass to Ethanol: Dilute-Acid Pretreatment and Enzymatic Hydrolysis of Corn Stover; 2011;
26. Agbor, V.B.; Cicek, N.; Sparling, R.; Berlin, A.; Levin, D.B. Biomass Pretreatment: Fundamentals toward Application. Biotechnol. Adv. **2011**, 29, 675–685, doi:10.1016/j.biotechadv.2011.05.005.
27. Alvira, P.; Tomás-Pejó, E.; Ballesteros, M.; Negro, M.J. Pretreatment Technologies for an Efficient Bioethanol Production Process Based on Enzymatic Hydrolysis: A Review. Bioresour. Technol. **2010**, 101, 4851–4861, doi:10.1016/j.biortech.2009.11.093.
28. Cantero, D.; Jara, R.; Navarrete, A.; Pelaz, L.; Queiroz, J.; Rodríguez-Rojo, S.; Cocero, M.J. Pretreatment Processes of Biomass for Biorefineries: Current Status and Prospects. Annu. Rev. Chem. Biomol. Eng. **2019**, 10, 289–310, doi:10.1146/annurev-chembioeng-060718-030354.
29. Cocero, M.J.; Cabeza, Á.; Abad, N.; Adamovic, T.; Vaquerizo, L.; Martínez, C.M.; Pazo-Cepeda, M.V. Understanding Biomass Fractionation in Subcritical & Supercritical Water. J. Supercrit. Fluids **2018**, 133, 550–565, doi:10.1016/j.supflu.2017.08.012.
30. Chen, W.-H.; Chu, Y.-S.; Liu, J.-L.; Chang, J.-S. Thermal Degradation of Carbohydrates, Proteins and Lipids in Microalgae Analyzed by Evolutionary Computation. Energy Convers. Manag. **2018**, 160, 209–219, doi:10.1016/j.enconman.2018.01.036.
31. Li, M.; Cao, S.; Meng, X.; Studer, M.; Wyman, C.E.; Ragauskas, A.J.; Pu, Y. The Effect of Liquid Hot Water Pretreatment on the Chemical–Structural Alteration and the Reduced Recalcitrance in Poplar. Biotechnol. Biofuels **2017**, 10, 237, doi:10.1186/s13068-017-0926-6.
32. Irvine, G.M. The Significance of the Glass Transition of Lignin in Thermomechanical Pulping. Wood Sci. Technol. **1985**, 19, 139–149, doi:10.1007/BF00353074.
33. Selig, M.J.; Viamajala, S.; Decker, S.R.; Tucker, M.P.; Himmel, M.E.; Vinzant, T.B. Deposition of Lignin Droplets Produced During Dilute Acid Pretreatment of Maize Stems Retards Enzymatic Hydrolysis of Cellulose. Biotechnol. Prog. **2007**, 23, 1333–1339, doi:10.1021/bp0702018.

34. Li, H.; Pu, Y.; Kumar, R.; Ragauskas, A.J.; Wyman, C.E. Investigation of Lignin Deposition on Cellulose during Hydrothermal Pretreatment, Its Effect on Cellulose Hydrolysis, and Underlying Mechanisms. Biotechnol. Bioeng. **2014**, 111, 485–492, doi:10.1002/bit.25108.
35. Samuel, R.; Pu, Y.; Raman, B.; Ragauskas, A.J. Structural Characterization and Comparison of Switchgrass Ball-Milled Lignin Before and After Dilute Acid Pretreatment. Appl. Biochem. Biotechnol. **2010**, 162, 62–74, doi:10.1007/s12010-009-8749-y.
36. Cao, S.; Pu, Y.; Studer, M.; Wyman, C.; Ragauskas, A.J. Chemical Transformations of Populus Trichocarpa during Dilute Acid Pretreatment. RSC Adv. **2012**, 2, 10925–10936, doi:10.1039/C2RA22045H.
37. 2. The Reactions Leading to Furfural. In Sugar Series; Zeitsch, K.J., Ed.; the chemistry and technology of furfural and its many by-products; Elsevier, 2000; Vol. 13, pp. 3–7.
38. 6. Furfural Loss Reactions. In Sugar Series; Zeitsch, K.J., Ed.; the chemistry and technology of furfural and its many by-products; Elsevier, 2000; Vol. 13, pp. 19–22.
39. Shinde, S.D.; Meng, X.; Kumar, R.; Ragauskas, A.J. Recent Advances in Understanding the Pseudo-Lignin Formation in a Lignocellulosic Biorefinery. Green Chem. **2018**, 20, 2192–2205, doi:10.1039/C8GC00353J.
40. He, J.; Huang, C.; Lai, C.; Huang, C.; Li, M.; Pu, Y.; Ragauskas, A.J.; Yong, Q. The Effect of Lignin Degradation Products on the Generation of Pseudo-Lignin during Dilute Acid Pretreatment. Ind. Crops Prod. **2020**, 146, 112205, doi:10.1016/j.indcrop.2020.112205.
41. Saeman, J.F. Kinetics of Wood Saccharification - Hydrolysis of Cellulose and Decomposition of Sugars in Dilute Acid at High Temperature. Ind. Eng. Chem. **1945**, 37, 43–52, doi:10.1021/ie50421a009.
42. Overend R. P.; Chornet E.; Gascoigne J. A.; Hartley Brian Selby; Broda P. M. A.; Senior P. J. Fractionation of Lignocellulosics by Steam-Aqueous Pretreatments. Philos. Trans. R. Soc. Lond. Ser. Math. Phys. Sci. **1987**, 321, 523–536, doi:10.1098/rsta.1987.0029.
43. Yang, B.; Wyman, C.E. Effect of Xylan and Lignin Removal by Batch and Flowthrough Pretreatment on the Enzymatic Digestibility of Corn Stover Cellulose. Biotechnol. Bioeng. **2004**, 86, 88–98, doi:10.1002/bit.20043.
44. Conrad, M.; Smirnova, I. Two-Step Autohydrolysis Pretreatment: Towards High Selective Full Fractionation of Wheat Straw. Chem. Ing. Tech. **2020**, n/a, doi:10.1002/cite.202000056.
45. Schmidt, L.M.; Pérez Martínez, V.; Kaltschmitt, M. Solvent-Free Lignin Recovered by Thermal-Enzymatic Treatment Using Fixed-Bed Reactor Technology – Economic Assessment. Bioresour. Technol. **2018**, 268, 382–392, doi:10.1016/j.biortech.2018.07.107.
46. Pearce, E.J.; Gerster, J.A. Furfural-Water System - Experimental and Theoretical Vapor-Liquid Relationships. Ind. Eng. Chem. **1950**, 42, 1418–1424, doi:10.1021/ie50487a043.
47. Bobleter, O.D.; Pape, G. Verfahren zum Abbau von Holz, Rinde oder andern Pflanzenmaterialien 1968.
48. Mok, W.S.L.; Antal, M.J. Uncatalyzed Solvolysis of Whole Biomass Hemicellulose by Hot Compressed Liquid Water. Ind. Eng. Chem. Res. **1992**, 31, 1157–1161, doi:10.1021/ie00004a026.
49. Cabeza, A.; Piqueras, C.M.; Sobrón, F.; García-Serna, J. Modeling of Biomass Fractionation in a Lab-Scale Biorefinery: Solubilization of Hemicellulose and Cellulose from Holm Oak Wood Using Subcritical Water. Bioresour. Technol. **2016**, 200, 90–102, doi:10.1016/j.biortech.2015.09.063.
50. Kilpeläinen, P.O.; Hautala, S.S.; Byman, O.O.; Tanner, L.J.; Korpinen, R.I.; Lillandt, M.K.-J.; Pranovich, A.V.; Kitunen, V.H.; Willför, S.M.; Ilvesniemi, H.S. Pressurized Hot Water Flow-through Extraction System Scale up from the Laboratory to the Pilot Scale. Green Chem. **2014**, 16, 3186–3194, doi:10.1039/C4GC00274A.
51. Ingram, T.; Rogalinski, T.; Bockemühl, V.; Antranikian, G.; Brunner, G. Semi-Continuous Liquid Hot Water Pretreatment of Rye Straw. J. Supercrit. Fluids **2009**, 48, 238–246, doi:10.1016/j.supflu.2008.10.023.
52. Reynolds, W.; Singer, H.; Schug, S.; Smirnova, I. Hydrothermal Flow-through Treatment of Wheat-Straw: Detailed Characterization of Fixed-Bed Properties and Axial Dispersion. Chem. Eng. J. **2015**, 281, 696–703, doi:10.1016/j.cej.2015.06.117.

53. Pronyk, C.; Mazza, G. Kinetic Modeling of Hemicellulose Hydrolysis from Triticale Straw in a Pressurized Low Polarity Water Flow-Through Reactor. Ind. Eng. Chem. Res. **2010**, 49, 6367–6375, doi:10.1021/ie1003625.
54. Torres-Mayanga, P.C.; Azambuja, S.P.H.; Tyufekchiev, M.; Tompsett, G.A.; Timko, M.T.; Goldbeck, R.; Rostagno, M.A.; Forster-Carneiro, T. Subcritical Water Hydrolysis of Brewer's Spent Grains: Selective Production of Hemicellulosic Sugars (C-5 Sugars). J. Supercrit. Fluids **2019**, 145, 19–30, doi:10.1016/j.supflu.2018.11.019.
55. Reynolds, W.; Smirnova, I. Hydrothermal Flow-through Treatment of Wheat Straw: Coupled Heat and Mass Transfer Modeling with Changing Bed Properties. J. Supercrit. Fluids **2017**, doi:10.1016/j.supflu.2017.08.001.
56. Archambault-Léger, V.; Shao, X.; Lynd, L.R. Simulated Performance of Reactor Configurations for Hot-Water Pretreatment of Sugarcane Bagasse. ChemSusChem **2014**, 7, 2721–2727, doi:10.1002/cssc.201402087.
57. Reynolds, W.; Conrad, M.; Mbeukem, S.; Stank, R.; Smirnova, I. Pressure Drop, Mechanic Deformation, Stabilization and Scale-up of Wheat Straw Fixed-Beds during Hydrothermal Pretreatment: Experiments and Modeling. Chem. Eng. J. **2018**, doi:10.1016/j.cej.2018.11.001.
58. Liu, C.; Wyman, C.E. The Effect of Flow Rate of Compressed Hot Water on Xylan, Lignin, and Total Mass Removal from Corn Stover. Ind. Eng. Chem. Res. **2003**, 42, 5409–5416, doi:10.1021/ie030458k.
59. Cheng, M.-H.; Dien, B.S.; Lee, D.K.; Singh, V. Sugar Production from Bioenergy Sorghum by Using Pilot Scale Continuous Hydrothermal Pretreatment Combined with Disk Refining. Bioresour. Technol. **2019**, 289, 121663, doi:10.1016/j.biortech.2019.121663.
60. Dai, J.; Cui, H.; Grace, J.R. Biomass Feeding for Thermochemical Reactors. Prog. Energy Combust. Sci. **2012**, 38, 716–736, doi:10.1016/j.pecs.2012.04.002.
61. Nachenius, R.W.; van de Wardt, T.A.; Ronsse, F.; Prins, W. Residence Time Distributions of Coarse Biomass Particles in a Screw Conveyor Reactor. Fuel Process. Technol. **2015**, 130, 87–95, doi:10.1016/j.fuproc.2014.09.039.
62. Sievers, D.A.; Stickel, J.J. Modeling Residence-Time Distribution in Horizontal Screw Hydrolysis Reactors. Chem. Eng. Sci. **2018**, 175, 396–404, doi:10.1016/j.ces.2017.10.012.
63. Heitz, M.; Capek-Ménard, E.; Koeberle, P.G.; Gagné, J.; Chornet, E.; Overend, R.P.; Taylor, J.D.; Yu, E. Fractionation of Populus Tremuloides at the Pilot Plant Scale: Optimization of Steam Pretreatment Conditions Using the STAKE II Technology. Bioresour. Technol. **1991**, 35, 23–32, doi:10.1016/0960-8524(91)90078-X.
64. Lischeske, J.J.; Crawford, N.C.; Kuhn, E.; Nagle, N.J.; Schell, D.J.; Tucker, M.P.; McMillan, J.D.; Wolfrum, E.J. Assessing Pretreatment Reactor Scaling through Empirical Analysis. Biotechnol. Biofuels **2016**, 9, 213, doi:10.1186/s13068-016-0620-0.
65. 10. Furfural Processes. In The chemistry and technology of furfural and its many by-products; Zeitsch, K.J., Ed.; sugar series; Elsevier, 2000; Vol. 13, pp. 36–74.
66. Rainey, T.J.; Covey, G. Pulp and Paper Production from Sugarcane Bagasse. In Sugarcane-Based Biofuels and Bioproducts; O'Hara, I.M., Mundree, S.G., Eds.; John Wiley & Sons, Inc: Hoboken, NJ, USA, 2016; pp. 259–280 ISBN 978-1-118-71986-2.
67. Muzzy, J.D.; Roberts, R.S.; Fieber, C.A.; Faass, G.S.; Mann, T.M. Pretreatment of Hardwood by Continuous Steam Hydrolysis. In Wood a Agricultural Residues; Academic Press, 1983; pp. 351–368 ISBN 978-0-12-654560-9.
68. Wayman, M.; Parekh, S.; Chornet, E.; Overend, R.P. SO2-Catalysed Prehydrolysis of Coniferous Wood for Ethanol Production. Biotechnol. Lett. **1986**, 8, 749–752, doi:10.1007/BF01032576.
69. Petersen, M.Ø.; Larsen, J.; Thomsen, M.H. Optimization of Hydrothermal Pretreatment of Wheat Straw for Production of Bioethanol at Low Water Consumption without Addition of Chemicals. Biomass Bioenergy **2009**, 33, 834–840, doi:10.1016/j.biombioe.2009.01.004.
70. Larsen J.; Østergaard Petersen M.; Thirup L.; Wen Li H.; Krogh Iversen F. The IBUS Process – Lignocellulosic Bioethanol Close to a Commercial Reality. Chem. Eng. Technol. **2008**, 31, 765–772, doi:10.1002/ceat.200800048.

71. Conrad, M.; Häring, H.; Smirnova, I. Design of an Industrial Autohydrolysis Pretreatment Plant for Annual Lignocellulose. Biomass Convers. Biorefinery **2019**, doi:10.1007/s13399-019-00479-1.
72. Jönsson, L.J.; Alriksson, B.; Nilvebrant, N.-O. Bioconversion of Lignocellulose: Inhibitors and Detoxification. Biotechnol. Biofuels **2013**, 6, 16, doi:10.1186/1754-6834-6-16.
73. Palmqvist, E.; Hahn-Hägerdal, B. Fermentation of Lignocellulosic Hydrolysates. II: Inhibitors and Mechanisms of Inhibition. Bioresour. Technol. **2000**, 74, 25–33, doi:10.1016/S0960-8524(99)00161-3.
74. Andersen, L.F.; Parsin, S.; Lüdtke, O.; Kaltschmitt, M. Biogas Production from Straw—the Challenge Feedstock Pretreatment. Biomass Convers. Biorefinery **2020**, doi:10.1007/s13399-020-00740-y.
75. Baerns, M.; Behr, A.; Brehm, A.; Gmehling, J.; Hinrichsen, K.-O.; Hofmann, H.; Palkovits, R.; Onken, U.; Renken, A. Technische Chemie; Zweite, erweiterte Auflage.; Wiley-VCH: Weinheim, 2013; ISBN 978-3-527-33072-0.
76. Wirtschaftlich optimale Prozeßführung. In Technische Chemie: Einführung in die Chemische Reaktionstechnik; Emig, G., Klemm, E., Eds.; Springer-Lehrbuch; Springer: Berlin, Heidelberg, 2005; pp. 33–93 ISBN 978-3-540-28887-9.
77. Chemistry and Processing of Sugarbeet and Sugarcane; Elsevier, 1988; Vol. 9; ISBN 978-0-444-43020-5.
78. Asadi, M. Beet-Sugar Handbook; Wiley-Interscience: Hoboken, N.J, 2007; ISBN 978-0-471-76347-5.
79. The Extraction of Vegetable Oils. In Fats and Oils Handbook; Elsevier, 1998; pp. 345–445 ISBN 978-0-9818936-0-0.
80. Green Vegetable Oil Processing.; Amer Oil Chemists Society, 2016; ISBN 978-0-12-810216-9.
81. Krotscheck, A.W. Pulp Washing. In Handbook of Pulp; John Wiley & Sons, Ltd, 2006; pp. 511–559 ISBN 978-3-527-61988-7.
82. Bari, I.D.; Dininno, G.; Braccio, G. BIOETANOLO DA RESIDUI DELLA LAVORAZIONE DEL MAIS. 127.
83. Voeste, T.; Weber, K.; Hiskey, B.; Brunner, G. Liquid–Solid Extraction. In Ullmann's Encyclopedia of Industrial Chemistry; American Cancer Society, 2006 ISBN 978-3-527-30673-2.
84. Sievers, D.A.; Kuhn, E.M.; Tucker, M.P.; McMillan, J.D. Effects of Dilute-Acid Pretreatment Conditions on Filtration Performance of Corn Stover Hydrolyzate. Bioresour. Technol. **2017**, 243, 474–480, doi:10.1016/j.biortech.2017.06.144.
85. Sievers, D.A.; Tao, L.; Schell, D.J. Performance and Techno-Economic Assessment of Several Solid–Liquid Separation Technologies for Processing Dilute-Acid Pretreated Corn Stover. Bioresour. Technol. **2014**, 167, 291–296, doi:10.1016/j.biortech.2014.05.113.
86. Handbook of Pulp; Sixta, H., Ed.; Wiley-VCH ; John Wiley, distributor]: Weinheim : [Chichester, 2006; ISBN 978-3-527-30999-3.
87. Crawford, N.C.; Nagle, N.; Sievers, D.A.; Stickel, J.J. The Effects of Physical and Chemical Preprocessing on the Flowability of Corn Stover. Biomass Bioenergy **2016**, 85, 126–134, doi:10.1016/j.biombioe.2015.12.015.
88. Thermische Trennverfahren: Grundlagen, Auslegung, Apparate; Sattler, K., Ed.; 3., überarb. u. erw. Aufl., [Nachdr.].; Wiley-VCH: Weinheim, 2007; ISBN 978-3-527-30243-7.
89. Sluiter, A. Determination of Total Solids in Biomass and Total Dissolved Solids in Liquid Process Samples: Laboratory Analytical Procedure (LAP). Tech. Rep. **2008**, 9.
90. Koch, G.; Kleist, G. Application of Scanning UV Microspectrophotometry to Localise Lignins and Phenolic Extractives in Plant Cell Walls. **2001**, 55, 563–567, doi:10.1515/HF.2001.091.
91. Schmitt, U.; Grünwald, C.; Gričar, J.; Koch, G.; Čufar, K. WALL STRUCTURE OF TERMINAL LATEWOOD TRACHEIDS OF HEALTHY AND DECLINING SILVER FIR TREES IN THE DINARIC REGION, SLOVENIA. IAWA J. **2003**, 24, 41–51, doi:10.1163/22941932-90000319.
92. DIN EN ISO 17828 Biogene Festbrennstoffe – Bestimmung Der Schüttdichte (ISO 17828:2015); Deutsche Fassung EN ISO 17828:2015.

93. VDI 4630 - Fermentation of Organic Materials Characterisation of the Substrate, Sampling, Collection of Material Data, Fermentation Tests; VDI-Handbuch Energietechnik VDI-Handbuch Nutztierhaltung: Emissionen/Immissionen VDI-Handbuch Technik Biomasse/Boden; Düsseldorf, 2016; pp. 1–132;.
94. Scherzinger, M.; Kaltschmitt, M.; Thoma, M. Effects of Vapothermal Pretreatment on Anaerobic Degradability of Common Reed. Energy Technol. **2021**, 9, 2001046, doi:10.1002/ente.202001046.
95. Sluiter, A. Determination of Structural Carbohydrates and Lignin in Biomass: Laboratory Analytical Procedure (LAP); Issue Date: 7/17/2005; 2008; p. 16;.
96. Adney, B.; Baker, J. Measurement of Cellulase Activities: Laboratory Analytical Procedure (LAP); Issue Date: 08/12/1996; 2008; p. 11;.
97. AD 2000-Regelwerk: Taschenbuch-Ausgabe 2021; Verband der TÜV, Ed.; 13. Auflage, Stand: Dezember 2021.; Beuth: Berlin Wien Zürich, 2022; ISBN 978-3-410-30950-5.
98. Conrad, M.; Smirnova, I. Counter-Current Suspension Extraction Process of Lignocellulose in Biorefineries to Reach Low Water Consumption, High Extraction Yields, and Extract Concentrations. Processes **2021**, 9, 1585, doi:10.3390/pr9091585.
99. Conrad, M.; Smirnova, I. Process for Continuous Extraction of Lignocellulose Material, LU102852, Patend Filled 2021.
100. Jørgensen, H.; Kristensen, J.B.; Felby, C. Enzymatic Conversion of Lignocellulose into Fermentable Sugars: Challenges and Opportunities. Biofuels Bioprod. Biorefining **2007**, 1, 119–134, doi:10.1002/bbb.4.
101. Reynolds, W.; Verlag Dr. Hut Modeling and Scale-up of Hydrothermal Pretreatment in Compressible Lignocellulosic Biomass Fixed-Beds with Changing Properties, 2019.
102. Ertas, M.; Han, Q.; Jameel, H.; Chang, H. Enzymatic Hydrolysis of Autohydrolyzed Wheat Straw Followed by Refining to Produce Fermentable Sugars. Bioresour. Technol. **2014**, 152, 259–266, doi:10.1016/j.biortech.2013.11.026.
103. Zerbe, B. Investigation of Fundamentals of Two-Stage, Dilute Sulfuric Acid Hydrolysis of Wood.; Energy from biomass and wastes X: Chicago: Institute of Gas Technology;, 1987; pp. 927–947.
104. Sanchis-Sebastiá, M.; Gomis-Fons, J.; Galbe, M.; Wallberg, O. Techno-Economic Evaluation of Biorefineries Based on Low-Value Feedstocks Using the BioSTEAM Software: A Case Study for Animal Bedding. Processes **2020**, 8, 904, doi:10.3390/pr8080904.
105. Sanchis-Sebastiá, M.; Erdei, B.; Kovacs, K.; Galbe, M.; Wallberg, O. Introducing Low-Quality Feedstocks in Bioethanol Production: Efficient Conversion of the Lignocellulose Fraction of Animal Bedding through Steam Pretreatment. Biotechnol. Biofuels **2019**, 12, 215, doi:10.1186/s13068-019-1558-9.

8. List of figures

9. List of tables

10. Appendix

10.1. Bulk Densitiy

The measured bulk density of untreated and LHW pretreated wheat straw is displayed as a function of the liquid to solid ratio L/S in Fig. 10-1. The bulk density shows a strong increase with increasing L/S. The model constants for the bulk density of the untreated biomass are determined to be: $a = 13.044, b = 74.071$ and $c = 112.17$. It can be noted, that the pretreatment has only a small influence on the bulk density under the experimental conditions. The addition of water leads to almost no change of the bulk volume. This can be explained by the air in the bulk being replaced by water. To visualize this effect, the density is calculated using the dry biomass instead of the sample mass and displayed in Fig. 10-1 (diamonds). It can be seen, that this dry matter based density remains almost constant at 110 g/L. This behavior simplifies the reactor scaling, in regard to possible fluctuations in the dry matter content.

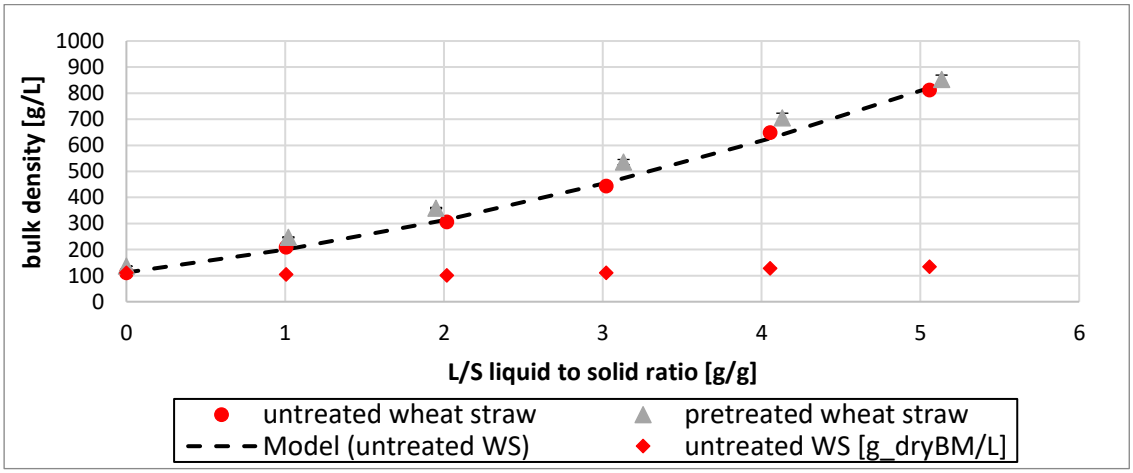

Fig. 10-1: Bulk density of untreated and pretreated wheat straw as a function of the liquid to solid ratio. Error of the measurements are displayed as standard deviations. The error of untreated straw for L/S=5 is not available

10.2. Two-Step Autohydrolysis LHW

In Fig. 10-2 the Degree of Solubilisation DS_{th} is displayed versus the overall severity factor S_0. It can be seen that all data sets follow the same increasing trend. The second step pretreatment DS shows higher values than the first step at the same overall severity factor. It is assumed that the water-soluble components like non-structural carbohydrates, ash, proteins are removed from the solids rapidly. The increase in DS with the treatment severity is due to the solubilization of structural carbohydrates, mainly hemicellulose. At higher severities, the solubilized pentoses can degrade to furfural and re-polymerize [38]. Thus, the DS slope would be lowered. The absence of an DS increase at high severities can indicate that the solubilization and the re-polymerization are of equal rates. This phenomenon can be observed with the single-step pretreatment in the range of $4.4 < \log(R_0) < 5.1$ but not with the two-step pretreatment. It is concluded that re-polymerization is reduced for A2 and reduced for B2 at a higher severity factor. The data from Reynolds show lower DS values in the first step at the same severity factor. This result is unexpected.

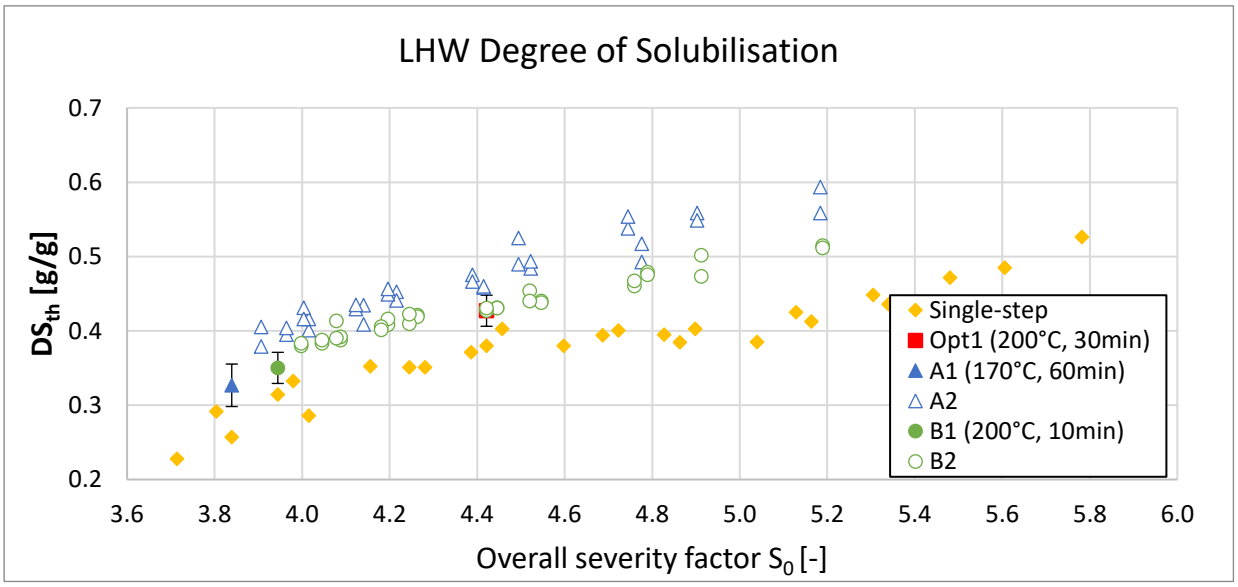

Fig. 10-2: Degree of solubilization of the first (full symbols) and the second step (hollow symbols) autohydrolysis pretreatment versus the overall severity factor. Opt1 (full square), A1 (full triangle), B1 (full circle), A2 (hollow triangle) and B2 (hollow circle). The error bars indicate the standard deviation for the first step hydrothermal pretreatment experiments (six repetitions). For the second step, all experimental results (duplicates) are shown.

In Fig. 5-12c glucose recovery is displayed. All data points, first and second treatment steps, are well below $R_{Glu,th}$ = 8 wt%. It is not possible to affect the glucose recovery

in the hydrolysate under the tested reaction conditions. Thus, it does not need to be considered in the selection of process conditions. The hemicellulose contains a small amount of glucose. Thus, it is suspected that the glucose in originated from the hemicellulose and not the cellulose.

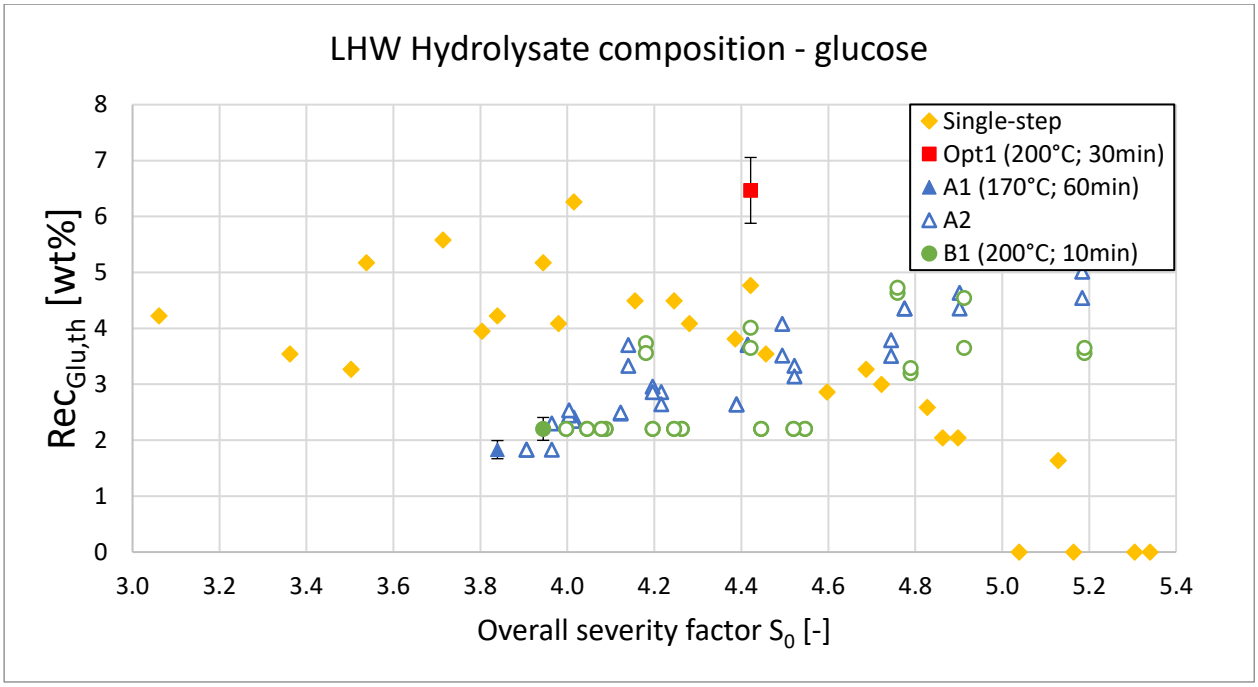

Fig. 10-3: Glucose recovery in the first (full symbols) and second step (hollow symbols) hydrothermal pretreatment. Opt1 (full square), A1 (full triangle), B1 (full circle), A2 (hollow triangle) and B2 (hollow circle). The error bars indicate the standard deviation for the first step hydrothermal pretreatment experiments (six repetitions). For the second step, all experimental results (duplicates) are shown.

10.3. pH vs Acid concentration in steam pretreatment

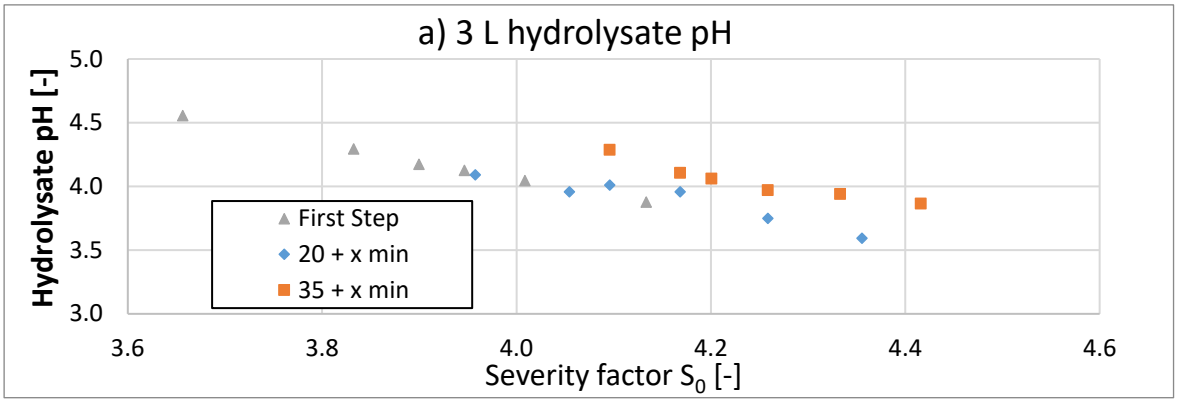

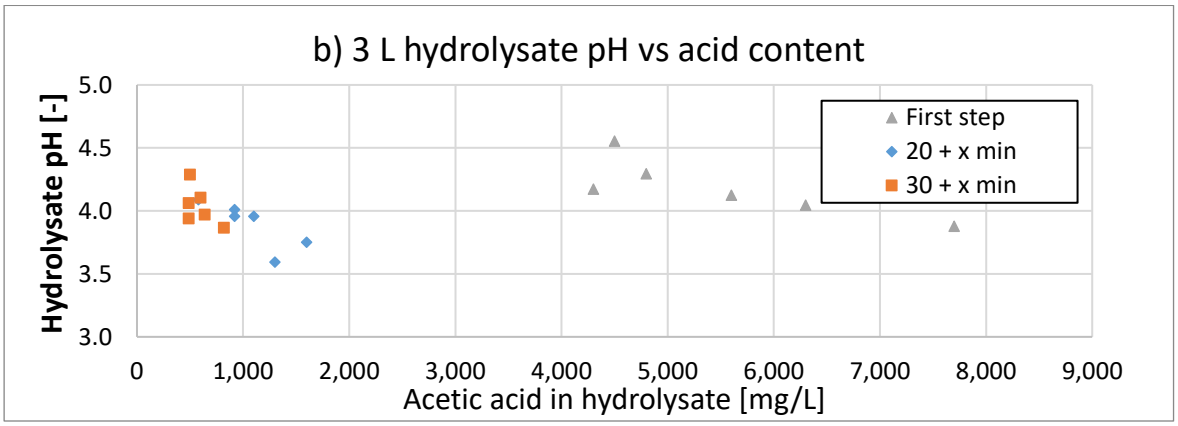

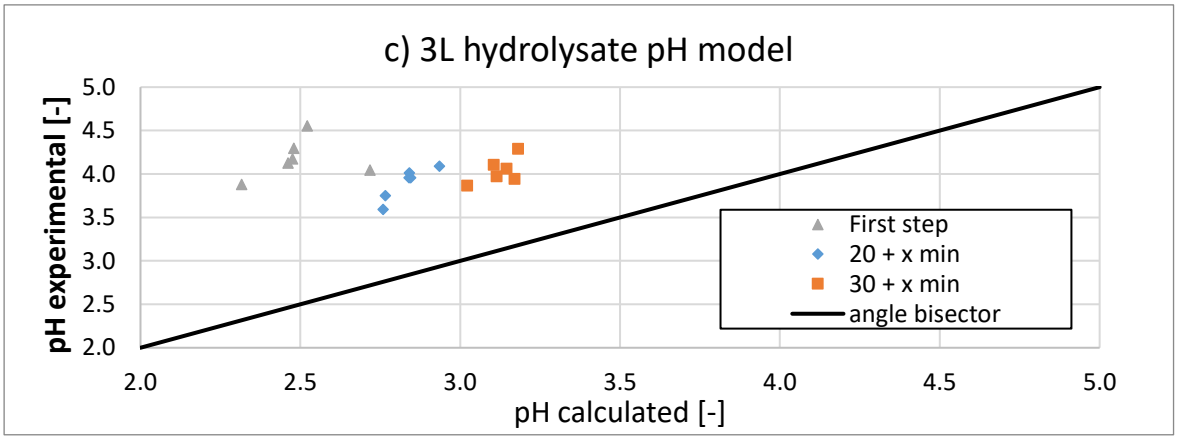

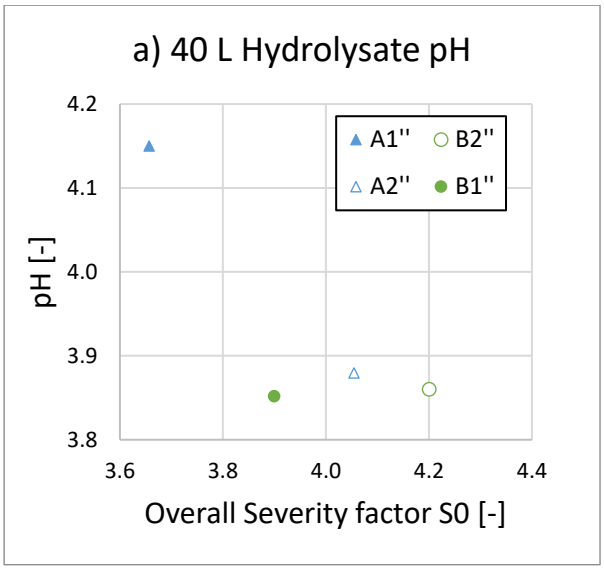
a) 40 L Hydrolysate pH
pH [-]
Overall Severity factor S0 [-]
A1''
B2''
A2''
B1''
4.2
4.1
4.0
3.9
3.8
3.6
3.8
4.0
4.2
4.4

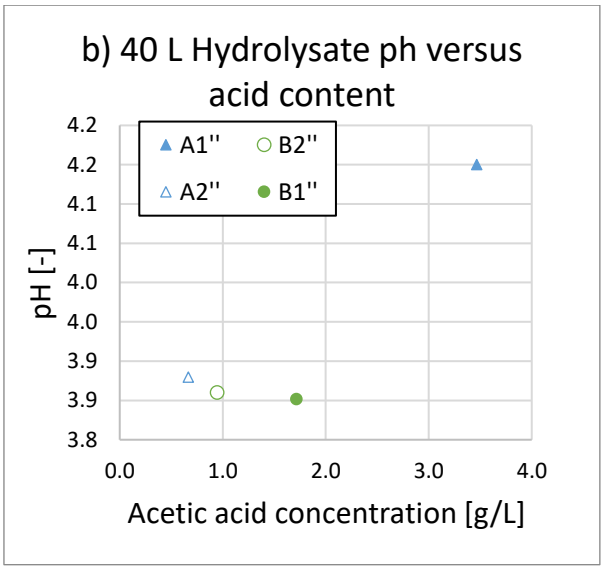
b) 40 L Hydrolysate ph versus acid content
pH [-]
Acetic acid concentration [g/L]
A1''
B2''
A2''
B1''
4.2
4.2
4.1
4.1
4.0
4.0
3.9
3.9
3.8
0.0
1.0
2.0
3.0
4.0

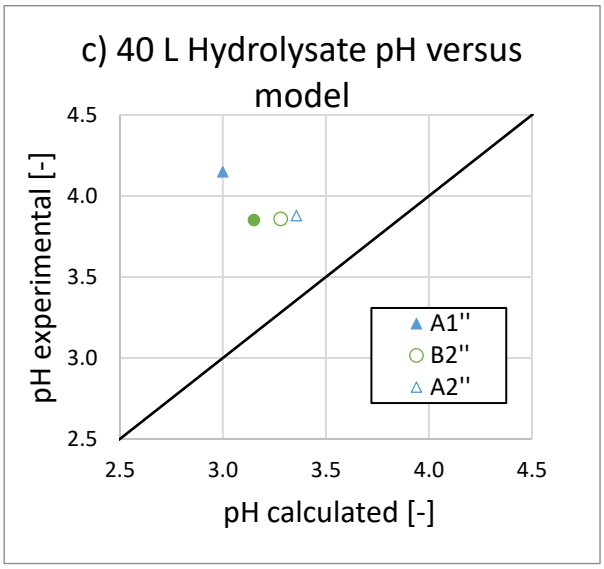
c) 40 L Hydrolysate pH versus model
pH experimental [-]
pH calculated [-]
A1''
B2''
A2''
4.5
4.0
3.5
3.0
2.5
2.5
3.0
3.5
4.0
4.5

10.4. AS-Lignin after milling

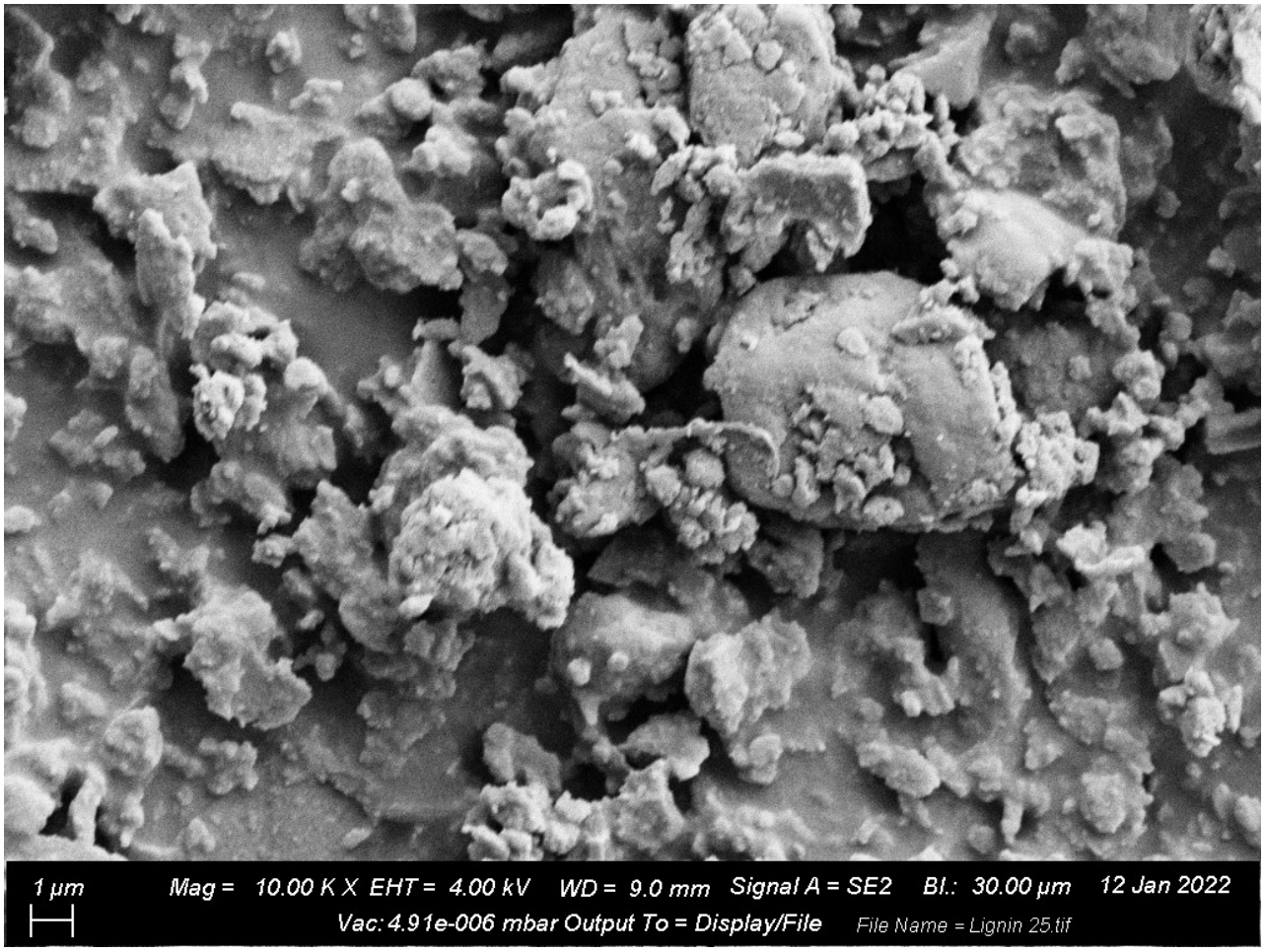

Fig. 10-4: Scanning electron microscopy (SEM) image of milled AS-lignin (B'') in Hosokawa impact mill.

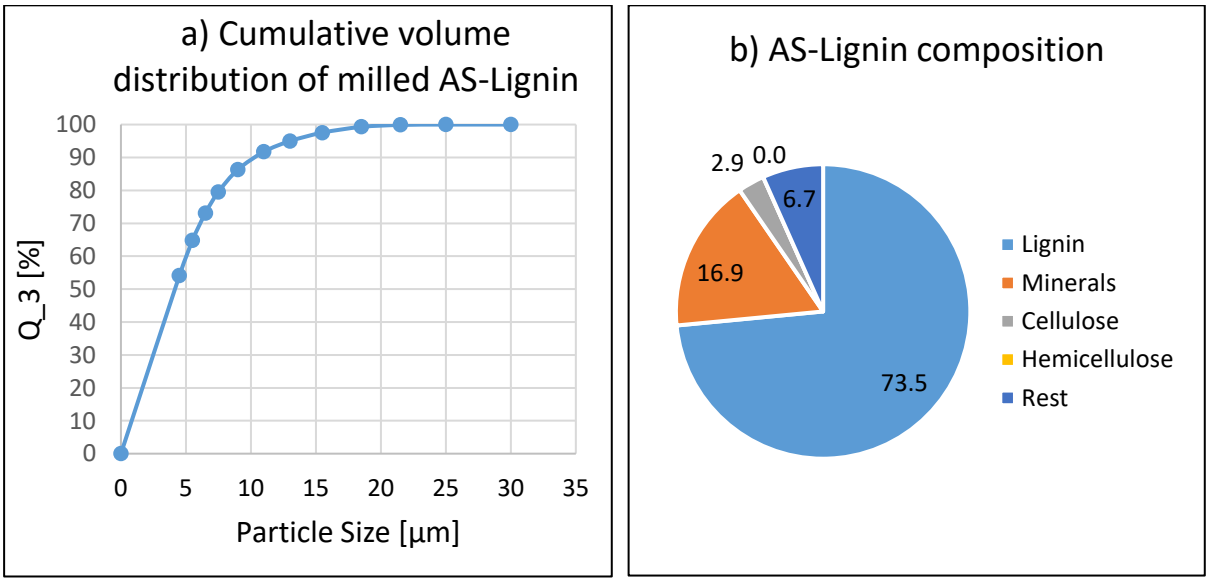

Fig. 10-5: AS-lignin (B'') **a)** Cumulative volume distribution of milled dispersed in water measured with laser diffractometer. **b)** composition.

10.5. Plug screw feeder in Lund (TK energy)

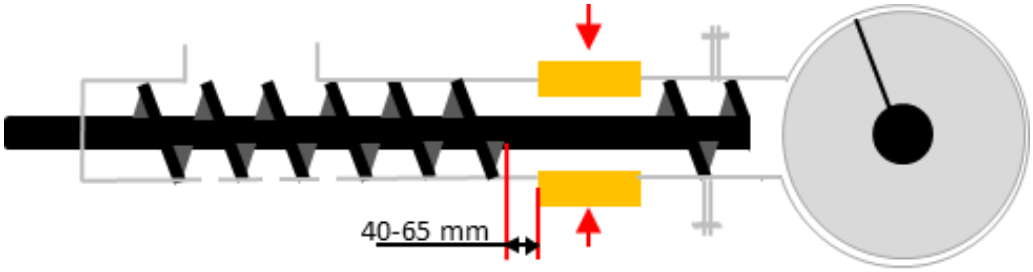

10.6. UMSP

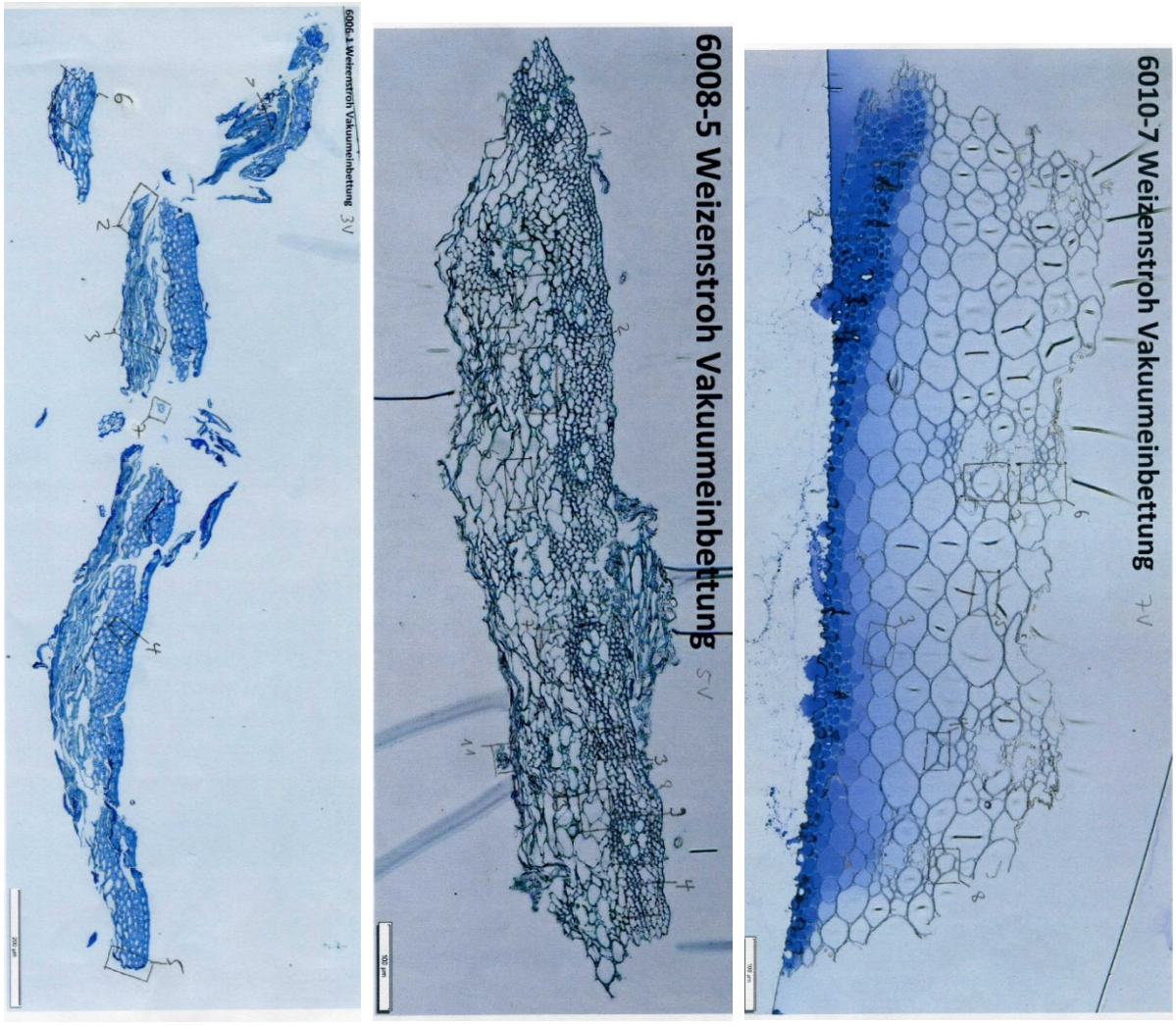

Fig. 10-6: Light microscope images of 1 µm thick of wheat straw slices, **left)** milled straw, after pretreatment at 200°C for 30 min in **middle)** flow-through reactor and **right)** LHW batch Flow-through LHW

The analyses were carried out using a UV microspectrophotometer (UMSP 80, Zeiss) equipped with a scanning stage enabling the determination of image profiles at defined wavelengths using the scan program APAMOS® (Automatic-Photometric-Analysis of Microscopic Objects by Scanning (Zeiss)). For the detection of the lignin distribution of softwoods and hardwoods wavelengths of 280 nm and 278 nm, respectively, were selected. The scan program digitizes rectangular fields with a local geometrical resolution of 0.25 µm² and a photometrical resolution of 4096 grey scale levels which are converted in 14 basic colors to visualize the absorbance intensities. The scans can be depicted as two- or three-dimensional image profiles including a statistical evaluation (histogram) of the semi-quantitative lignin distribution.

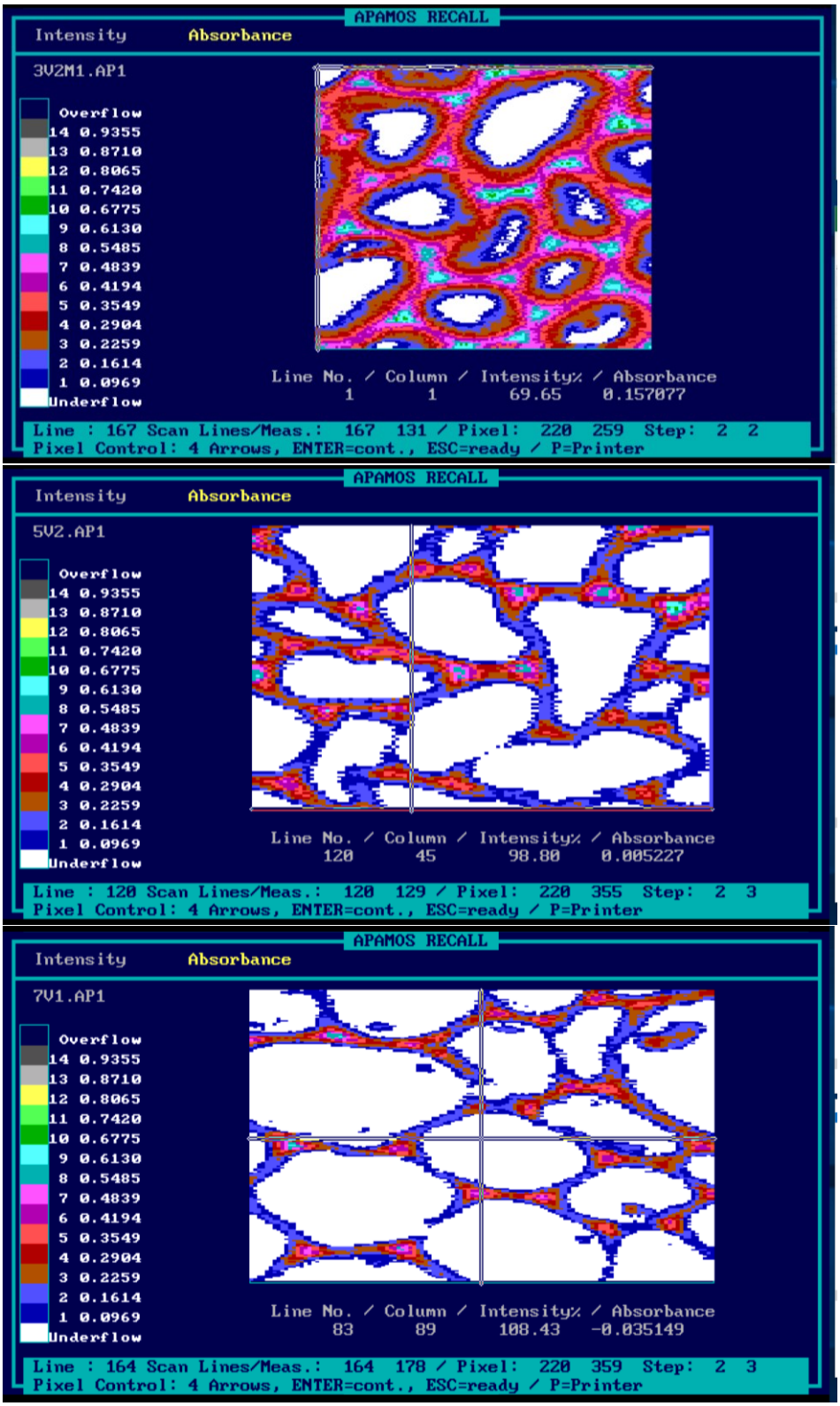

Fig. 10-7: Scanning UV microspectrophotometry (UMSP) images with 0.25 µm x 0.25 mm resolution wheat straw, left) milled straw, after pretreatment at 200°C for 30 min in midde) flow-through reactor and right) LHW batch Flow-through LHW

10.7. Recent publications for SCR use

#	1	2	3	4	5	6	7	8	9	10	11	12	13	14	15	16	17
Organisation	Quaker Oats	Georgia IT	Sherbrooke	Université de Sherbrooke	Université de Sherbrooke	Soustons, France	ENEA, Italy	Inbicon	NREL	FPI Quebec	Inbicon	Ceske		ACIB, Austria	Illinois	NREL	Beijing
year	1960s	1983	1986	1988	1991	1987	2007	2008	2011	2011	2012	2012	2016	2016	2019	2019	2014
material	bagasse	tulip poplar		pine, aspen, corn stover	populus temuloides	agricultural residues, hardwood, softwood	wheat, barley, oat straw	wheat straw	corn stover	bad spruce	wheat straw	rye straw	bagasse	wheat straw	sorghum bagasse	corn stover	corn cob
size		chips 1"			20x20x20 mm (chips)		chopped	5-10		20 mm	5	pellets/ cut		0.6 (min)			4
[cm]																	
chem. Add. [y/n]	sulphuric acid	no	SO_2	SO_2	no		no	no	dilute sulfuric acid	sulphuric acid	no	no	yes	sulphuric acid	no	sulfuric acid	non/ various
dry matter content in reactor [wt%]	45	45				60	50	40		42	35				50		
technology/ supplier		STAKE; Stake Tech Biomass	stake II	stake II	Stake II	Stake II	Stake I	IBUS	Andritz	Andritz	based on IBUS	Pharmix Ltd	Pandia digester	SCR	SUPR 2G	Metso	
flow pattern	co-current	co-current		co-current		co-current	co-current	co-current	co-current			co-current	co-current	co-current	co-current	co-current	
preparation	low pressure steam	debarking/ chipping				chopping, stone trap, fines blower, hammer milled		non		acid soaking; preheaming	washed with recycle condensate containing acetic acid	preheating; washing; addition of used rapeseed oil			shredding, dreiengy, grinding (3mm)	hammer milled; knife-milled (13 mm); washed	
feeding	auger press "french press"	screw piston feeder			co-axial feeder (dense plug), against choke		coaxial screw reziproging feeder	particle pump (dense plug)	Plug screw feeder (Andritz)	plug screw	?	High pressure screw pump	screw feeder	screw conveyor	open flight and full pitch equalizing screw feeder	compression screw feeder	
relese	double lock (ram valves)	screw compaction; ball vale			auger + single blow valve	hot-blow	stake I	particle pump	hot blow	in disk refiner	?	SE		single ball valve	two ball vale lock; hot blow		
steam recyl.	??	?					no	for evaporation		no	?			?			
diameter [m]	1.8	?			??		?	?	2.6	?	?				0.15		0.019
length [m]	16	?			??		?	?	9	?	?				1.37		3.5
volume [qm]	40.7	?			??		?	?	47.8	?	?				0.024		0.001
L/D	8.9								3.5						9.1		184.2
throughput kg/h	2 x 60,000	500		1,500	2,000	4,000	150	100	83,333	50-200	4,000					21	
medium	superheated steam	saturated steam		saturated steam	saturated steam		saturated steam	saturated steam	saturated steam	saturated steam	saturated steam	saturated steam	saturated steam	saturated steam	saturated steam	saturated steam	saturated steam
Temperatur [°C]	650	230		208	180-230	180-240	195-198	180-200		16	180-201	17.5		165	160-190	175	
pressure [barg]	10.9	24				10-32								7	20.7		25
residence time [min]	60	2-6		2	0.7-4.0	1-10	1.5-2.5	5-15	2	?	10-20	8.3		10	10	10-25	
Y_HC,Hyd,max					65%									?			
application	furfural	fractionation or furfural		ethanol	fractionation	Fractionation, ethanol	fractionation/ cattle feed	Ethanol		Ethanol	Ethanol	biogas fermentation	pulp	Ethanol	Ethanol	Ethanol	
source	[Zeitsch, 2000, 10. Furfural Processes]	[Zeitsch, 2000]; [Muzzy, 1983, in Wood and agricultural residues]	[Wayman, 1986, SO2-catalysed,]	[Wayman, 1988]	[Heitz, 1991]	[Native], 1992, The Biotechnology Facilities..] [Ropars, 1992, Large-scale enzymatic..]	[Viola, 2008]	[Larsen 2008]	[Humbird, 2011, Process Design...	[Fang, 2011]	[Larsen, 2012]	[Marousek, 2012]	[Rainey 2016 sugar cane based biofuels and bioproducts]	[Monschein, 2016]	[Cheng, 2019]	[Sievers, 2019]	[Zhang, 2014, A novel cleaning process for

11. Publications list

1. Reynolds, W.; Conrad, M.; Mbeukem, S.; Stank, R.; Smirnova, I. Pressure Drop, Mechanic Deformation, Stabilization and Scale-up of Wheat Straw Fixed-Beds during Hydrothermal Pretreatment: Experiments and Modeling. Chem. Eng. J. **2018**, doi:10.1016/j.cej.2018.11.001.
2. Conrad, M.; Häring, H.; Smirnova, I. Design of an Industrial Autohydrolysis Pretreatment Plant for Annual Lignocellulose. Biomass Convers. Biorefinery **2019**, doi:10.1007/s13399-019-00479-1.
3. Conrad, M.; Smirnova, I. Two-Step Autohydrolysis Pretreatment: Towards High Selective Full Fractionation of Wheat Straw. Chem. Ing. Tech. **2020**, doi:10.1002/cite.202000056.
4. Ruiz, H.A.; Conrad, M.; Sun, S.-N.; Sanchez, A.; Rocha, G.J.M.; Romaní, A.; Castro, E.; Torres, A.; Rodríguez-Jasso, R.M.; Andrade, L.P.; et al. Engineering Aspects of Hydrothermal Pretreatment: From Batch to Continuous Operation, Scale-up and Pilot Reactor under Biorefinery Concept. Bioresour. Technol. **2020**, 299, 122685, doi:10.1016/j.biortech.2019.122685.
5. Conrad, M.; Smirnova, I. Counter-Current Suspension Extraction Process of Lignocellulose in Biorefineries to Reach Low Water Consumption, High Extraction Yields, and Extract Concentrations. Processes **2021**, 9, 1585, doi:10.3390/pr9091585.

12. Patents

1. Conrad, M.; Smirnova, I. Process for continuous extraction of lignocellulose material, application number LU102852, filled in Luxembourg. 2021.

13. Students participation

The several students contributed to this work in the form of examination relevant thesis work or as student workers.

13.1. Thesis

- Delgado, Daniel (**2019**); Mater Thesis “2-step Liquid Hot Water Hydrolysis of Wheat Straw in a Lignin Biorefinery Cascade”
- Álvarez, Alicia (**2019**); Bachelor thesis “Application of Reaction Additives to Suppress Degradations Reactions in a HydrothermalPretreatment in a Wheat Straw Biorefinery”
- Kumar, Aditya (**2020**); Project work “Autohydrolysis of Wheat Straw at Low pHInvestigation of Reaction kinetics”
- Nicholls, Cherisa Michelle (**2020**); Master Thesis “Two Step Steam Hydrolysis of WheatStraw in a Biorefinery Cascade”
- Karimi, Mohammad Ali (**2020**); Bachelor Thesis “Hemizellulose-Extraktion von dampfaufgeschlossenem Weizenstroh: Prozessentwicklung in einem Bioraffinerie-Konzept”
- Brenke, Benjamin (**2021**); Bachelor Thesis “Bewertung eines zweistufigen Dampf-Autohydrolyse Aufschlusses mit Weizenstroh in einer Bioraffinerie-Kaskade im Pilot-Maßstab”

13.2. Hiwi

- Scherwinski, Timo
- Delgado, Daniel
- Karimi, Mohammad Ali
- Schnur, Jonas